Universidade de Lisboa

Faculdade de Farmácia

Small molecule PGC-1α activators:
A novel class of anti-neurodegenerative therapeutics

Catarina Isabel Ambrósio Ranito

Dissertation supervised by Professor Jorge Manuel Lira Gonçalves Ruas and co-supervised by Doctor Andreia Margarida Gonçalves das Neves Carvalho

Master in Biopharmaceutical Sciences

2019

Universidade de Lisboa

Faculdade de Farmácia

Small molecule PGC-1α activators: A novel class of anti-neurodegenerative therapeutics

Catarina Isabel Ambrósio Ranito

Dissertation supervised by Professor Jorge Manuel Lira Gonçalves Ruas and co-supervised by Doctor Andreia Margarida Gonçalves das Neves Carvalho

Master in Biopharmaceutical Sciences

2019

2019

Part of the results discussed in this dissertation were exhibited in the following meeting:

Catarina Ranito, Elsa Rodrigues, Andreia Neves Carvalho, Maria João Gama and Jorge Ruas. *Small molecule PGC-1α activators: a novel approach to anti-neurodegenerative therapeutics*. 11th iMed.ULisboa Postgraduate Students Meeting & 4rd i3DU Meeting, 15th July 2019, Lisbon Portugal [Abstract and Poster]

This work was supported by FEDER and national funds from Fundação para a Ciência e Tecnologia (FCT): LISBOA-01-0145-FEDER-030194 | PTDC/MED-FSL/30194/2017, PTDC/NEU-OSD/0502/2012 and UID/DTP/04138/2019

ABSTRACT

Parkinson's disease (PD) is an age-related neurodegenerative disorder, affecting primarily, the central nervous system. The major hallmark of PD is the death of dopaminergic neurons in the *substantia nigra pars compacta*, with consequently decreased levels of dopamine in the *striatum*. During aging many cellular processes suffer alterations, such as increased mitochondrial damage, ROS accumulation and decreased proteostatic mechanisms. Altogether, these events can ultimately lead to degeneration of neuronal cells and the development of neurodegenerative diseases.

Peroxisome proliferator-activated receptor γ (PPARγ) coactivator1α (PGC-1α) is the most studied member of the PGC-1 family and can be induced, in a tissue-specific manner, by physiological cues, such as exercise, fasting and cold exposure. PGC-1α1 is directly linked to mitochondrial biogenesis and cell detoxification of reactive oxygen species. Several studies have shown that PGC-1α1 expression tends to decrease with aging. Conversely, its activation prevents dopaminergic neuron loss, in both genetic and toxin-induced cellular models of PD. PGC-1α1 does not have predictable DNA- or ligand-binding domains, which poses a challenge to a direct pharmacological intervention. Thus, being able to target this coactivator through its stabilization is of utmost importance, in order to help find new approaches against neurodegeneration.

The aim of this study is to validate in a neuronal cellular system, eleven small-molecules that were previously identified as PGC-1α1 stabilizers in brown adipocytes, where this coactivator was first identified. The validation process comprehended: selection of the cellular model for compound screening; screening of the small PGC-1α1 activators on the chosen cellular model, through dose-dependent cell viability assays and evaluation of mRNA relative expression levels of PGC-1α1 downstream target genes; and, finally the evaluation of the effects of each selected compound in a cellular model of PD.

We were able to select five of the eleven small-molecules tested as effective modulators of PGC-1α downstream targets, in a N2a mouse neuroblastoma cell line. Upon pre-conditioning of cells with the compounds followed by treatment with 1-methyl-4-phenylpyridinium (MPP^+), some of the selected compounds increased both cellular ATP levels and cellular viability, restoring control levels. Altogether, the results from the present study revealed that a small group of the tested compounds demonstrated protective effects against MPP^+-treated cells, possibly by stabilizing PGC-1α1.

Keywords: Parkinson's disease; MPP^+; PGC-1α1 stabilizers; screening.

RESUMO

A doença de Parkinson (DP) é uma doença associada ao envelhecimento que afeta, principalmente o sistema nervoso central. A doença manifesta-se por diversos sintomas, nomeadamente distúrbios do sono, depressão, disfunção olfatória e gastrointestinal, assim como disfunção autonómica e cognitiva; e sintomas motores, característicos da doença, como tremores, instabilidade postural, desequilibro, bradicinesia e hipocinesia, cujo seu aparecimento/desenvolvimento ocorre já numa fase em que cerca de 80% da dopamina no estriado se encontra depletada e em que já ocorreu degenerescência de cerca de 60% a 70% dos neurónios dopaminérgicos, da *substantia nigra pars compacta*. Uma vez que os sintomas motores são característicos desta patologia, o diagnóstico da mesma torna-se possível, através da observação clínica de pelo menos quatro destes sinais motores. Uma das características principais desta doença é o surgimento de inclusões proteicas, constituídas maioritariamente por α-sinucleína, ubiquitina, neurofilamentos e *chaperones* moleculares. Estas inclusões são designadas por corpos de *Lewy* e pensa-se que a agregação que leva à sua formação está associada ao desenvolvimento de espécies intermediárias tóxicas para as células. Como mecanismo de proteção, os sistemas de defesa das células promovem a agregação destas espécies intermediárias, que são observáveis em amostras de tecido de cérebros de pacientes com a DP. Pensa-se que o aparecimento dos corpos de *Lewy* ocorre anos antes da morte dos neurónios dopaminérgicos, prevendo-se que o seu surgimento seja anterior ao desenvolvimento da fase sintomática da doença.

O envelhecimento é caracterizado pela alteração de processos celulares, tais como aumento de danos mitocondriais, acumulação de espécies reativas de oxigénio e ainda pela regulação negativa dos mecanismos de homeostase proteica. Consequentemente, estes eventos podem levar à degenerescência das células neuronais e ao desenvolvimento de doenças neurodegenerativas.

A família do co ativador 1 do recetor γ ativado por proliferadores de peroxissomas (PGC-1) é constituída por três membros fundadores: o PGC-1α, o PGC-1β e o co ativador relacionado com o PGC-1 (PRC). Tanto o PGC-1α como o PGC-1β podem apresentar funções complementares ou sobrepostas, essencialmente em tecidos oxidativos, como o cérebro, o coração, o tecido adiposo e o músculo esquelético. Por sua vez o PRC é expresso em todos os tecidos.

O PGC-1α é um dos membros mais estudados da família do PGC-1, sendo induzido de uma forma especifica para cada tecido, em função de fatores como o exercício, o jejum e a exposição

ao frio. Está ainda diretamente envolvido na biogénese mitocondrial e na destoxificação de espécies reativas de oxigénio. Este membro da família PGC-1 pode ser expresso sob a forma de diversas isoformas, que podem resultar na substituição do promotor do gene usado (proximal ou distante) e/ou de *splicing* alternativo, dependendo do estímulo ao qual a célula é sujeita. Cada isoforma pode apresentar funções distintas e ser específica de determinados tecidos. O PGC-1α1, inicialmente apenas conhecido como PGC-1α, foi a primeira isoforma a ser descoberta e corresponde ao transcrito canónico. Mais ainda, modificações pós-tradução, tais como a fosforilação, acetilação/deacetilação, SUMO-ilação e metilação, parecem estar envolvidas na modulação da atividade deste co ativador.

Estudos revelaram uma redução da expressão do PGC-1α1 com o envelhecimento. Por outro lado, a sua ativação previne a perda de neurónios, em modelos celulares da DP. Outros estudos conseguiram ainda relacionar mutações genéticas, associadas ao desenvolvimento da DP, com a diminuição dos níveis de expressão do PGC-1α1. Mutações no gene da parquina, que levam à perda da sua função, podem promover a repressão da transcrição deste co ativador através da acumulação da PARIS, um substrato de interação com a parquina.

Dado que não foram ainda identificados no PGC-1α1 domínios funcionais de ligação ao DNA nem a ligandos, a sua intervenção farmacológica torna-se um desafio. Assim, a estabilização deste co ativador poderá possibilitar o desenvolvimento de novas abordagens terapêuticas contra a neurodegenerescência.

Através de um estudo realizado pelo Dr. Jorge Ruas e colaboradores, em que procederam à realização de um *high-throughput screening*, baseado em modelos celulares, foi identificado um grupo de compostos químicos com capacidade de ativar e estabilizar o PGC-1α1 em culturas de adipócitos do tecido adiposo castanho. A capacidade destes compostos para estabilizarem o PGC-1 foi avaliada através da medição dos níveis de expressão proteica deste co ativador, assim como dos níveis de expressão relativos do mRNA dos genes regulados pelo mesmo e ainda pela medição da respiração mitocondrial, no mesmo modelo celular.

Desta forma, com base no estudo anterior, o objetivo do presente projeto assenta na validação, num sistema celular neuronal, de onze moléculas que foram previamente identificadas como estabilizadoras do PGC-1α1 e selecionadas para validação no sistema celular aqui descrito. O processo de validação foi decomposto em: seleção do modelo celular mais adequado; *screening* dos compostos, recorrendo a ensaios de viabilidade celular e à avaliação dos níveis de expressão relativos do mRNA de genes regulados pelo PGC-1α1; e à avaliação dos efeitos de cada composto selecionado, num modelo celular da DP. Nesta avaliação foram testados novamente os níveis de expressão relativos do mRNA de genes regulados pelo PGC-1α1 e outros fatores

como a influência destes compostos na viabilidade celular, nos níveis de produção de ATP e na produção de espécies reativas de oxigénio, no modelo celular da doença. A capacidade protetora destes compostos, face a um insulto com 1-metil-4-fenilpiridina (MPP+), nestas condições foi também avaliada.

Dos onze compostos, cinco foram selecionados como moduladores efetivos de genes regulados pelo PGC-1α1, numa linha celular de neuroblastoma de ratinho (células N2a). Após pré-condicionamento das células com os compostos e tratamento com MPP^+, alguns dos compostos selecionados promoveram o aumento dos níveis de ATP e de viabilidade celular, recuperando os níveis do controlo. Subsequentemente, alguns destes compostos mostraram ainda uma tendência para aumentar os níveis relativos de mRNA de genes como o da UCP1 (proteína desacopladora localizada nas mitocôndrias, que leva ao desacoplamento de eletrões da cadeia transportadora de eletrões e que, de entre as suas diversas funções se encontra envolvida na produção de calor, em adipócitos e na destoxificação de espécies reativas de oxigénio). O NRF-1, associado à respiração mitocondrial e o Glut-4, membro dos transportadores de glucose, correspondem também a outras classes de genes que pareceram aumentar na presença de alguns dos compostos selecionados.

Os resultados do presente estudo revelaram ainda que um pequeno grupo dos compostos testados parecem ter efeitos protetores em células tratadas com MPP^+, possivelmente por promoverem a estabilização do PGC-1α1. No caso particular de um dos compostos testados, o PGC-1α1 parece ser ativado pela via do cAMP/p-CREB/CRE, uma das principais vias de ativação deste co ativador. Apesar de os outros compostos não terem demonstrado alterações nesta via, poderão estabilizar ou ativar o PGC-1α1 através de vias alternativas. Uma das hipóteses é que estes compostos possam promover modificações pós-tradução responsáveis por regular tanto a estabilidade como a função e localização deste co ativador.

Dado que o mecanismo de ação destes compostos não é conhecido, é de extrema importância avaliar a sua capacidade de estabilizar o PGC-1α1 em diferentes sistemas celulares. Uma vez que a atividade biológica deste co ativador depende da presença de fatores de transcrição específicos, a sua estabilização pode não ser suficiente para a sua ativação nos diferentes sistemas celulares.

Através dos diversos estudos que envolvem o PGC-1α tem-se vindo, cada vez mais a realçar o papel preponderante deste co ativador em diversos tecidos, com maior relevância para os tecidos oxidativos. Desta forma, encontrar compostos capazes de modular e estabilizar este co ativador, mantendo os seus níveis fisiológicos nestes tecidos é de extrema relevância, de forma

a possibilitar o desenvolvimento de estratégias terapêuticas comuns a patologias de diferentes origens, em que o PGC-1α poderá estar envolvido.

Palavras-chave: Doença de Parkinson; MPP^+; estabilizadores do PGC-1α1; *screening*.

ACKNOWLEDGMENTS

Gostaria de começar por agradecer à Prof.ª Doutora Cecília Rodrigues, coordenadora do mestrado em Ciências Biofarmacêuticas, em que estive inscrita nos últimos dois anos e investigadora principal no grupo de investigação *Cellular Function and Therapeutic Targeting*, no qual estive inserida neste último ano a realizar a minha dissertação de mestrado. Muito obrigada pela orientação ao longo de todo o meu percurso neste mestrado e disponibilidade no esclarecimento quer de questões científicas, como de outras questões relacionadas com a faculdade e o mestrado.

Ao Prof. Doutor Jorge Ruas, meu orientador, por na fase final do meu trabalho me ter ajudado a interpretar os meus resultados de uma perspetiva diferente e mais motivadora.

Um enorme e especial agradecimento à Andreia, minha coorientadora, por tudo! Foste uma "santa"! Não tenho palavras para descrever o quanto agradecida estou pelos nossos caminhos se terem cruzado e por todos os esforços que puseste neste meu percurso, para que o conseguisse finalizar com sucesso. Obrigada pela tua sinceridade ao longo deste período e por sempre que foi preciso me relembrares que é preciso continuar a lutar. "Não desiste, insiste" é uma das tuas muitas frases que nunca vou esquecer e que tenho a certeza, vão sempre fazer parte do meu modo de pensar, para me tornar uma pessoa e uma profissional melhor. Quero ainda agradecer-te por todas as boleias até à outra margem e por todo o companheirismo. Neste percurso foste uma excelente profissional, coorientadora, companheira de bancada e amiga. Vou sentir saudades, em especial dessa tua memória de "peixinho dourado", como dizes, que sempre nos fez rir. Muito obrigada!

Um especial agradecimento à Prof.ª Doutora Maria João Gama, em primeiro lugar por me ter acompanhado e ajudado sempre no meu percurso neste mestrado, desde a disciplina de Projeto I, mostrando sempre total disponibilidade para me receber no seu gabinete e para me esclarecer qualquer dúvida. Em segundo lugar e algo que nunca vou esquecer, agradecer também a forma bem-disposta e positiva como sempre tentou levar as situações comigo, tentando sempre fazer-me ver o lado positivo das coisas, com a frase que eu nunca vou esquecer: "Não stresses, melher!".

À Prof.ª Doutora Elsa Rodrigues por toda a disponibilidade que demonstrou em ajudar-me, sempre que foi necessário, nas questões científicas e pela paciência ao ensinar-me alguns dos

primeiros passos dentro de uma sala de cultura e na manipulação de células. Agradecer também pela boa disposição, capaz de contagiar os que a rodeiam.

À Maria João Nunes, também pela boa disposição dentro do laboratório, por toda a ajuda e esclarecimentos que me foste prestando ao longo deste meu pequeno percurso e ainda por me ajudares a crescer e a tornar-me numa pessoa mais cuidadosa no meu trabalho.

À Prof.ª Doutora Margarida Castro-Caldas por sempre se mostrar prestável e disponível a ajudar-me e por participar muitas vezes na discussão de resultados e dúvidas que foram surgindo ao longo deste projeto.

Queria ainda agradecer a todos os elementos do grupo CellFun por toda a boa disposição e momentos de descontração. Agradeço também toda a ajuda que todos sempre me disponibilizaram para resolver questões científicas e me explicarem as boas práticas laboratoriais. Obrigada também por me fazerem aprender a cerca de outros temas, através dos vossos *lab meetings*.

Ainda dentro do grupo CellFun, um especial agradecimento às minhas colegas e amigas Rita Almeida e Viviana Ciraci por todo o apoio que me deram nesta fase tão importante e stressante, para mim. Obrigada por me fazerem rir, por me acompanharem e por me ouvirem, sempre que estava mais desmotivada. Obrigada pelos jantares e bons momentos que me proporcionaram, dentro e fora do CPM. Acima de tudo, obrigada pelo vosso companheirismo e amizade! Espero que apesar de tudo, perdure.

À Inês Caria, minha companheira de secretária e única mestranda a tempo inteiro, tal como eu, que me fizeste muitas vezes companhia tanto junto à secretária como no laboratório. Foi bom ter alguém na mesma situação perto de mim para poder partilhar preocupações e receios, ao estilo de quem nunca passou por eles.

À Daniela Costa, um grande e especial agradecimento, por tudo…por tudo o que me ensinaste ao longo deste percurso, no laboratório; por sempre estares disposta a ouvir-me e dar-me conselhos; por me teres dado uma perspetiva diferente da vida e da ciência. Ajudaste-me a crescer, durante este processo. Obrigada por tentares fazer com que gostasse de *metal*, mas para além de tudo isto, muito obrigada pela tua amizade e por teres sido das primeiras pessoas a integrar-me neste grande grupo que é o CellFun.

Queria também agradecer aos meus colegas de curso, em especial à Rita Manguinhas e à Rita Costa, pois este percurso não podia ter sido feito sem vocês. As minhas colegas de grupo, com

quem passei momentos muito importantes e divertidos. Obrigada pela vossa amizade e por me terem ensinado a gostar de estudar em grupo!

Um agradecimento muito especial a toda a minha família. À minha mãe por todo o apoio e força que me tem dado, não apenas no decorrer desta fase, mas durante toda a minha vida, incitando-me sempre a continuar o meu percurso e a lutar pelo que sempre me fazia feliz, consciencializando-me da ponderação necessária e associada a importantes decisões. Considero-te parte da minha primeira linha de defesa, pois és sempre das primeiras pessoas a quem recorro para desabafar, quer seja sobre frustrações, quer seja de sucessos. Ao meu pai, também por todo o apoio, por sempre te mostrares disponível a ouvir-me, especialmente nos momentos mais frustrantes do meu percurso. Obrigada por teres tentado sempre entender aquilo que faço em laboratório e tentares sempre fazer perguntas a cerca do meu trabalho, sem nunca te mostrares enfadado. Aos dois, obrigada por acreditarem em mim e me darem força para continuar. Aos meus irmãos, Ricardo e Tiago, que apesar de estarem longe sempre que precisei conseguiram apoiar-me e dar-me força, cada um na vossa maneira especial de se expressarem, que significa muito para mim. Ao Jorge, pelo apoio, por sempre me defender e, acima de tudo, pela boa disposição que sempre me contagiou, mesmo nos momentos mais *stressantes* e ansiosos. À Catriona, pela preocupação, pela motivação constante e por sempre se mostrar disposta a ajudar-me. Aos meus tios, Filomena, Tó, José António e João Paulo por sempre se disponibilizarem a ajudar-me e a aconselhar-me, independentemente do que eu poderia precisar. Todos vocês, cada um à sua maneira, me ajudou e me permitiu percorrer este percurso e terminá-lo com sucesso.

As minhas últimas palavras de agradecimento vão para o André o meu companheiro de vida e maior cúmplice. Quero agradecer-te por tudo, pelo companheirismo, pela tua amizade, compreensão e paciência para lidares com as minhas frustrações e por saberes sempre como me ajudar a ultrapassá-las. Obrigada por me fazeres rir, ajudando-me a descontrair e por tentares sempre motivar-me.

TABLE OF CONTENTS

FIGURES

TABLES

ABBREVIATIONS

AMP	Adenosine monophosphate
ATP	Adenosine triphosphate
BAT	Brown adipose tissue
BBB	Blood-brain barrier
cAMP	Cyclic adenosine monophosphate
cDNA	Complementary DNA
CPT1α	Carnitine palmitoyltransferase 1α
CRE	cAMP response element
CREB	cAMP response-element binding protein
Cyt C	Cytochrome C
DA	Dopamine
DAT	Dopamine transporter
DEPC	Diethyl pyrocarbonate
DMEM	Dulbecco's Modified Eagle Medium
DMSO	Dimethyl sulfoxide
DNA	Deoxyribonucleic acid
DRP1	Dynamin-related protein
EEF	Eukaryotic elongation factor
ER	Endoplasmic reticulum
ERR	Oestrogen related receptor
ETC	Electron transport chain
FBS	Fetal bovine serum
Glut-4	Glucose transporter type 4
LDH	Lactate dehydrogenase
L-Dopa	Levodopa
MPP^+	1-methyl-4-phenylpyridinium
MPTP	1-methyl-4-phenyl-1,2,3,6-tetrahydropyridine
mRNA	Messenger RNA
mtDNA	Mitochondrial DNA
MTT	Methylthiazolyldiphenyl-tetrazolium bromide
NADH	Nicotinamide adenine dinucleotide
NRF	Nuclear respiratory factor

PARIS	Parkin interacting substrate
PBS	Phosphate buffered saline
PCR	Polimerase chain reaction
PD	Parkinson's Disease
PGC-1α	PPARγ coactivator1α
PINK1	PTEN-induced putative kinase 1
PPAR	Peroxisome proliferator-activated receptor
PTEN	Phosphatase and tensin homolog
PTMs	Post-translational modifications
RedoX	Reduction/Oxidation reactions
RNA	Ribonucleic acid
ROS	Reactive Oxygen Species
RT-qPCR	Reverse Transcription quantitative PCR
SDS	Sodium dodecyl sulphate
SIRT1	Sirtuin 1/ Silent information regulator 1
SN*pc*	*Substantia nigra pars compacta*
SREBP1c	Sterol regulatory element-binding protein 1c
TBS	Tris-buffered saline
TBS-T	TBS tween-20
Tfam	Mitochondrial transcription factor A
TH	Tyrosine hydroxylase
UCP	Mitochondrial uncoupling protein
UPS	Ubiquitin-Proteasome system
XBP1s	X-box-binding protein 1 s

I. INTRODUCTION

1. Parkinson's Disease

Parkinson's disease (PD) is the second most prevalent neurodegenerative disorder, after Alzheimer´s disease, affecting primarily, the central nervous system[1]. Its age of onset ranges from 55 to 60 years old with an incidence of 20 patients per 100,000 people worldwide. Since it is an age-related progressive disease its incidence increases significantly by the age of 70, affecting 120 patients per 100,000 people worldwide[2]. PD prevalence is higher in men, since it is believed that the female hormone oestrogen confers protective effects[1].

1.1. Symptomatology of PD

Symptomatically, PD is characterized by the appearance of a diverse array of symptoms, both non-motor as well as motor symptoms. Non-motor symptoms have extra-striatal effects and often correspond to gastrointestinal and olfactory disorders, sleep disturbances, autonomic dysfunction, depression and cognitive impairment[3,4]. Motor symptoms, can include resting tremor, rigidity, postural instability, balance impairment, bradykinesia and hypokinesia[4] (i.e. slowness and difficulty in movement and in movement initiation, respectively)[5].

In a first stage of the disease some of the non-motor symptoms start to develop. At this stage, PD is very difficult to diagnose, since these symptoms are also commonly associated with aging. In a second stage, along with the non-motor symptoms, motor symptoms start to appear. Since these are characteristic of this pathology, when they are noticed, diagnostic becomes easier with the clinical observation of, at least four of the fundamental motor signs[6]. However, at this point in disease progression, approximately 80% of the putamenal dopamine is depleted and 60% to 70% of all *substantia nigra pars compacta* (*SNpc*) dopaminergic neurons have already been lost[2] (Figure I.1.).

1.2. Etiology and Pathogenesis of PD

Parkinson's disease can be classified, according to its origin, as sporadic or familial PD. Sporadic PD, also known as idiopathic, is often developed during aging and/or from prolonged exposure to some toxic compounds, such as herbicides (e.g. paraquat), pesticides (e.g. rotenone) and toxic solvents[1]. These promote damaging alterations in cellular functions, predominantly at the mitochondrial level[7]. On the other hand, familial PD arises in general from a genetic predisposition for the development of this disorder, caused by PD-associated gene mutations[8].

The discovery of these mutations helped elucidating the main molecular pathways involved in the development and progression of PD. However, when combined with environmental factors, a more complex understanding of the disease emerges, suggesting common signalling pathways in both forms, although triggered by different factors.

To date, eighteen PD-related genetic loci, termed PARK1-18[9] have been identified. The most common mutations are described in Table I.1.

Table I.1. Most common PD-associated gene mutations and mode of inheritance. (Adapted from Winklhofer & Haass[4])

PD Locus	Gene Product	Mode of Inheritance
PARK1/4	α-Synuclein	Autosomal Dominant
PARK2	Parkin	Autosomal Recessive
PARK 5	UCHL1	Autosomal Dominant
PARK6	PINK1	Autosomal Recessive
PARK7	DJ-1	Autosomal Recessive
PARK8	LRRK2	Autosomal Dominant
PARK9	ATP13A2	Autosomal Recessive

As shown in Table I.1., mutations associated with the monogenic familial forms of PD can be inherited either by an autosomal dominant or autosomal recessive form. Since sporadic and familial forms of PD share some important clinical, pathological and biochemical characteristics, the discovery of these monogenic familial forms also helped on the understanding of the pathology of the sporadic form of the disease [4].

The major hallmark of PD is the death of dopaminergic neurons in the *SNpc*, with consequently decreased levels of dopamine in the *striatum* (Figure I.1.). Along with this phenomenon there is the emergence of Lewy bodies (Figure I.1.C), which result from the aggregation of α-synuclein with other proteins and components, such as ubiquitin, neurofilaments[10] and molecular chaperones[11]. This aggregation process initiates with the conversion of the soluble unstructured monomeric α-synuclein into a partially soluble oligomeric nuclei and a rapid elongation and gathering into insoluble mature fibrils[12]. The accumulation of mature fibrils in neuronal cells is thought to confer neuroprotection, since it is believed that the true toxic forms of α-synuclein are the soluble oligomeric intermediates promoting cytotoxicity and leading to neuronal pathogenesis. In order to protect the cells, defence mechanisms presumably promote

the elongation, forming fibrils which accumulate and can be detected in *postmortem* PD brain samples[13,14]. The appearance of these proteinaceous inclusions, called Lewy bodies, is thought to occur years before the death of neurons and therefore, before the symptomatic stage of the disease starts to develop[15]. Mitochondrial dysfunction, oxidative stress, apoptosis, autophagy and chronic neuroinflammation represent other cellular and molecular pathways, whose malfunction also contribute to PD progression[16].

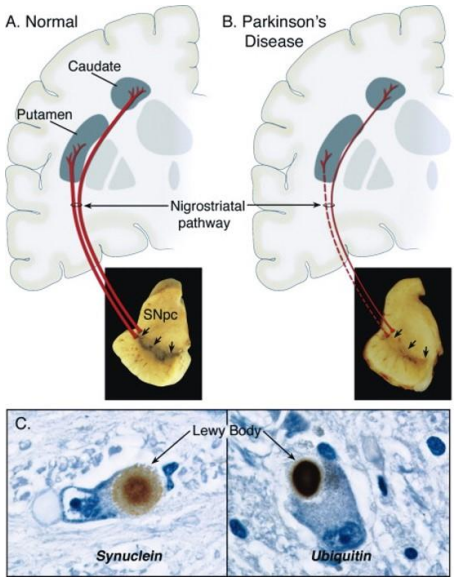

Figure I.1. Brain regions affected in Parkinson's disease. The main affected brain regions in PD are the midbrain, in particular the *substantia nigra pars compacta (SNpc)*, due to death of dopaminergic neurons and consequently the basal ganglia where the *striatum* exhibits decreased levels of dopamine, particularly at the putamenal subregion. Depicted here is a schematic representation of the normal nigrostriatal pathway (A) and of a degenerated nigrostriatal pathway (B), as occurs in PD. The photographs demonstrates the normal pigmentation of the *SNpc*, produced by neuromelanin (A) that is lost in PD brains (B). Red arrows indicate the nigrostriatal pathway. Immunohistochemical staining of Lewy bodies (C) reveals immunoreactivity for α-synuclein and ubiquitin (adapted from Dauer, W. *et. al* [2]).

1.3. Current Therapeutic Strategies in PD

Although there are already some therapeutic approaches that ameliorate and delay some of the motor features, most of the available therapies are symptomatic and unable to prevent disease progression. Therefore, it is of critical importance to find new and more effective therapies as well as possible biomarkers to detect the disease at earlier stages.

Since PD is a disease with a multifactorial etiology affecting multiple pathways and neurological processes, both at cognitive and motor levels, the actual best approach for retardation of its progression is based on polypharmacy[18]. The most common therapy used is

the administration of Levodopa (L-Dopa), which is a dopamine (DA) precursor enabling the increase of brain dopamine levels. Although many therapies have been discovered throughout the years, L-Dopa remains the best available pharmacological approach for clinical symptomatic relief. This DA precursor has the advantages of being relatively cheap and of crossing the blood-brain barrier (BBB). Moreover, L-Dopa is very effective in ameliorating motor symptoms, such as akinesia, bradykinesia, rigidity and partial response to tremor. However, this therapy is not efficient against non-motor features, such as hallucinations and cognitive impairment and cannot retard disease progression nor reverse the associated biochemical alterations. Furthermore, response to L-Dopa medication starts to be affected, after long-term usage by the patients, resulting in the deterioration of some of the most common motor functions, such as speech, gait, posture and balance instability, also presenting fluctuations in the motor features first described to be ameliorated by this therapy.

Therefore, a combined therapy with different drugs targeting other receptors, such as Monoamine Oxidase B (MAO-B) and Catechol-O-Methyl Transferase (COMT) inhibitors, as well as dopamine receptor agonists and anticholinergic drugs are often considered.

Dopamine receptor agonists rely on the direct stimulation of the post-synaptic DA receptors, in the *striatum*[19]. This family of drugs is able to delay the onset of motor features and in some cases, when in combination with L-Dopa, it is able to reduce by 50% the chance of developing motor function complications, when compared with L-Dopa monotherapy[20]. However, this therapy also contributes to the occurrence of side effects, namely sleep disturbances, cognitive problems, confusion and hallucinations, especially in older patients[6].

MAO-B and COMT inhibitors increase plasma half-life of DA and its precursor, L-Dopa, by hampering DA conversion and metabolization of L-Dopa, respectively. Additionally, MAO-B inhibitors ameliorate motor symptoms and delay the addition of L-Dopa as a therapy, by several months[21].

Anticholinergic drugs are the cheapest and oldest therapy approaches against parkinsonian symptoms. These drugs are usually used in combination with L-Dopa, although they are only effective against mild symptoms of tremors and rigidity[6].

Nevertheless, a great number of other pharmacological approaches are being studied, in order to find the most effective in halting disease progression.

Despite pharmacological therapies, there are also surgical approaches against PD, namely infusion techniques and deep brain stimulation (DBS). Infusion systems usually work as continuous administrators of dopaminergic drugs and apomorphine, a strong dopamine receptor agonist that is usually administered in combination with other antiparkinsonian drugs.

However, in addition to being extremely expensive it can cause local inflammatory responses at the subcutaneous administration site[22]. Conversely, DBS of the subthalamic nucleus was found to be the most effective approach to control levodopa-sensitive off symptoms, induced dyskinesias and tremors, being this the safest area of the brain to carry-out the procedure. This is considered a highly effective therapy for patients who suffer from advanced PD[23]. Although this procedure has no effect in halting disease progression, it appears to increase the patient quality of social and day-to-day life.

2. Mitochondrial dysfunction in Parkinson's disease

2.1. Mitochondria in cellular function

Mitochondria are vital organelles that play crucial roles in cellular homeostasis. These include regulation of calcium release, cell death (through cytochrome-c release) and energy production (through the mitochondrial respiratory chain and oxidative phosphorylation). A common by-product of oxidative phosphorylation is the production of reactive oxygen species (ROS). ROS are part of the normal cellular signalling processes, but can also lead to mitochondrial dysfunction upon accumulation[24].

Although mitochondria are semiautonomous organelles, they still depend on nuclear gene expression, which provides the majority of elements necessary for its metabolic systems and molecular architecture[25,26]. One such system is a complex structure known as the electron transport chain (ETC) and the ATP synthase complex (Figure I.2.). The four complexes (I-IV) composing the ETC are responsible for catalysing the electron transfer of reducing equivalents, from high-energy compounds produced in the Krebs cycle into oxygen, through a series of coupled redox reactions. This electron transfer leads to an electrochemical gradient, or proton-motive force, through the inner mitochondrial membranes, resulting in ATP synthesis by ATP synthase (complex V)[27]. This force is created through a pH gradient (ΔpH) and an electrical potential (Δψ), leading to ATP production, as protons re-enter the matrix through complex V[28]. This process constitutes the core of mitochondrial respiration and is known by oxidative phosphorylation (Figure I.2.).

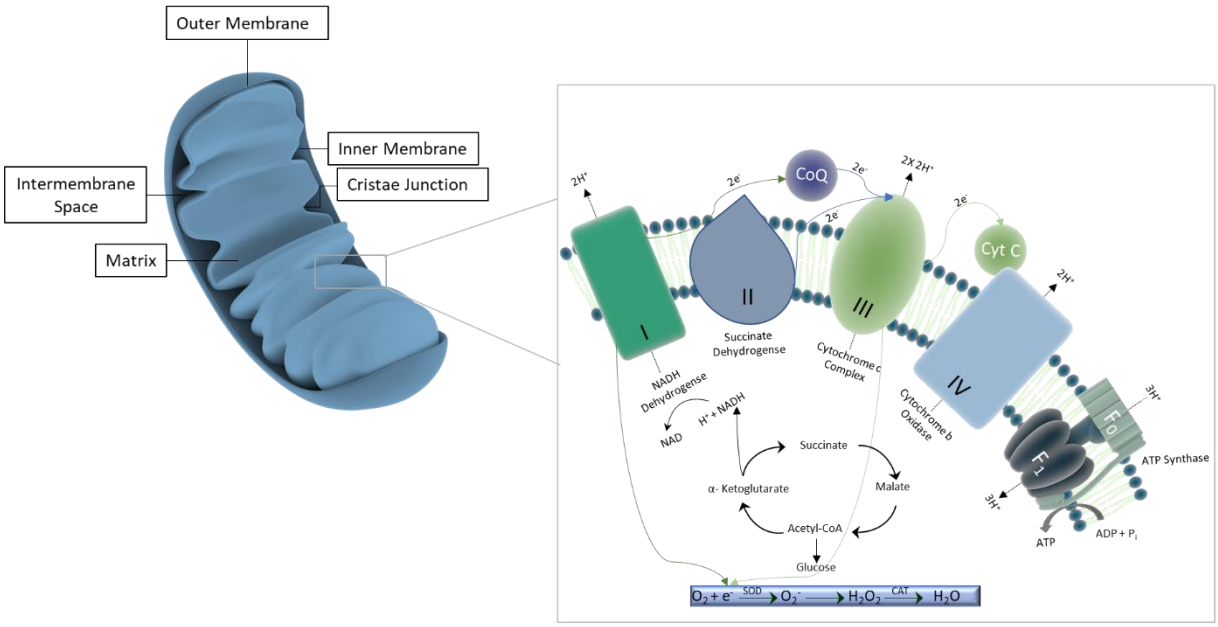

Figure I.2. Structural composition of mitochondria and the electron transport chain. Mitochondria are composed of two membranes, an outer and an inner membrane, an intermembrane space separating both membranes and a matrix where the mitochondria genetic material is present. The electron transport chain (ETC) is embedded in the inner membrane of the mitochondria and is composed of enzymatic complexes I-IV, responsible for catalysing the electron transfer of reducing equivalents into oxygen, through a series of coupled redox reactions. The reducing equivalents, namely NADH and $FADH_2$, enter the ETC at complexes I and II, respectively, and their electrons are transferred from complex to complex, until they reduce oxygen into water, in complex IV, creating an electrochemical gradient. This will ultimately result in the synthesis of ATP by ATP synthase (complex V). During this process a series of different ROS are produced in the mitochondrial matrix and consequently converted by specific enzymes into water. CoQ as well as Cyt C are the main molecules responsible for the electron transfer between complexes. CoQ – Co-enzyme Q10; Cyt C – Cytochrome C; O_2^{2-} - Superoxide anion; SOD – Superoxide dismutase; CAT – Catalase (adapted from Dorn II[29]).

Mitochondrial respiration can be divided in two types: ATP turnover and basal proton leak. ATP turnover, or coupled respiration, corresponds to the fraction of mitochondrial respiration coupled to ATP production (described above) and is sensitive to oligomycin (an ATP synthase inhibitor). On the contrary, basal proton leak, or uncoupled respiration, is insensitive to oligomycin. As its name implies, this type of respiration results from the leak of protons through anion carriers across the mitochondrial inner membrane, uncoupling cellular respiration from ATP production and thus, generating heat. Although the relevance of this phenomenon is quite cell type-specific, it is estimated that approximately 20% of mitochondrial respiration, in mammals, is due to this proton leak[30,31]. Importantly, there is a family of uncoupling proteins

(UCP) that facilitate proton leak, which is thought to have an important role in the protection against ROS and in the modulation of the cellular ATP levels[32,33].

Both, coupled and uncoupled, mitochondrial respiration are so important to cellular function that metabolic efficiency depends on the balance between ATP turnover and proton leak. Thus, when total mitochondrial respiration is altered, metabolic efficiency can only be preserved if the two fractions are affected in a similar way[30].

2.2. Mitochondrial dynamics

Mitochondrial function critically depends on their structure and localization that in turn are dependent on mitochondrial dynamics. Mitochondrial dynamics comprises the processes of fission and fusion, which play important roles in neurotransmission, synaptic maintenance and neuronal survival[34]. Fusion is thought to be essential for normal mitochondrial function as it plays a protective role, by providing a possibility to mix contents between the different mitochondria existent in the cell. This process allows protein complementation, mitochondrial DNA (mtDNA) repair and equal distribution of metabolites[35]. On the other hand, fission enables an equal segregation of these organelles into daughter cells, during cell division and enhances mitochondrial distribution along cytoskeletal tracks. Moreover, this process allows the detection of damaged segments of mitochondria, targeting them to the autophagic process, called mitophagy[36].

Mediating these two processes, there are fusion and fission promoting proteins which mainly correspond to guanosine-triphosphatases (GTPases) and are part of the dynamin family. Mitofusin 1 and mitofusin 2 (MFN1 and MFN 2) along with optic atrophy 1 (OPA1) are responsible for regulating the fusion process[37]. While MFN1 and MFN2 are mainly responsible for promoting fusion of the outer mitochondrial membrane (OMM) by forming homo and hetero-oligomeric complexes, OPA1 mediates the fusion of the inner mitochondrial membrane (IMM) [38]. Dynamin-related protein 1 (DRP1) is a GTPase that is recruited from the cytosol to the OMM, to promote fission of mitochondria[39]. DRP1 interacts with mitochondrial receptors proteins, such as mitochondrial fission protein 1 (Fis1), mitochondrial fission factor (MFF)[40] and mitochondrial dynamics proteins that help on the process of mitochondrial division[41].

Hence, mitochondria are dynamic organelles that meet cellular energy demands by responding to diverse stimuli, from developmental to environmental signals[25].

2.3. Mitochondrial dysfunction

During aging many cellular processes suffer alterations, such as morphological changes, increased mitochondrial damage and ROS accumulation, DNA damage and telomere shortening. Aging is also associated to decreased cellular turnover and impaired proteostatic mechanisms which consequently lead to endoplasmic reticulum (ER) stress and increased amount of misfolded proteins. This in turn, leads to accumulation of protein aggregates both in the cytosol and in the lysosomal system[42]. Altogether, these events can result in oxidative damage to the mtDNA as well as proteins and lipids, consequently disturbing the redox signalling pathways[28]. In the brain, these events can ultimately lead to degeneration of neuronal cells and the development of neurodegenerative diseases.

Due to absence of histones and less efficient repairing mechanisms than nuclear DNA, mtDNA is more vulnerable to the occurrence of mutations[4]. Furthermore, accumulation of ROS produced from oxidative phosphorylation is thought to induce mtDNA damage. The high copy number of mitochondrial DNA confers a protective effect and leads to genetic redundancy, allowing point-mutations or largescale deletions to co-exist with wild-type DNA, without negatively affecting the normal cellular function[43,44,45]. This process is known as heteroplasmy. However, clonal expansion and accumulation of somatic mtDNA mutations, associated with the aging process, can occur in several tissues, namely the brain, contributing to neurodegeneration[43,46,47].

Since several of the respiratory chain subunits are encoded by mtDNA, oxidative damage may negatively affect the ETC and, therefore, lead to a vicious circle of oxidative stress and bioenergetic failure, where each oxidative event compromises other cellular pathways that should be protecting the normal cellular function.

The superoxide anion (O_2^{2-}) is the first ROS to be produced in the mitochondrial matrix, during oxidative phosphorylation, due to electron transfer from complexes I and III. This anion is rapidly converted to hydrogen peroxide (H_2O_2) in a reaction catalysed by manganese dependent-superoxide dismutase (MnSOD). Furthermore, in the presence of metal ions, namely Fe^{2+}, H_2O_2 can also be converted into a highly reactive hydroxyl radical (HO·), through a chemical reaction known as Fenton reaction[4].

Moreover, mitochondrial dysfunction is not only characterized by the accumulation of ROS, but also by a consequent decrease in the ETC complex I enzyme activity, cytochrome-c release due to caspase-3 activation and formation of micropores in the mitochondrial membranes and,

ultimately to ATP depletion[24]. These reactive species not only lead to cellular damage but also activate cell death signalling pathways[48].

2.3.1. Mitochondrial dysfunction in Parkinson's Disease

Post-mitotic nerve cells, such as neurons, showed to be more susceptible to cumulative oxidative damage than proliferating tissues[49]. Additionally, nigral dopaminergic neurons are more vulnerable than other populations of neurons, exhibiting a higher basal rate of oxidative phosphorylation, increased levels of basal oxidative stress as well as higher density of axonal mitochondria and a more complex axonal arborization[50,51]. Dopamine oxidative metabolism, by monoamine oxidases, is thought to be one of the reasons for these differences between brain areas[52].

Furthermore, the iron content in the *SNpc* DA neurons was also shown to be higher, which may be due to the increased release from ferritin, caused by O_2^{2-} and/or from iron-sulfur proteins by peroxynitrite ($ONOO^-$) formation[52]. Additionally, the accumulation of H_2O_2 through the Fenton reaction in conjugation with the cytosolic monoamine oxidases and tyrosine hydroxylase (TH) activities leads to an amplification of the oxidative damage effect, resulting in defective detoxifying mechanisms, such as MnSOD and the glutathione system[49]. Additionally, both mechanisms were shown to be altered in PD patients. Furthermore, iron-mediated oxidative stress may promote the formation of partially folded α-synuclein intermediates, that are susceptible to aggregation[53].

Beyond the general markers of oxidative stress, such as high levels of oxidatively modified lipids, proteins and DNA that were all found in the *SNpc* of PD patients[54,55,56], respiratory complex I deficit appears to have some specificity related to the development of PD[49]. This impairment has been observed not only in the *SNpc* of PD patients, but also in peripheral cells, like fibroblasts[57], platelets and skeletal muscle[58,59], all of which were thought not to be affected in this pathology. Thus, these findings suggest a systemic ETC impairment[60,61].

Regarding complex I impairment and its specificity to PD pathology, in the 1970s, in the United States of America, young drug addicts started to develop a progressive and irreversible form of parkinsonism, after self-administering an illicit drug, intravenously[24]. Later, it was found that during the synthesis of a meperidine analogue a neurotoxic by-product had accidentally been generated. This by-product is known today as 1-methyl-4-phenyl-1,2,3,6-tetrahydropyridine (MPTP)[62,63]. Furthermore, one of these young adults also presented degeneration of the *SNpc*, without clearly exhibiting the presence of Lewy bodies. Confirmation of this discovery was obtained after other patients exhibit similar patterns upon MPTP self-administration[64].

Interestingly, both the short-term effectiveness and the long-term adverse effects of L-Dopa therapy in MPTP-treated patients and non-human primates were comparable to those in patients suffering from sporadic PD. With this knowledge it was possible to establish a MPTP monkey model for neuropathological, neurophysiological and preclinical therapeutic studies and later a similar model in mice[2].

MPTP is extremely lipophilic and is able to cross the BBB[65]. This neurotoxin binds mainly to astrocyte lysosomes[66] and is metabolized by monoamine oxidase B to the active toxic metabolite, 1-methyl-4-phenylpyridinium (MPP^+), which is not able to cross the BBB[52]. MPP^+ is then released to the extracellular space and rescued by dopaminergic neurons through the dopamine transporter (DAT)[67,68,69]. Its affinity to the DAT leads to its accumulation in neurons. Once inside the neurons, MPP^+ can pursue, at least three different pathways: it can either bind to the vesicular monoamine transporter 2 (VMAT2) and translocate to the synaptosomal vesicles, in a process that appears to be protective to cells, since this avoids its toxic action in the mitochondria[70]. MPP^+ can also remain in the cytosol and interact with cytosolic enzymes, especially the ones carrying negative charges[71] or, finally it can enter mitochondria through a process that involves an alteration in mitochondrial transmembrane potential[72].

By entering mitochondria, MPP^+ will inhibit complex I of the respiratory chain[73,72,74]. From this step forward, a series of cascade events will ultimately lead to neurodegeneration and cell death. This cascade includes decreasing ATP production and increasing ROS formation[75], inhibiting mitochondrial complexes III and IV[76], decreasing mitochondrial genes expression[77], affecting mitochondrial proteins, namely chaperones, metabolic enzymes, inner and outer membrane mitochondrial proteins[78], dopamine signalling, impairing the ubiquitin-proteasome system (UPS), calcium signalling, oxidative stress response and ultimately leading to cell death[79]. Altogether, these events will lead to the manifestation of the symptoms associated with PD, which are displayed in human patients and animal models[24].

As a consequence of oxidative phosphorylation inhibition, neurons start to rely on glycolysis for ATP production[52]. Curiously, it has been found that regulating the levels of cellular ATP via glycolysis attenuates MPP^+-induced toxicity and conversely, depriving cells from glucose exacerbates the toxic effect[80,81]. However, previous studies in neuroblastoma cells and in rat brain showed that at MPP^+ concentrations below 1 mM, its toxicity depends on glucose depletion, whereas at MPP^+ concentrations ranging from 1 to 10 mM, cells experience a metabolic collapse, switching from oxidative phosphorylation to glycolysis, consequently leading to cell death[82,83]. This suggests a biphasic mechanism involved in MPP^+ toxicity, where: at low concentrations depends on a DAT-mediated mechanism selective for DA neurons; and

at higher concentrations, an oxidative mechanism is triggered[83]. This metabolic shift in combination with the series of cellular events that occur in MPP^+/MPTP models and in PD patients, leads to the prospect of Parkinson's disease as a metabolic syndrome-like disorder[84].

2.3.2. Genetic contribution for mitochondrial dysfunction in PD

Upon discovery of the different monogenic forms of PD, several studies have revealed an interplay between the affected *loci*. A great relevance has been given to the ones inherited by an autosomal recessive mechanism, such as Parkin (PARK2), PINK-1 (PARK6) and DJ-1 (PARK7). Interestingly, these *loci* share mitochondrial-associated functions, namely in the maintenance of mitochondrial integrity[85,86,87].

The parkin gene encodes an E3 ubiquitin ligase. Mutations in this locus have been demonstrated to lead to alterations in protein solubility, leading to its aggregation and reduced ubiquitin-ligase activity[3].

Phosphatase and tensin homolog (PTEN)-induced putative kinase 1 (PINK1) gene encodes a serine/threonine kinase, localized in the mitochondria. It can be found either in the inner and outer membranes or in the intermembrane space[3,24]. In addition, PINK1 plays a key role in the maintenance of mitochondrial homeostasis and is known to phosphorylate the 75 kDa heat shock protein, which is a mitochondrial molecular chaperone that confers protection against oxidative stress[88].

As for DJ-1, it is known to encode a small protein, highly conserved amongst prokaryotes and eukaryotes. Although no specific function has been found for this protein[3], it is known to have a predominantly cytosolic localization, but can also be found in the nucleus and mitochondria[4]. It was also found that DJ-1 translocates to the matrix and intermembrane space of mitochondria after an increase in oxidative stress, impairing its degradation[24]. Additionally, overexpression of DJ-1 demonstrated to be protective against oxidative stress-induced damage, in neurons, while its deficiency led to more susceptible cells, under oxidative damage[4,89,90].

Once large deletions, in these three genes, have been found in patients with autosomal recessive parkinsonism, understanding their functions and interplay, under physiological and stress-induced conditions is of utmost importance, in order to pin-point them as therapeutic targets for the treatment of PD[3].

Each of these three genes have shown cytoprotective properties when overexpressed. PINK1 overexpression in human neuroblastoma cells, for example, stabilizes mitochondrial respiration networks, by regulating mitochondrial membrane potential and suppressing autophagy[91].

Regarding DJ-1, although it was initially identified as an oncogene, it has also shown neuroprotective effects under oxidative stress[92]. Finally, by overexpressing parkin, cells became more protected from ER and mitochondrial stress[93]. Accordingly, loss of parkin expression led to an increase in cellular vulnerability to stress and to mitochondrial impairments, in the striatum of parkin-null drosophila[94,95].

Undoubtedly, PINK1, DJ-1, and parkin play an important role in protecting cells against oxidative stress. Moreover, under physiological conditions, PINK1 and parkin promote the fission process in mitochondria, while inhibiting fusion[52]. Impairment or loss of either proteins lead to altered mitochondria morphology and DRP1-dependent fragmentation, changes in mitochondrial membrane potential and ultimately, to a decrease in ATP production[96,97].

Additionally, loss of DJ-1 promotes increased mitochondria fragmentation and autophagy, which can be reverted by PINK1 and parkin[98]. DJ-1 was also demonstrated to be involved in the degradation of misfolded proteins[99].

Although, parkin is thought to have an important role in mitochondrial biogenesis in combination with PINK1, accumulation of its substrates may contribute to dopaminergic neurodegeneration[100,101]. Parkin is responsible for regulating the levels of its interacting substrate, PARIS, *via* the UPS. PARIS was shown to accumulate in PD brains of patients and of models of inactive parkin[92, 102]. Peroxisome proliferator-activated receptor γ (PPARγ) coactivator-1α (PGC-1α) expression is regulated by PARIS through transcriptional repression. Therefore, although parkin and PGC-1α have shown to be protective against neurodegeneration, the parkin-PARIS-PGC-1α pathway may contribute to degeneration of DAnergic neurons, in PD, due to parkin loss of function. This leads to PARIS accumulation and repression of PGC-1α transcription, consequently causing alterations in mitochondria function and behaviour, under oxidative stress conditions (Figure I.3.)[102].

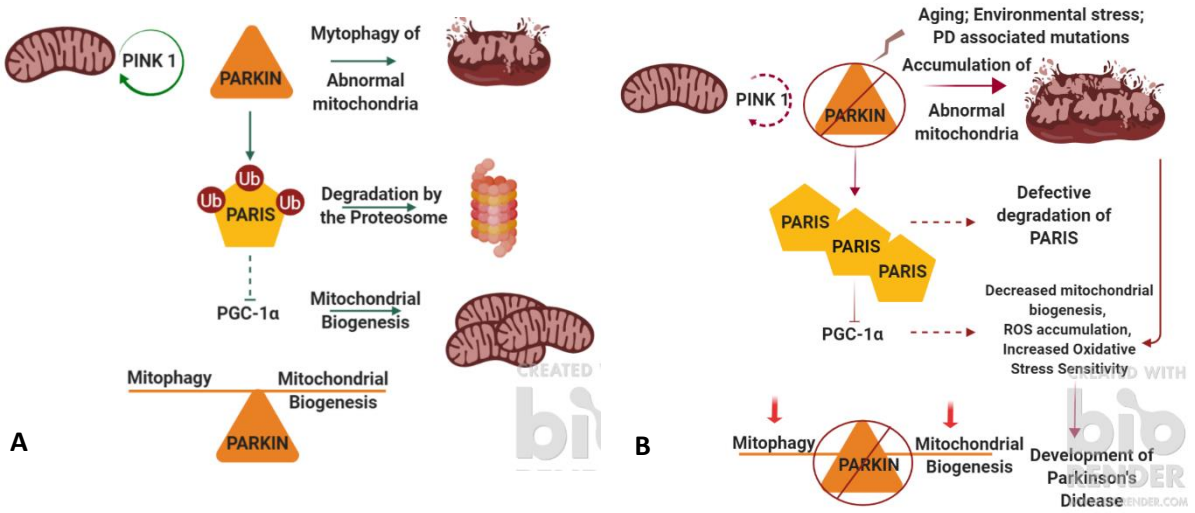

Figure I.3. Interplay between Parkin, PINK1 and PARIS and its influence in the maintenance of cellular integrity. On the left panel (A) it is depicted the events occurring under homeostatic conditions, where parkin is responsible for PINK1 normal function and for targeting PARIS to degradation by the UPS. Under physiological conditions, ubiquitination of PARIS allows PGC-1α expression, leading to mitochondrial biogenesis. On the right panel (B) it is represented the cellular events that occur upon parkin and PINK1 loss of function, where maintenance of mitochondria normal function is impaired. Parkin altered function also leads to accumulation of PARIS, direct repression of PGC-1α and consequent accumulation of damaged mitochondria, neurodegeneration and the development of Parkinson's disease (adapted from Chhangani & Mishra[103]).

2.4. Mitochondria and the ubiquitin proteasome system in Parkinson's disease pathogenesis

The UPS is responsible for the selective degradation of short-lived intracellular and plasma membrane proteins. In addition, it also plays an important role in the degradation of misfolded and damaged proteins[24].

Ubiquitin (Ub) conjugation involves the covalent attachment of one (monoubiquitination) or more ubiquitin molecules (polyubiquitination) to substrate proteins[104]. This link is formed between the C-terminal glycine residue of Ub and lysine residues of the substrate and depends on the successive action of the ubiquitin-activating enzyme (E1), the ubiquitin conjugating enzymes (E2) and the ubiquitin protein ligases (E3)[104,105].

The UPS is characterized by a multi-step catalytic process, that initiates with E1 enzyme activating Ub, in an ATP-dependent reaction. Subsequently, one of the E2 enzymes transfers the activated Ub from E1 to the substrate, catalysing the covalent attachment of Ub to a lysine residue in the substrate proteins, acting in concert with E3 enzymes, to determine the recognition of specific substrates [105,106,107]. The consecutive addition of activated Ub moieties

to internal lysine residues on the previously conjugated Ub molecule leads to the formation of a polyubiquitin chain that in a final step, will allow 26S proteasome to catalyse the degradation of the polyubiquitylated protein (more than four Ub molecules attached), releasing the ubiquitin for further reuse[108].

The UPS together with autophagy represent the two major mechanisms in the proteostasis control system, although autophagy enables cellular component degradation through a lysosomal dependent machinery.

This system largely contributes to the maintenance of mitochondrial homeostasis, by regulating the proteome and the process of mitophagy, where mitochondria renew themselves[109]. However, UPS dysfunction resulting in the accumulation of damaged and misfolded proteins is thought to participate in the death of dopaminergic neurons and eventually, in the development of Parkinson's disease (Figure I.4.)[110].

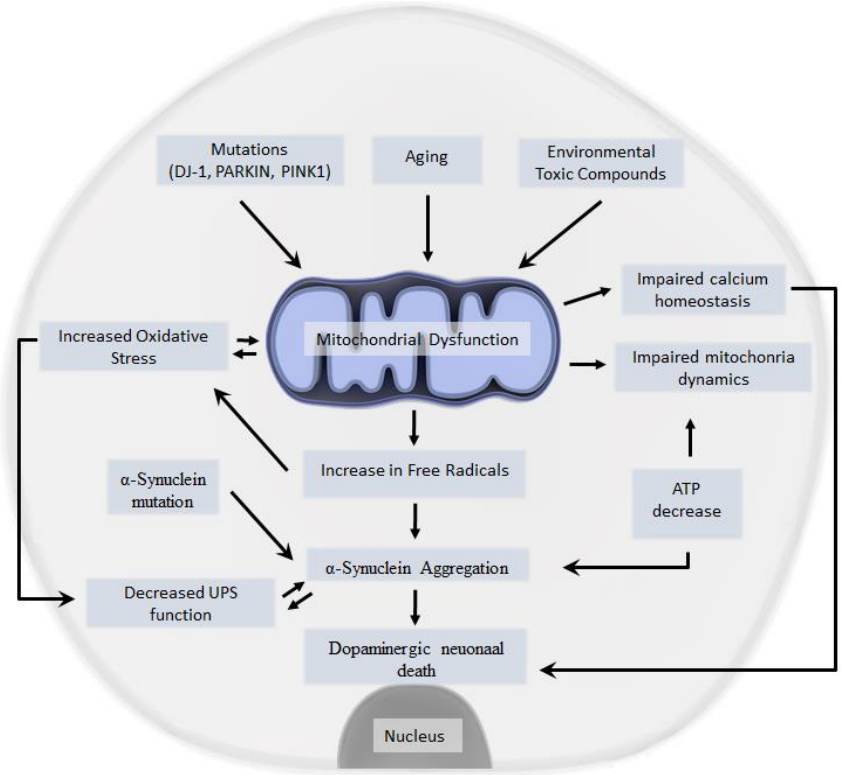

Figure I.4. Schematic representation of some of the cellular events that lead to mitochondrial dysfunction and Parkinson's disease development. Mitochondrial dysfunction is a key phenomenon involved in the pathogenesis of Parkinson's disease. PD-associated mutations, the process of aging and even environmental factors are the major responsible events for altered function of mitochondria. Increasing oxidative stress as well as impaired calcium homeostasis and impaired mitochondria dynamics, can either be responsible for or triggered by mitochondrial dysfunction. Examples of downstream events are the increase in the free radicals' content, α-synuclein aggregation, ATP decreased levels and UPS decreased function. Some of these events can, again, contribute to the dampening of mitochondrial function, leading to a vicious circle of events. All of these events will ultimately lead to dopaminergic neuronal death, contributing to PD pathology (adapted from Moon & Paek[24]).

3. PGC-1α – Roles in Cellular Function

The PGC-1 family of transcriptional coactivators have a variety of biological functions that tends to be tissue-specific. Almost all forms of the coactivator are strong regulators of cellular bioenergetics, through the regulation of genes involved in mitochondrial biogenesis and oxidative metabolism[111]. Furthermore, it is thought that this coactivator is able to modulate cellular and mitochondrial metabolism *via* mitochondrial biogenesis and organelle remodelling, through alteration of the intrinsic properties of mitochondria[111].

The PGC-1 family has three founding members encoded by distinct genes: PGC-1α, PGC-1β and PGC related coactivator (PRC). PGC-1 proteins possess no known intrinsic enzymatic

activities and their main function relies on interacting with different transcription factors and other coactivators, participating in different biological functions[111]. While PRC is ubiquitously expressed, PGC-1α and PGC-1β can present overlapping functions and are mainly expressed in oxidative tissues, including the brain, heart, kidney, muscle, liver, brown adipose tissue (BAT) and pancreas[112,113].

PGC-1α was the first member of the family to be identified in BAT cDNA library and shown to be a cold-inducible coactivator involved in adaptive thermogenesis[114]. BAT uses glucose and fatty acids in thermogenic futile cycles that help regulate body temperature[115]. Furthermore, PPARγ was discovered to have a specific role in BAT, while was being upregulated by a novel protein, upon exposure to cold[114]. This coactivator was named PGC-1α and it revealed high expression levels in BAT, under the same conditions. Moreover, its overexpression, in cultured muscle cells, induced UCP1 and a number of enzymes involved in oxidative phosphorylation[114].

The PGC-1α gene is expressed as several splicing isoforms with distinct functions. They result from alternation in the gene promoter used (proximal or alternative) and/or alternative splicing, depending on the stimulus that is given to the cell[116]. The combination of these two events generates PGC-1α-a, b and c[117], NT-PGC-1α a, b and c[118,119,120] and PGC-1α1, 2, 3 and 4[121]. Of note, PGC-1α-a is PGC-1α1 (previously PGC-1α, the original, canonical transcript), and NT-PGC-1αb is PGC-1α4. PGC-1α1 activation is modulated by post-translational modifications (PTMs) which include phosphorylation[122], deacetylation[123], small ubiquitin-like modifier (SUMO)-ylation[124] and methylation[125]. While deacetylation is responsible for activating PGC-1α transcription, acetylation, methylation and SUMOylation are responsible for the opposite effect. Phosphorylation, can induce or inhibit PGC-1α1 activity, depending on the kinase involved. PTMs allow specific targeting of genes, by PGC-1α1[111], as well as regulation of protein properties, such as stability, structure, function and localization[126]. Depending on the external signal different PTM patterns are induced leading to different cellular functions in a nuclear receptor (NR)-mediated manner[127,128]. These functions are directly related to regulation of cellular processes, including metabolism and differentiation[129]. PGC-1α1 is mostly induced by physiological cues like exercise, fasting and cold[130] and it is directly linked to cell detoxification of ROS and mitochondrial biogenesis[30,131,132] (Figure I.5.).

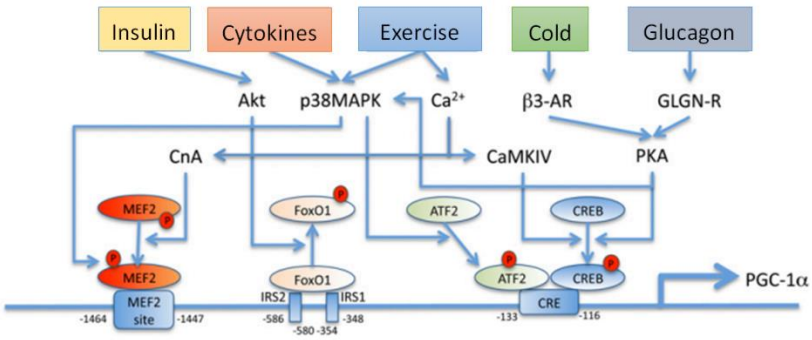

Figure I.5. Regulation of PGC-1α gene expression by different stimuli. Modulation of PGC-1α transcription involves distinct molecular pathways, that usually depend on the stimulus given to the cell and on the tissue context. Cold in adipocytes and fasting in liver cells, although through different types of stimulation, lead to activation of Protein Kinase A (PKA) that consequently induce phosphorylation of cAMP response element binding protein (CREB) that will bind to cAMP response element (CRE) on the PGC-1α gene promoter and induce its expression. Other stimuli, such as inflammation, oxidative stress and insulin levels are capable of promoting PGC-1α expression, not only through CRE, but also through Insulin Receptor Substrate 1 (IRS1) site and Myocyte Enhancer 2 (MEF2) site. Different stimuli can induce similar pathways, such as p38 mitogen-activated protein kinase (p38MAPK) that is induced by both inflammation response and exercise. Protein kinase B (Akt) pathway is thought to be activated through insulin, while Ca^{2+} signalling is believed to be induced by exercise. β3-AR – β3 Adrenergic Receptor; GLGN-R – Glucagon Receptor; CaMIV - Calcium/calmodulin-dependent protein kinase type IV; CnA – Calcineurin A; FoxO1 - Forkhead box protein O1; ATF2 – Activating transcription factor 2 (adapted from Fernandez-marcos & Auwerx[133]).

Furthermore, studies revealed that activation of PGC-1α1 allows the induction of other UCPs, in muscle cells, such as UCP2 and other different transcription factors, such as nuclear respiratory factors (NRFs), namely NRF-1 and NRF-2, peroxisome proliferator-activated receptors (PPAR α, β and δ) and oestrogen related receptors (ERRs), depending on the external stimulus[115]. ERRα, together with the above described NRFs, are responsible for regulating the expression of other nuclear-encoded mitochondrial genes, like cytochrome c (Cyt C), components of complexes I-V, and mitochondrial transcription factor A (Tfam)[115].

Since PGC-1α is not known to bind DNA or have ligand-binding domains, designing direct pharmacological intervention has remained a challenge. Thus, new strategies must be developed in order to induce this coactivator activity, either through gene transcriptional regulation, PTM or modulation of protein-protein interactions of binding partners[112].

3.1. Role of PGC-1α1 in the pathogenesis of Parkinson's disease

Overexpression of PGC-1α1 in animal models of PD has generated some positive results, since it decreases ROS, which significantly contribute to the pathogenesis of this neurodegenerative disorder[134]. Several studies have shown that PGC-1α1 expression is reduced with age. Although the precise mechanism behind the progressive loss of PGC-1α1 expression isn't known, it has been speculated that it could be related to the decrease in the expression levels of sirtuin 1 (SIRT1)[135], which is responsible for PGC-1α1 deacetylation[133]. This mechanism seems plausible since PGC-1α feeds forward on its own gene expression[136]. In line with this, administration of resveratrol decreases PGC-1α1 acetylation, leading to its activation and an increase in the expression of its downstream genes[137]. Activation of p53 through the telomere shortening process would also suppress transcription of this coactivator by binding to its promoter[138]. In addition, the presence of single nucleotide polymorphisms (SNPs) in the gene encoding PGC-1α (PPARGC1A) is associated with the development of several human diseases[112].

PGC-1α activation promotes expression of nuclear-encoded subunits of the mitochondrial respiratory chain, preventing dopaminergic neuron loss, in both genetic and toxin-induced cellular models of PD[139]. Activation of PPARγ through its agonist, pioglitazone has also demonstrated positive results in animal models of PD, with acute administration of MPTP. Namely, pioglitazone administration blocked dopaminergic neurodegeneration and reduced astrocyte and microglia activation. However, it was not able to reduce loss of TH-positive fibres, in the *striatum* and to avoid the decrease in dopamine levels[140].

Ppargc1a-null mice (whole body knockouts) exhibit increased sensitivity to oxidative agents, in the hippocampus and *SNpc*[131]. The same mouse model presented a decrease in neurite outgrowth, in the *striatum*, when compared to wild-type (wt) animals. This model also exhibited spongiform lesions, predominantly in the *striatum*, but also in the motor cortex, *SNpc* and hippocampus[141]. These data show that PGC-1α1 not only plays a significant role in regulating mitochondrial function but can also be important in regulating neuronal growth and function. Although, the comprise in neuronal growth could be caused by a deficit in energy production.

Figure I.6. depicts some of the ways by which PGC-1α1 has been reported to be involved in neurodegeneration. Stimulation of PGC-1α1 expression triggers a series of neuroprotective events, such as increased mitochondrial biogenesis and levels of ROS scavengers (e.g. SOD and catalase). This decreases ROS levels and reduces dopaminergic neuronal death. However,

when PGC-1α1 expression is impaired, cells become more susceptible to neurotoxins, such as MPTP/MPP^+. In addition, PD-associated mutations, can potentially lead to alterations in mitochondria function and to an increase in the levels of ROS. MPTP/MPP^+, by inhibiting mitochondrial complex I, will dampen oxidative phosphorylation, causing a decrease in ATP levels. These events, in combination with decreased PGC-1α1 levels, will also lead to decreased levels of its downstream targets, namely NRFs and Tfam, which are responsible for the regulation of the expression of mitochondrial genes, affecting mitochondrial biogenesis and cell survival.

Being able to increase PGC-1α1 levels and/or activity through its modulation or stabilization could help find new approaches against neurodegeneration.

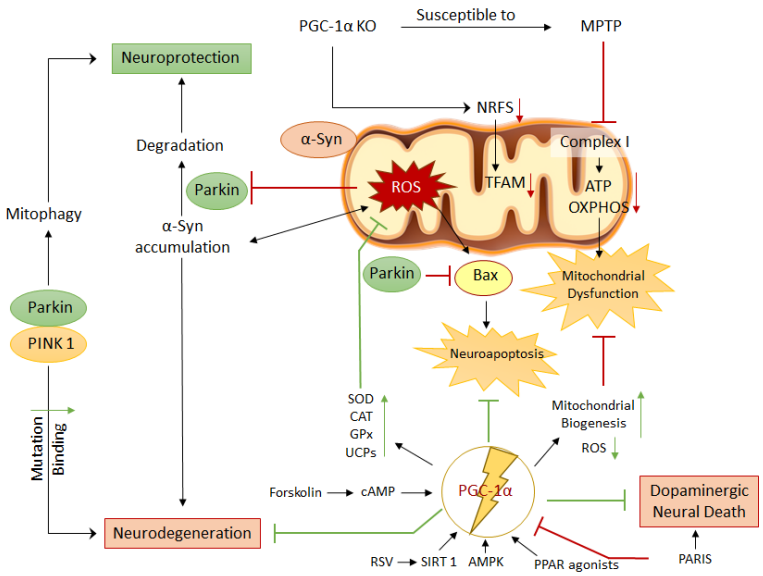

Figure I.6. PGC-1α1 modulation and its role in Parkinson's disease pathogenesis. This figure elucidates the role of PGC-1α1 in preventing neurodegeneration. This coactivator promotes mitochondrial biogenesis and induces the expression of ROS detoxifying agents and defence mechanisms, such as superoxide dismutase (SOD), catalase (CAT) and glutathione peroxidase (GPx). In this way, PGC-1α1 affect a series of pathways that are altered in neurodegeneration. PGC-1α1 can be induced through several different pathways depending on the stimulus. This induction can occur *via* cAMP/CREB/CRE, through its deacetylation by SIRT1, phosphorylation by AMPK or *via* PPAR agonists, such as pioglitazone. Parkin interacting substrate, PARIS is thought to also play an important role in the repression of PGC-1α1. Alterations in one of these pathways can be sufficient for the development of neurodegeneration and, in addition, can also be part of a solution for stopping neuronal death (adapted from Lv, J. *et al.*[142]).

4. Cellular Models of Parkinson's Disease

Because PD is a very complex disorder with many features and unknown causes, it becomes difficult to develop a model where most features are displayed, particularly for the sporadic form. Throughout the years, different cellular models of PD have been engineered that allow to explore several molecular and biochemical features associated to this complex pathology, rather quickly and reliably[143]. In the case of neuronal cell lines, they can be differentiated into different types of neurons, such as dopaminergic or cholinergic[143,144].

Currently, two of the most studied features of PD in cellular models are the formation of the α-synuclein aggregates and the neuronal death to recapitulate, to some extent, the loss of dopaminergic neurons in the *SNpc*[143].

Among the several immortalized neuronal cell lines that are commercially available, the most commonly used to study PD are the human neuroblastoma SH-SY5Y cell line and the rat pheochromocytoma PC12 cell line[143,145,146,147].

Another common cell line is the N2a murine neuroblastoma[82]. These cells display neuronal morphology and exhibit a higher sensitization upon treatment with MPP^+, when compared to other cell lines, namely SH-SY5Y and PC12 cells, under glucose and cell density controlled conditions[82]. Additionally, this cell line possesses high content of TH and also low levels of some neurotransmitters, namely dopamine, norepinephrine and serotonin, as well as low levels of MAO[148]. Therefore, N2a cells have been extensively used in a wide variety of studies, from toxicological to in vitro models of neurodegenerative disorders, such as Alzheimer's disease[149], Huntington's disease and PD[78,150].

However, these cell lines are often tumour-derived and therefore, they have the capacity of dividing virtually indefinitely, unlike neurons that are post-mitotic cells. Thus, these cells possess the disadvantage of carrying important physiological differences, depending on the cell type from which they derive[144]. Furthermore, the fact that they derive from tumorigenic cells could contribute for a resistance to the stimulus administered, unlike what happens in primary cultures.

Primary cell cultures could present an advantage to cell lines, and to better recapitulate the features of neuronal cells in vivo, since they are directly isolated from human or rodent tissues. However, the availability of fresh tissue for primary cell isolation is limited, the variability between donors is high and the process of separating the different cell types can be challenging and slow (compromising cell viability). Additionally, primary culture conditions can be more demanding and need to be more controlled, than immortalized cell lines, particularly in the case of primary neurons[144].

When deciding on the appropriate disease model, there are other aspects that must be considered, including using a stimulus that is suitable for the cells to exhibit the feature of interest for the study.

5. Cell-based High-throughput screenings

High-throughput screening (HTS) refers to the process where a large number of entities (e.g. chemical compounds, genetic manipulations) are tested to identify desired biological activities. Potential hits/candidates are then further validated in several distinct biological or pharmacological experiments[151]. It started as a system carried-out by many of the industrial biotechnology companies to try to reduce costs in drug development[152]. Furthermore, compound libraries were also increasing in the pharmaceutical industry and lack of structural

information was preventing their potential use as drugs[153]. This highly efficient approach was adapted to cell-based assays, which allow for a variety of screenings[152].

Biochemical and cell-based assays comprehend two types of assays that can be developed in HTS. While biochemical assays are direct and usually target-specific, conferring less variability due to the homogeneous nature of the reactions, cell-based assays are often carried out to identify modulators of a specific pathway and its effects in the regulatory networks and control mechanisms, within the cell environment[151].

Developing the most profitable screening strategy involves the balance between the maintenance of the appropriate biological structure and viability, where reagent availability and its adaptation to process automation needs to be considered[151].

In the case of cell-based assays, choosing the appropriate biological system, the assay approach, whether the readout will be uniform or high-content, considering the follow-up experiments and determining the strategies to interpret the output data are all very important aspects to the development of the screening. Each choice and consideration will influence the readout output. Additionally, cell-based assays also require other optimization steps, such as cell density, cell reagents, determination of optimal concentrations of modulators, determination of incubation periods with the screened compounds and, ultimately the sensitivity of the cell system to the compound solvent, namely dimethyl sulfoxide (DMSO)[151]. Finally, after positive hit validations of compounds, cytotoxicity experiments, such as half maximal inhibitory concentration (IC_{50}) determinations are usually carried out, as follow up experiments and secondary assays. These give more precise information about the compounds in the tested biological system and help to isolate the more promising compounds[154].

After careful consideration of all the former described aspects, the actual screening can be finally conducted. HTS comprehend several steps from target identification to reagent preparation, compound management, assay development and screening of the selected library[155].

Screenings can be divided into different categories depending on the number of compounds that are being analysed. Low-throughput screenings usually involve 1 to 500 samples tested per day, medium-throughput screenings include a range between 500 and 10 000, while high-throughput screenings involve 10 000 to 100 000 samples and ultra-high-throughput screenings comprise a number of samples tested per day, higher than 100 000[156].

Miniaturization techniques associated to the modern lead discovery *via* HTS, allowed the evaluation of a greater number of compounds in less time and less associated read-outs, resorting to a much smaller amount of biological material as well as the chemical to be tested.

The optimization of this process in order to reach a successful HTS lays on the 'magic triangle', where time, cost and quality represent the fundamental principles of performance management[157] (Figure I.7.).

Therefore, HTS provide a highly efficient approach to drug discovery, from already existing compounds gathered in enormous compound decks. These can be analysed by *in silico* strategies, creating several sub libraries, based on the *in silico* predicted activities (enzymatic activity, such as kinases[158] or transferases[159] and receptor-ligand binding properties)[157].

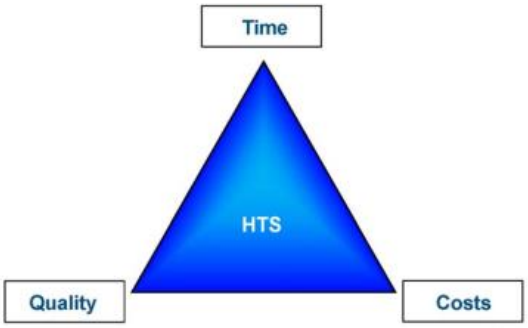

Figure I.7. Magic Triangle in HTS performance management. The optimization process towards a successful HTS lays on time and cost saving methodologies, where the time spent in each well, the number of wells that are analysed per day, within the project time, along with the type of reagents, instruments used and qualified personnel needs to be considered. Quality is also a fundamental principle that needs to be considered, since by reducing time and costs hit validations must be obtained, avoiding false negatives and false positives (adapted from Mayr & Bojanic[157]).

Transcriptional coactivators have been attracting attention (over transcription factors) as potent regulatory nodes for physiological stimuli[160]. Modulating PGC-1α1 by inducing specific PTM might allow its stabilization and thus the activation of target gene networks, involved in specific pathways. Therefore, identifying compounds that can modulate PGC-1α1 and increase this coactivator's activity could present great benefits for several diseases. In one such effort, an HTS was developed to identify small molecules capable of inducing PGC-1α gene expression in cultured myotubes. This led to the identification of microtubule and protein synthesis inhibitors as modulators of this coactivator and mitochondrial biogenesis[161].

In addition, another study has resorted to HTS assays to identify possible inhibitors of ERRα and/or of the PGC/ERR pathway, since uncontrolled overexpression of this nuclear receptor is present in cancer cells and is involved in cancer progression[162].

6. Main Goals

A study conducted by Dr. Jorge Ruas and colleagues identified a group of small molecules, from a cell-based HTS, that can activate and stabilize PGC-1α1, in cultured brown adipocytes[163]. Compound activity was verified by measuring PGC-1a1 protein accumulation, target gene expression and uncoupled mitochondrial respiration, in the same cellular model.

The main goal of the present project is to explore the biological activity of a group of eleven chemical compounds, selected from the previous screening, on PGC-1α1 in a neuronal cellular system, under physiological conditions and a neurodegenerative disease model. Screening the ability of these chemical compounds to stabilize PGC-1α1 in a neuronal system is of great importance, since this coactivator does not possess any known enzymatic activity to be targeted. In proving that this modulation might present neuroprotective effects, a new therapeutic approach can be formulated against neurodegenerative diseases, such as Parkinson's disease.

The first step to accomplish this project's goal was to select an adequate neuronal cell line to be used as a cellular model of PD and conduct the following validation steps. Having performed this, the following stage was to select the concentration of each compound, considering its toxicity to cells. Following this step, the compounds' biological effects were evaluated, namely cell viability, ATP levels and ROS production as well as their ability to stabilize PGC-1α1 by inducing its downstream targets and its associated protein expression levels.

II. MATERIALS AND METHODS

1. Reagents

1-methyl-4-phenylpyridinium (MPP+) iodide, Bovine Serum Albumin (BSA) (fraction V), Triton X-100, Ammonium Persulfate (APS) and Methylthiazolyldiphenyl-tetrazolium bromide (MTT) were purchased from Sigma Aldrich (St Louis, MO, USA); MG132 was secured from Enzo Life Sciences (Farmingdale, NY, USA); Minimum essential medium (MEM), Dulbecco's Modified Eagle Medium High Glucose (DMEM), Reduced Serum Medium (Opti-MEM® I), Ham's F-12 medium, fetal bovine serum (FBS), Penicillin/Streptomycin, L-glutamine and TripLE Express were obtained from GIBCO® (Life Technologies, Inc., Grand Islands, USA); phosphate buffered saline (PBS) was obtained from Corning® (Manassas, VA, USA); TRIzol reagent and Lipofectamine™ 3000 were secured from Invitrogen™ Life Technologies (Carlsbad, Ca, USA); Recombinase DNase I enzyme was acquired from Merck (Kenilworth, NJ, USA); Random hexamers mix for reverse transcribed complementary DNA (cDNA), dNTPs NZY mix and NZY First-Strand cDNA Synthesis Kit were purchased from NZYTech Lda. (Lisbon, Portugal); SensiFAST™ SYBR® Hi-ROX kit was acquired from Bioline (London, UK); Complete Mini protease inhibitors cocktail was secured from Roche Diagnostics (Penzberg, Germany); BSA 2 mg/mL ampules were purchased from ThermoFisher Scientific (Waltham, MA, USA); ECL Western blotting HRP substrate was secured from Advansta (San Jose, CA, USA); SuperSignal® West Femto Maximum Sensitivity was acquired from Thermo Scientific (Rockford, USA); Bio-Rad's Protein Assay Reagent, mouse and rabbit IgG and pre-stained protein ladder molecular weight marker were purchased from Bio-Rad Laboratories (Hercules, CA, USA); Polyvinylidene difluoride (PVDF) membrane was obtained from Millipore (Burlington, MA, USA) and from ThermoFisher Scientific (Waltham, MA, USA). Tris, glycine, methanol, absolute ethanol, acetic acid and isopropanol reagents were purchased from VWR (Radnor, PA, USA); Sodium Chloride and Potassium Chloride were obtained from Fisher Chemical (Hampton, NH, USA); Cytotoxicity Detection LDH kit was secured from Roche, Sigma Aldrich (Indianapolis, USA); 2',7'-dichlorofluorescein diacetate (H_2DCF-DA) probe was purchased from Molecular Probes, Inc., Invitrogen (Eugene, OR, USA); ATP-Glo™ Bioluminometric Cell Viability Assay Kit was obtained from Biotium, Inc. (Freemont, CA, USA).

2. Cell culture

All adherent cells used were kept at 37◦C in a humidified 5% CO_2 incubator. As cells grown in monolayer reached confluency, they must be sub-cultured. Cell sub-culturing was achieved by enzymatic dissociation using TrypLE express, to promote detachment of adherent cells from the flask. Cells were then transferred into new T75-flasks (Falcon™, BD Biosciences, San Jose, California, EUA) and freshly prepared growth medium was added.

Mouse neuroblastoma cells (N2a cell line) were cultured in a medium composed of a mix (1:1) of Opti-MEM and DMEM high glucose 4,5 g/L, 10% FBS, 2 mM L-glutamine and 100 µg/mL streptomycin and 100 U/mL penicillin (Pen/Strep).
Human neuroblastoma cells (SH-SY5Y cell line) were maintained in MEM and Ham's F-12 mixture (1:1) supplemented with 15% FBS, 1% non-essential amino acids, 2 mM L-glutamine and 100 µg/mL streptomycin and 100 U/mL penicillin.
Human glioblastoma cells (U118 cell line) were cultured in a medium of DMEM high glucose, 4,5 g/L, 10% FBS, 2 mM L-glutamine and 100 µg/mL streptomycin and 100 U/mL penicillin.

During the earlier passages of cells, half were set aside to freeze a new batch, and the other half was used for maintenance. The freezing step starts with the same process of sub-culturing, as described above. After this process, half of the volume of medium with resuspended cells was centrifuged at 500 × *g*, for 5 minutes, at 20 ◦C. Cells were resuspended in fresh medium and 10% FBS and 10% Hibry-Max™ (Sigma Aldrich, St Louis, MO, USA) were added. Cells were aliquoted into crio-vials that were kept at -20 ◦C, for 30 minutes and finally transferred and kept at -80 ◦C, until further use.

3. Cell culture treatments

In the course of this project, cells were treated with the eleven selected compounds at different concentrations, depending on the aim of each performed assay. Additionally, cells were also treated with the proteasome inhibitor MG132, in the experiments to select the cellular model, and with MPP^+, as a cellular model of PD. In this section, are described the different treatments that were performed, according to the corresponding validation step.
Cells were plated according to the experiment to be performed, as follows: for Western Blot, cells were plated in 100 mm diameter culture dishes at a density of $4{,}5 \times 10^6$ cells/dish. Regarding RT-qPCR experiments, cells were plated in 60 mm diameter culture dishes at a

density of $1{,}5 \times 10^6$ cells/dish. For cell viability assays (MTT, LDH and ATP), as well as for ROS production assays, cells were plated at a density of 15 000 cells/well, in 96 multiwell microplates. For each condition, a series of 3 replicates were conducted, to assess the variability associated to each experiment. Independently of the assay, after plating of cells, they were let to grow for approximately 24 hours.

3.1. Selection of the cellular model for the compound screening

3.1.1. Transfection assay

The three tested cell lines were transfected with 1000 ng of the plasmid pcDNA3.1-Flag-mPGC1α1-HIS, to obtain PGC-1α1 overexpression. The plasmid was kindly given by Dr. Jorge Ruas. The backbone of pcDNA3.1-Flag-mPGC1α1-HIS corresponds to the pcDNA3.1 plasmid, where Flag-mPGC1α1-HIS is flanked by BamHI and XhoI sites. Plasmid transfection was performed resorting to Lipofectamine™ 3000 (Life Technologies) and according to the manufacturer's instructions. For each cell line, four culture dishes were plated ($1{,}5 \times 10^6$ cells/dish) and two of them were transiently transfected with recombinant PGC-1α plasmid.

For the transfection assays a DNA mix (mix 1; containing Opti-MEM, P3000 and 1 µg of plasmid DNA per condition) and a Lipofectamine mix (mix 2; containing Opti-MEM and Lipofectamine 3000), were separately prepared.

Mix 2 was then added, dropwise, to mix 1 and incubated for 15 minutes. This master mix was finally added, dropwise, to each plate of cells into fresh medium.

The culture medium was replaced with fresh medium 6 h and 24 h after transfection. 72 h after plating, cells were treated with the proteasome inhibitor MG132, in order to assess PGC-1α1 stabilization, by Western Blot. Cells were treated with a concentration of **10 µM MG132**, as described by Ruas and col.[163] and incubated for **7 h**, at 37 ◦C and 5 % CO_2. Figure II.1. is a representative image of the performed treatments for the validation of the cellular line.

Control MG132 *p*PGC-1α *p*PGC-1α + MG132

Figure II.1. Schematic representation of treatments for cell line validation. After plating of cells, from each cell line (SH-SY5Y, U118 and N2a cells), transfection was performed, as described above. 6 h after transfection, the culture medium of each cell plate, including the ones not transfected, was replaced to maintain the same experiment conditions in every dish. 24 hours passed, another medium replacement was carried out and cells were let to grow until the following day. On the third day after plating of cells, one plate with transfected cells and another with not transfected cells were then treated with 10 µM MG132. (Control – untreated cells; MG132 – cells treated with MG132; *p*PGC-1α – cells transfected with PGC-1α plasmid; *p*PGC-1α + MG132 – cells transfected with PGC-1α plasmid and treated with MG132).

3.2. Screening of the small molecule PGC-1α1 stabilizers

For the screening, cells were treated with the **eleven compounds** at **0,1 µM**, **1 µM**, **2,5 µM**, **5 µM** and **10 µM** (only for the MTT assay) and incubated for **7 h**, at 37 ◦C and 5 % CO_2. After this period, cells were processed for the **LDH** and **MTT** cell viability assays as described in section II.6.1. and II.6.2 and for **RT-qPCR** (section II.5.).

For the cell viability assays two control conditions were performed, one containing untreated cells and another containing DMSO-treated cells (at the same proportion of volume as the most concentrated condition of compound).

3.3. Evaluation of the effects of each selected compound in a cellular model of Parkinson's disease

Compounds **CR4**, **CR5**, **CR9**, **CR10** and **CR11** were selected from the initial group of eleven small molecules. Cells were treated with these compounds at **1 µM** and incubated for **7 h**, at 37 ◦C and 5 % CO_2. After the incubation period, half of the cells treated with the compounds had their medium replaced by new one. The other half of the cells had their medium replaced by new one, containing **MPP^+** at a final concentration of **1 mM**.

Cells were then incubated for an additional period of **3 h**, at 37 ◦C and 5 % CO_2 so that **ATP** and **ROS** production assays could be performed. For **MTT** assay, **RT-qPCR** and **Western blot** cells were incubated for **16 h**, at 37 ◦C and 5 % CO_2. For each assay a control of untreated cells and another of cells treated only with MPP^+, were performed.

4. Western Blot analysis

4.1. Total protein extraction

After cells were treated, they were washed with cold 1x PBS and to each dish was added cell lysis buffer, containing: 50 mM Tris-HCl pH 7,4, 180 mM NaCl, 1% Triton-X100, 1 mM EDTA plus Complete Mini protease inhibitors cocktail (Roche Diagnostics). After this process cells were stored at -80 ˚C.

For total protein extraction each sample was scrapped and transferred to different eppendorf's where each sample was sonicated three times, for five seconds each time, using an ultrasonic processor UP100H (Hielscher - Ultrasound Technology, Teltow, Germany; cycle: 1, amplitude: 100%). Finally, samples were centrifuged for 15 minutes, 12 000 rpm, at 4 ˚C, using an Allegra 2IR centrifuge (Beckman Coulter, Brea, CA, USA). Supernatants were transferred to new eppendorf's and pellets were discarded. Protein extracts were stored at -80 ˚C, until further use.

4.2. Total protein quantification

For total protein quantification the Bradford method was used. Briefly, a standard curve was created, using known concentrations of BSA protein, from a working solution of 0,1 mg/mL. To all samples was added Bradford assay dye (Bio-Rad's Protein Assay Reagent), on a proportion of 1:500 and respective absorbances were then measured at 595 nm, in a Bio-Rad microplate reader model 680 (Hercules, CA, USA).

4.3. Preparation of samples and SDS-page

For the Western Blot, 100 µg of total protein were used and SDS-loading buffer (Tris-HCl pH 6,8, 4% SDS, 4 % glycerol, 1% β-mercaptoetanol and bromophenol blue) was added to each sample. Samples were then heated, for 5 minutes at 95 ˚C, for denaturing, using a dry bath and kept on ice or at -20 ˚C, until further use.

Western Blot gels system was assembled according to manufacturer's instructions and a gel of 7,5 % composed of 30% acrylamide/bis-acrylamide (37,5:1), from Bio-Rad (Hercules, CA, USA), was prepared with addition of polymerization catalysts, tetramethylethylenediamine (TEMED) and APS. After polymerization of this gel, a 4% gel of 30% acrylamide/bis-acrylamide (37,5:1) (stacking gel), was prepared for loading of samples.

The system was then assembled into the running vat, containing the running buffer solution (tris-glycine/SDS). For each gel an electric current of 35 mA was applied, for approximately 3

h. During this period the system was under a refrigeration system, due to possible over-heating caused by the continuous generated electric current.

4.4. Transfer of proteins to the membrane

Once the gel achieved complete separation, it was equilibrated in transfer buffer (tris-glycine/methanol). Proteins were then electro-transferred to a PVDF membrane (previously activated in methanol and equilibrated in transfer buffer), in a transfer vat, filled with the same buffer, to assure a wet transfer. An electric current of 500 mA was applied, for approximately 2 h. During this period the system was also under refrigeration. Finally, the membranes were stained with Amido Black (Sigma-Aldrich, St Louis, MO, USA), for control of loaded samples and transfer efficiency.

4.5. Immunodetection

For immunodetection, membranes were reactivated in absolute ethanol, washed in double-distilled water and then in tris-buffered saline solution with 0,1 % Tween-20 (TBS-T). The membrane was then blocked with 5% non-fat dry milk, diluted in TBS-T, for 1 h, at room temperature (r.t.) and further incubated with the respective primary antibody (Table II.1.), overnight at 4 ◦C. Afterwards, the membrane was incubated with anti-rabbit or anti-mouse horseradish peroxidase-conjugated secondary antibodies (1:5000, 5% non-fat dry milk), for 1 h, at r.t., after being washed three times with TBS-T, to remove the excess of primary antibody. The chemiluminescent immunocomplexes were detected using ECL or Femto reagents and visualized in a ChemiDoc MP Imaging System (Bio-Rad, Hercules, CA, USA). Detection analysis was performed through Image Lab 5.0 software (Bio-Rad, Hercules, CA, USA).
Following detection, membranes were stripped using an acidic solution composed of acetic acid, glycine, 10% SDS and Tween-20, in order to remove the immunocomplexes earlier formed. The membrane was then washed in bi-distilled water and in TBS-T, before being dried or blocked and re-probed.

Table II.1. Information on the primary antibodies used for Western blot analysis.

Antibody	Commercial Source	Reference	Host	Concentration	Molecular Weight (kDa)
PGC-1α	Calbiochem	ST1202	Mouse (mAb)	1:500	113
β-Actin	Sigma Aldrich	A 5441	Mouse	1:40 000	42
p-CREB	Santa Cruz Biotech	sc-101663	Rabbit	1:200	43
Total CREB	Cell Signalling Technology, Inc.	#9104	Mouse (mAb)	1:1000	43

5. RT-qPCR analysis

5.1. Total RNA extraction

After treatment, cells were washed in cold sterile 1x PBS, TRIzol™ reagent (Invitrogen™) was added and samples were stored at -80 ◦C.

The RNA extraction protocol was performed according to manufacturer's instructions, as follows. First, samples were thawed while kept on ice. Each cell plate was scrapped, and cells were transferred into new sterile tubes. Samples were kept for 5 minutes, at r.t. and after, 0,2 mL of chloroform was added per mL of TRIzol™ used. Each tube was briefly vortexed, left to incubate at r.t. and then centrifuged at 12 000 × *g*, for 15 minutes at 4 ◦C.

After centrifugation, the aqueous phase of each sample, was transferred into new sterile tubes and 0,5 mL of isopropanol per mL of TRIzol™ was added, to precipitate RNA. Samples were then mixed by inversion, incubated at r.t. and centrifuged at 12 000 × *g*, for 10 minutes at 4 ◦C. The supernatant was removed, and the RNA pellet washed in 70% ethanol (1 mL per mL of TRIzol™). The samples were then briefly vortexed and centrifuged at 12 000 × *g*, for 10 minutes at 4 ◦C. Finally, the supernatant was discarded, and pellets were left to air dry. The RNA pellets were resuspended in DEPC water, briefly vortexed and incubated in a water bath, at 55 ◦C, for 10 minutes, to help its solubilization.

Samples were then quantified using a Nanodrop 1000 (Thermo Scientific, Rockford, USA) and stored at -80 ◦C, until further use.

5.2. Treatment of RNA samples with DNase

Before proceeding to RT-qPCR, samples were treated with DNase, to remove possible contaminations with DNA. In this step, a mix was prepared containing 1x DNase buffer, the recombinant DNase I enzyme 10 U/µL (Merck) and 1 µg of RNA diluted in DEPC water. The

samples were incubated for 20 minutes at 37◦C, followed by 10 minutes at 75 ◦C in a thermocycler (VWR, Radnor, PA, USA).

5.3. Synthesis of cDNA

NZY First-Strand cDNA Synthesis Kit (NZYTech Lda) was used in order to synthesize the cDNA, according to the manufacturer's instructions.

Briefly, a mix was prepared containing random hexamers (25 µg/500 µL), dNTPs (25mM) and 500 ng of RNA treated with DNase. This mixture was incubated for 5 minutes at 65 ◦C. Afterwards, reverse transcriptase enzyme and buffer (1x) was added to the tubes, reaching a final volume of 20 µL. The cDNA synthesis was performed in a thermocycler and the program was as follows: 10 minutes, at 25 ◦C; 50 minutes, at 50 ◦C; and 5 minutes, at 85 ◦C. cDNA was then stored at -20 ◦C, until further use.

5.4. RT-qPCR

Quantitative Real-Time PCR (qPCR) was performed using SensiFAST™ in a QuantStudio™ 7 Flex System (Thermo Fisher Scientific, Waltham, MA, USA) in a 384-well reaction plate. A mix containing SensiFAST™ (1x) and 500 nM of the primers forward and reverse was prepared to amplify each gene (Table II.2.). cDNA samples were used for each reaction (5 µL of total reaction volume), and each sample was assayed in duplicate as well as the negative control, for each primer mix (the reaction was prepared with miliQ water instead of cDNA).

Finally, the microplate was covered with a transparent adhesive, briefly centrifuged at $500 \times g$ and inserted into the QuantStudio™ 7 Flex detection system, with the following amplification program: 2 minutes, at 95 ◦C and 40 cycles of 5 seconds, at 95 ◦C; 30 seconds, at 60 ◦C. A melting curve analysis was also performed.

In order to quantify the amplified gene sequences, in each sample, comparative $\Delta\Delta C_T$ method was used. The relative mRNA levels of the genes of interest were normalized to the relative mRNA levels of the eukaryotic elongation factor (EEF) and were expressed as fold over control.

Table II.2. Sequence of primers tested by RT-qPCR.

Gene	Forward (5'-3')	Reverse (5'-3')
EEF	ACACGTAGATTCCGGCAAGT	AGGAGCCCTTTCCCATCTC
TFAM	CACCCAGATGCAAAACTTTCAG	CTGCTCTTTATACTTGCTCACAG
ESRRA (ERRα)	GGGGAGCATCGAGTACAGC	AGACGCACACCCTCCTTGA
NRF1	AGCACGGAGTGACCCAAAC	TGTACGTGGCTACATGGACCT
CPT1A	CACTGCAGCTCGCACATTAC	CCAGCACAAAGTTGCAGGAC
GLUT4	AAAAGTGCCTGAAACCAGAG	TCACCTCCTGCTCTAAAAGG
UCP1	CAATGAACACTGCCACACCTC	GGCATTCAGAGGCAAATCAGCT
SREBP1c	GCAGGAAACTGAGAGACCCC	GTACCCACTGGCCTTCTCAC
XBP1s	TCCGCAGCAGGTGCAG	CCAACTTGTCCAGAATGCCC

6. Cytotoxicity detection assays

To assess the selected compounds' toxicity in neuroblastoma N2a cells and the cellular response to the compounds in the presence/absence of MPP^+, the following assays were conducted.

6.1. Lactate Dehydrogenase (LDH) release assay

For LDH assessment, Cytotoxicity Detection LDH kit (Roche) was used, according to manufacturer's instructions. After plating and treatment of cells, the 96 well microplate was centrifuged at 250 × *g*, for 5 to 10 minutes. A volume of culture supernatant was transferred into a clean reading 96 well microplate. A mix of two solutions was prepared in a ratio of 1:45 (Solution 1: Solution 2) and an equal volume of mix was also added to each well. Finally, the microplate was covered in foil, to avoid light contact and incubated, at r.t., for 20 minutes. After this period, absorbance at 495 nm was measured with a reference absorbance of 600 nm.

In each conducted assay three different controls were used: a background control, providing information about any interaction between LDH activity and the culture medium; a "low control", to assess LDH activity released from untreated cells; a "high control", to asses maximum release of LDH activity. To this end a lysis buffer was added to cells, before centrifuging the microplate. Additionally, during the first assay, a "substance control" was included to assess possible interactions between the tested compounds and LDH activity.

6.2. Methylthiazolyldiphenyl-tetrazolium bromide (MTT) assay

After plating of cells and 2h before completion of cells treatment, MTT was added to each well. An MTT stock solution was prepared (5 mg/mL) in miliQ water and added to each well, to a final concentration of 0,5 mg/mL.

All the cell culture medium with the MTT was then removed into a toxic residue container and DMSO was added into each well, to help solubilize the violet crystals retained inside the cells. The microplate was subjected to vigorous agitation, to help on the solubilization process. After this step, absorbance at 470 nm was measured with a reference absorbance of 620 nm, in a microplate multimode reader GlowMax® (Promega, Madison, WI, USA).

In each conducted assay two different controls were included: a background control, providing information about any interaction between MTT and the culture medium; and a positive control, to assess the viability from untreated cells, which was considered 100% of cell viability.

7. ATP assay

To measure ATP levels an ATP-Glo™ Bioluminometric Cell Viability Assay Kit was used (Biotium, Inc). After treatment of cells, the cell culture medium from each well was replaced with sterile miliQ water. The plate was then stored at -80 ◦C, until further use.

Prior to plate reading, an assay buffer solution containing D-luciferin (luciferase substrate), with a final concentration of 0,4 mg/mL, was prepared. Immediately before plate reading, luciferase was added to the previously prepared buffer solution in a proportion of 1:100. The solution was then heated at 37 ◦C in a water bath. Readings were performed in a FB12 luminometer (Berthold Detection Systems, Pforzheim, Germany) using proper assay tubes. To each tube the sample, diluted in miliQ water, and assay buffer with luciferase were added (1:1). The sample was quickly mixed by flicking the tube and then read with a 10s delay time. Oxidation of D-luciferin by luciferase is directly dependent on consumption of the ATP produced by cells. A background control was performed containing miliQ water and assay buffer (1:1). This value was subtracted to each obtained value in order to abrogate any unspecific luciferase activity.

To assure that the measured values from the luminometer were only a consequence of luciferase activity and since this activity was dependent on ATP release from the cells, a protein normalization was performed using Bradford assay dye.

An ATP standard curve was also performed, from serial dilutions of a stock solution of 2 mM (provided in the assay kit). Preparation of the buffer solution and readings were processed as previously described.

8. ROS production assay

After plating and treatment of cells, the cell culture medium from each well was removed and the 2',7'-dichlorofluorescein diacetate (H_2DCF-DA) probe prepared in cellular medium was added to the cells, at a final concentration of 20 μM. Cells were incubated for 30 minutes at 37 ◦C and 5 % CO_2. After the incubation period, the medium from each well was removed and cells were washed twice, in sterile 1x PBS. The PBS from the last washing step was kept in the wells to perform the reading in a microplate multimode reader GlowMax®, with a proper filter for maximum emission λ of 485 nm and a maximum excitation λ of 535 nm.
To assure that the measured values relatively to the ROS production were only a consequence of the probe oxidation, considering the cells within each well, a protein normalization was performed using Bradford assay dye.

9. Statistical analysis

All data are expressed as mean ± standard error of the mean (SEM) and analysis of variance (ANOVA) testing was performed using one-way analysis with Tukey's post-hoc as a multiple comparison test. Differences were considered statistically significant when $p<0.05$. All analysis was performed using GraphPad/Prism, 5.0 software for Windows (San Diego, CA, USA).

III. RESULTS

A group of eleven chemical compounds were selected from a previous HTS (see section I.6.), where they were identified by their ability to stabilize and activate PGC-1α1 in brown adipocytes[163]. Since the mechanism of action of these compounds is still not known, it is important to evaluate their capacity to stabilize PGC-1α1 in other cellular systems. In addition, since the biological activity of the coactivator depends on the presence of specific transcription factors, PGC-1α1 stabilization might not be sufficient for its activation in all cell types. All the experiments, during the time of this study, were conducted as blind tests for all the tested compounds. At the begin of this study, each of the eleven compounds was randomly nominated with the initials CR followed by the respective number, CR1 to CR11. All the correspondent designations, from the previous study, were saved and kept away from the main interveners of the conducted experiments.

1. Selection of the cellular model for compound screening

The first step of this small-scale screening was to evaluate different cell lines, in order to choose the most adequate to proceed with the study (mainly in terms of PGC-1α1 stabilization). To that end, we tested three different neuronal cell lines: a murine neuroblastoma N2a cell line, a human glioblastoma U118 cell line and a human neuroblastoma SH-SY5Y cell line. Since it is known that PGC-1α1 degradation is mediated by the ubiquitin-proteasome system[163], we started by treating each of the cell lines with the proteasome inhibitor MG132 at 10 μM for 7 h. Cells were previously transfected, as described in 'Materials and Methods' with a recombinant DNA plasmid to overexpress PGC-1α1.

PGC-1α1 expression levels were evaluated by Western Blot, using an anti-PGC-1α1 antibody that recognizes the main four isoforms[121]. All tested cell lines appeared to have PGC-1a1 stabilized upon treatment with MG132 (Figure III.1.). From all the tested cell lines, N2a cells seem to be the ones with the highest endogenous levels of PGC-1α1. Moreover, despite of exhibiting a low transfection efficiency, ectopic expression of PGC-1α1 seem to be stabilized in this cell line (Figure III.1. A, B).

Since our priority for this study was to evaluate changes in the endogenous levels of PGC-1α1, upon administration of the compounds, the N2a cell line was selected to proceed with the following experiments. Furthermore, this cell line was also demonstrated to be more sensitive to MPP^+ when compared to other cell lines[82].

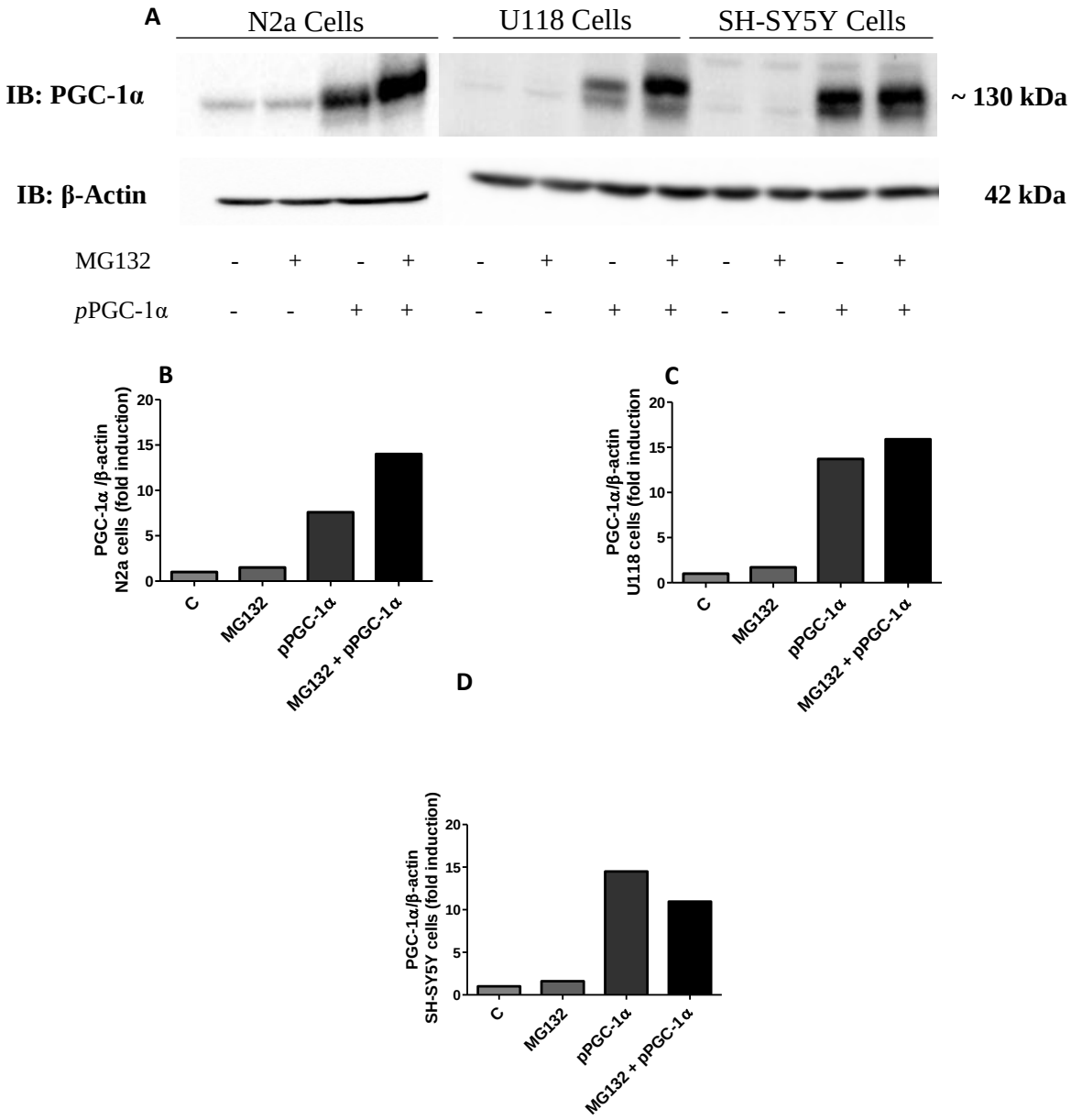

Figure III.1. Endogenous and ectopic PGC-1α1 protein expression levels under control conditions and after treatment with the proteasome inhibitor MG132. Three different cell lines - murine neuroblastoma N2a cell line, human glioblastoma U118 cell line and human neuroblastoma SH-SY5Y cell line - were transfected with a PGC-1α1 expression plasmid. After transfection, SH-SY5Y, U118 and N2a cells were treated with DMSO (C; control) or the proteasome inhibitor MG132 (10 μM) for 7 h. **A.** Protein extracts were separated by SDS/PAGE and the corresponding immunoblots were probed with an anti-PGC-1α mouse monoclonal antibody. Analysis of β-Actin was performed in parallel as a loading control. PGC-1α/β-Actin ratios are shown as fold induction over untransfected, untreated control in **B.** N2a cells, **C.** U118 cells and **D.** SH-SY5Y cells.

2. Screening of the small PGC-1α1 stabilizers

2.1. Evaluation of the toxicity of the selected compounds

As part of the validation process, we determined the effect of each compound on the viability of the chosen cellular model using two cell viability assays: an LDH assay, to assess cell death by measuring the amount of lactate dehydrogenase released to the medium of each condition and an MTT assay, to assess cell viability. In general, both assays were coherent and cell death increased in an inversely proportional way, relatively to cell viability, in a concentration-dependent manner (Figure III.2.). In addition, during the first experiment of each assay, an additional condition was tested to assess any possible interactions between the tested compounds and the tetrazolium salt.

Initially, we assessed cell viability by treating cells with each compound at a concentration of 10 µM, since this was the concentration previously used in brown adipocytes[163] (data not shown; n=3). However, since in our model at this concentration several of the tested compounds displayed some toxicity (with a minimum percentage of cell viability of 16 ± 1.3 %, 55.9 ± 6.6% and 64.8 ± 6.2 %, respectively for the compounds CR2, CR3 and CR10) we decided to lower the doses tested.

Using concentrations ranging from 0.1 µM to 5 µM, the majority of the compounds didn't present significant toxicity to cells, with a maximum percentage of LDH release of 17.4 ± 6.7%, corresponding to compound CR1 at a concentration of 0.1 µM, and a minimum percentage of cell viability of 70.5 ± 3.8 %, corresponding to the compound CR11 at a concentration of 5 µM (Figure III.2.). However, two of the eleven compounds, namely CR2 and CR10, showed significant toxicity, considerably affecting cell viability, achieving a maximum percentage of LDH release of 69.7 ± 23.5 %, for CR2, at a concentration of 5 µM and a minimum percentage of cell viability of 51.2 ± 26.3 % and 65.7 ± 10 %, respectively.

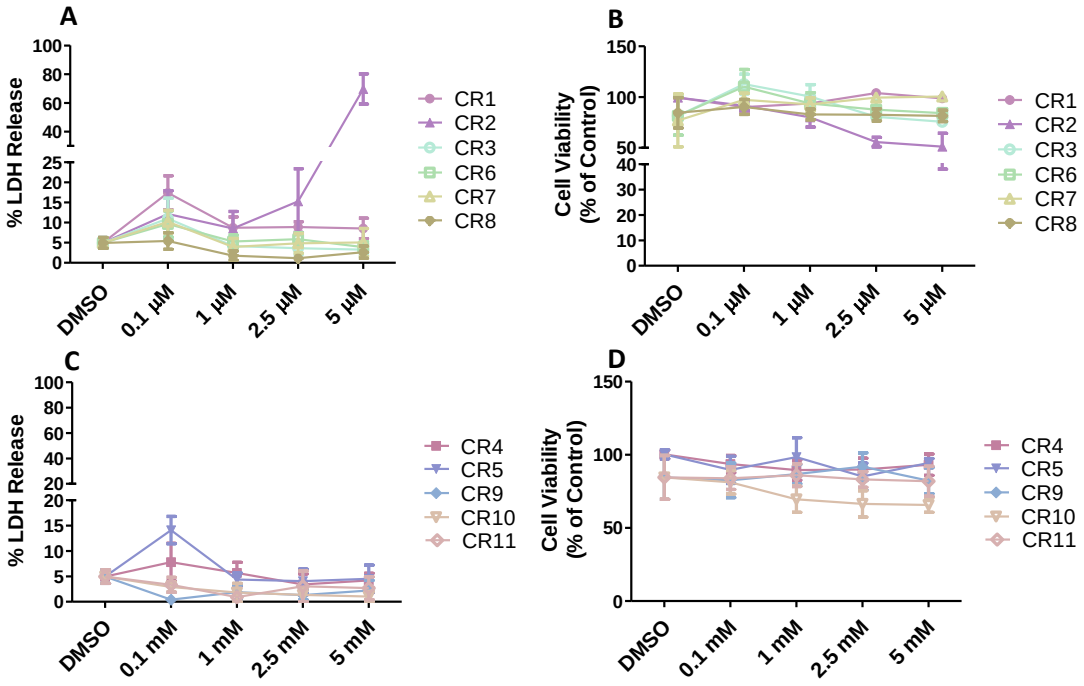

Figure III.2. N2a cell viability/cell death assessed by MTT and LDH assays, after treatment with the CR compounds at different concentrations. N2a cells were treated with each of the eleven compounds, at four different concentrations: 0.1 µM, 1 µM, 2.5 µM and 5 µM; and then incubated for 7 h, as described in 'Materials and Methods'. % of LDH release (left panel – A, C) and cell viability by MTT (right panel – B, D) were determined as a percentage of control (untreated cells). A negative control (DMSO) was also conducted, to assess its own toxicity in cells. Results are representative of 5 independent experiments.

2.2. Evaluation of PGC-1α1 stabilization and downstream targets expression levels upon treatment with selected compounds

In parallel, we assessed if compound treatment (at 10 μM) affected PGC-1α1 protein expression levels. Furthermore, RT-qPCR was also conducted to assess mRNA levels of the following PGC-1α1 target genes: ERRα, Tfam, NRF-1, CPT1α, Glut-4 and PPARα (data not shown).

These two sets of experiments allowed us to assess whether some compounds could be stabilizing PGC-1α1, even if higher (and more toxic doses) were required to achieve that goal. The rational for this is to identify compounds with a positive effect on PGC-1α1 expression and on its target genes expression, since their structure can be modified later, to obtain similar but less toxic compounds.

Therefore, from the Western Blot in combination with the RT-qPCR we chose five compounds that seemed to elevate more PGC-1α1 expression, leading to its accumulation and increasing the expression of most of its downstream targets: CR4, CR5, CR9, CR10 and CR11. Finally, we explored the effects of lower concentrations of these five compounds on PGC-1α1 downstream targets. To this end, we used the compound concentrations tested in section 2.1. and evaluated the expression of the same target genes as in the previous RT-qPCR. This was done with exception of PPARα, since the obtained C_T values were very high, compared to the rest of the genes, suggesting that N2a cells express low levels of this gene.

The compounds tested showed a tendency to increase relative mRNA levels of ERRα (Figure III.3.), at least in one of the tested concentrations, although no statistical significance was found. In this case, only CR10 and CR11 didn't seem to follow this pattern, with CR10 even significantly decreasing these levels.

As for CPT1α mRNA levels (Figure III.4.), a similar pattern was observed, with CR10 showing a tendency to increase these levels at the lowest concentration and at higher concentrations an inversion of this behaviour was observed. However, no statistical significance was observed in these experiments.

In addition, CR4 significantly increased NRF-1 mRNA levels, when compared to the control (* $p < 0.05$ vs. control; Figure III.5. C). CR9 exhibited a trend to slightly increase both Glut-4 (Figure III.5. A) and NRF-1 mRNA levels (Figure III.5. D). Moreover, CR10 tended to increase the relative mRNA levels of Glut-4 (Figure III.5. B), to a higher extent, when compared to CR9. However, none of the results achieved statistical significance.

Although Tfam was also tested for the same conditions as the targets above described, no compound showed a significant increase in its mRNA levels (data not shown).

The main goal of these experiments was to find a compromise between potential compound toxicity and positive effects on PGC-1α1 downstream targets. Since no selected compound (with exception to CR10) showed significant toxicity to N2a cells, at a concentration of 1 μM, this was the selected concentration to proceed with the following tests. Although no statistical significance was found, the selected concentration showed a tendency to increase the mRNA levels of most of the tested PGC-1α1 targets.

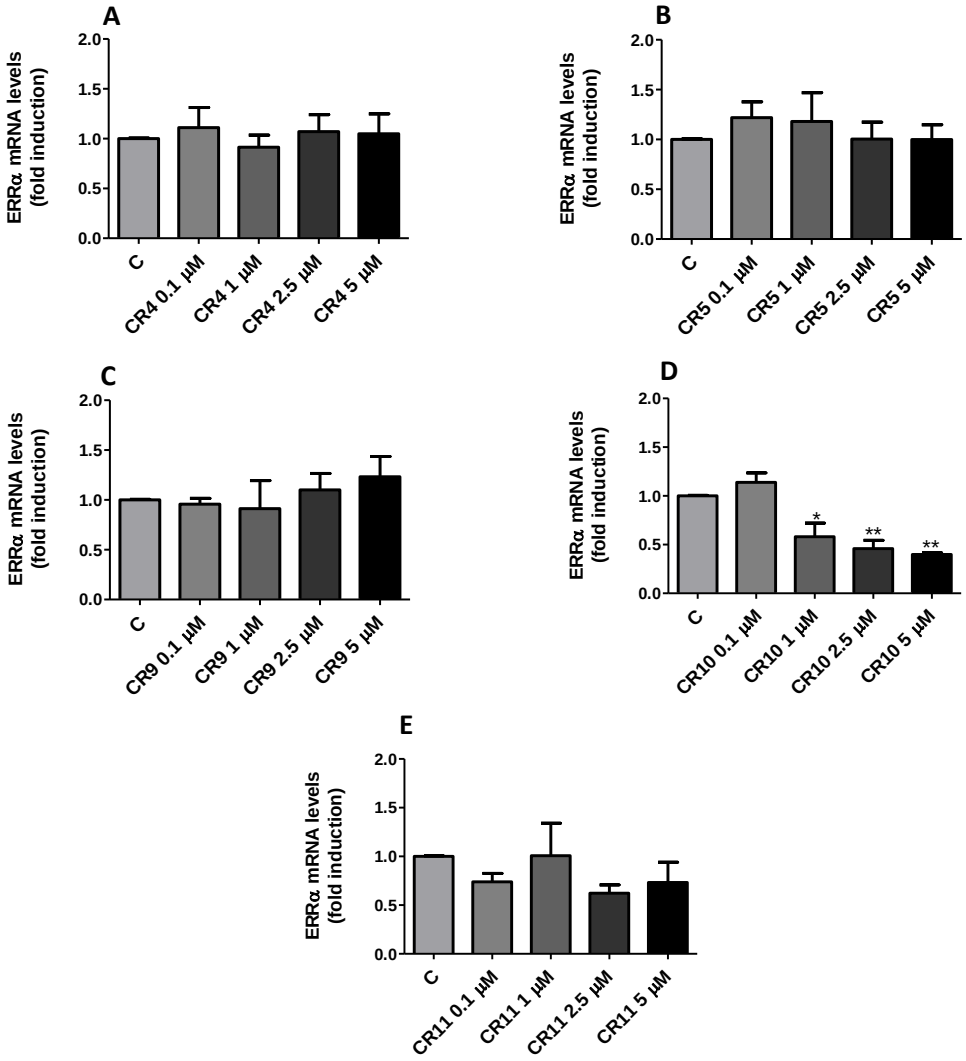

Figure III.3. Relative ERRα mRNA levels, in N2a cells after treatment with the selected compounds (CR4, CR5, CR9, CR10, CR11) at different concentrations. Cells were treated with each of the five selected compounds, at four different concentrations: 0.1 μM, 1 μM, 2.5 μM and 5 μM; and then incubated for 7 h, as described in 'Materials and Methods'. Total RNA was extracted from each sample and ERRα mRNA levels were determined by reverse transcription quantitative PCR. ERRα mRNA levels in N2a treated with: **A.** CR4; **B.** CR5; **C.** CR9; **D.** CR10 and **E.** CR11 are depicted. mRNA relative levels of EEF were determined in parallel as a housekeeping gene and used as a normalization tool, resorting to the $\Delta\Delta C_T$ method. Results are representative of 3 independent experiments (* $p < 0.05$, ** $p < 0.01$, *** $p < 0.001$); the symbol '*' refers to the change vs control, except if otherwise indicated.

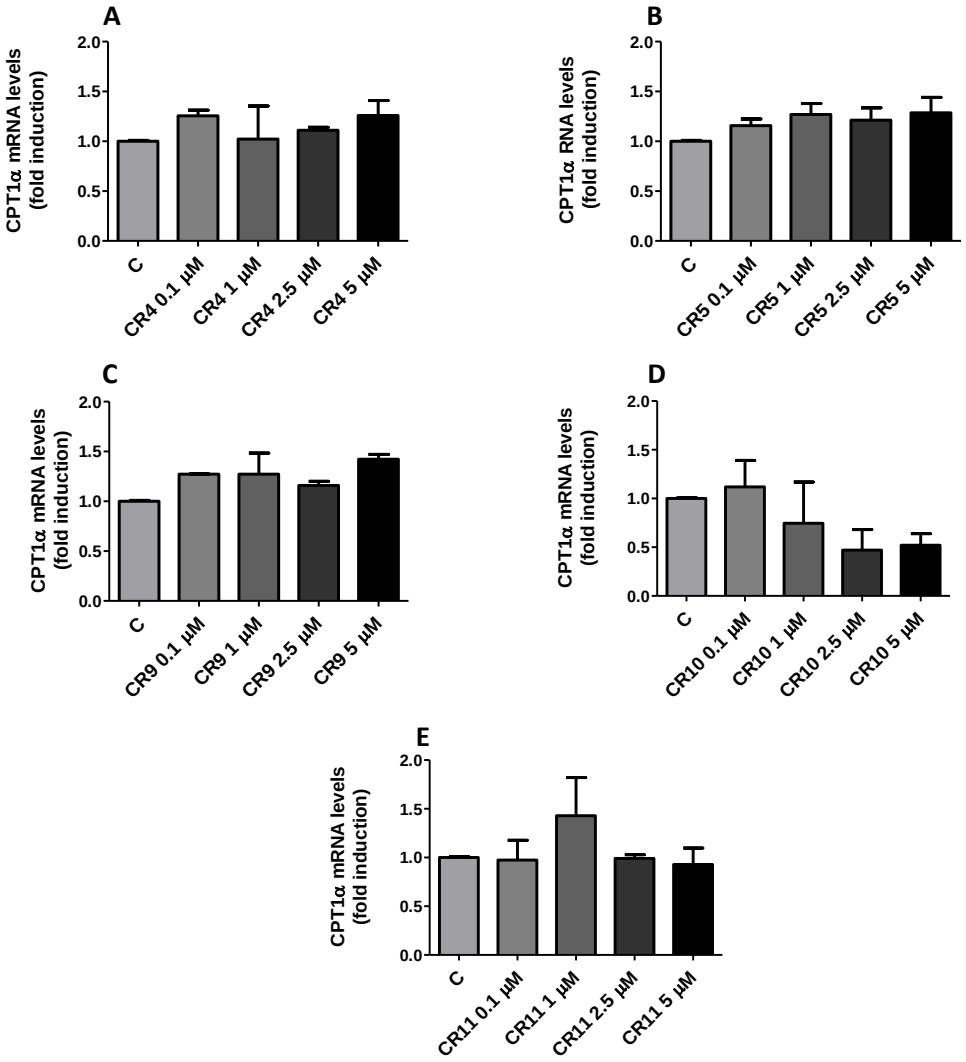

Figure III.4. Relative CPT1α mRNA levels, in N2a cells after treatment with the selected compounds (CR4, CR5, CR9, CR10 and CR11) at different concentrations. Cells were treated with each of the five selected compounds, at four different concentrations: 0.1 µM, 1 µM, 2.5 µM and 5 µM; and then incubated for 7 h, as described in 'Materials and Methods'. Total RNA was extracted from each sample and CPT1α mRNA levels were determined by reverse transcription quantitative PCR. CPT1α mRNA levels in N2a treated with: **A.** CR4; **B.** CR5; **C.** CR9; **D.** CR10 and **E.** CR11 are depicted. mRNA relative levels of EEF were determined in parallel as a housekeeping gene and used as a normalization tool, resorting to the $\Delta\Delta C_T$ method. Results are representative of 3 independent experiments.

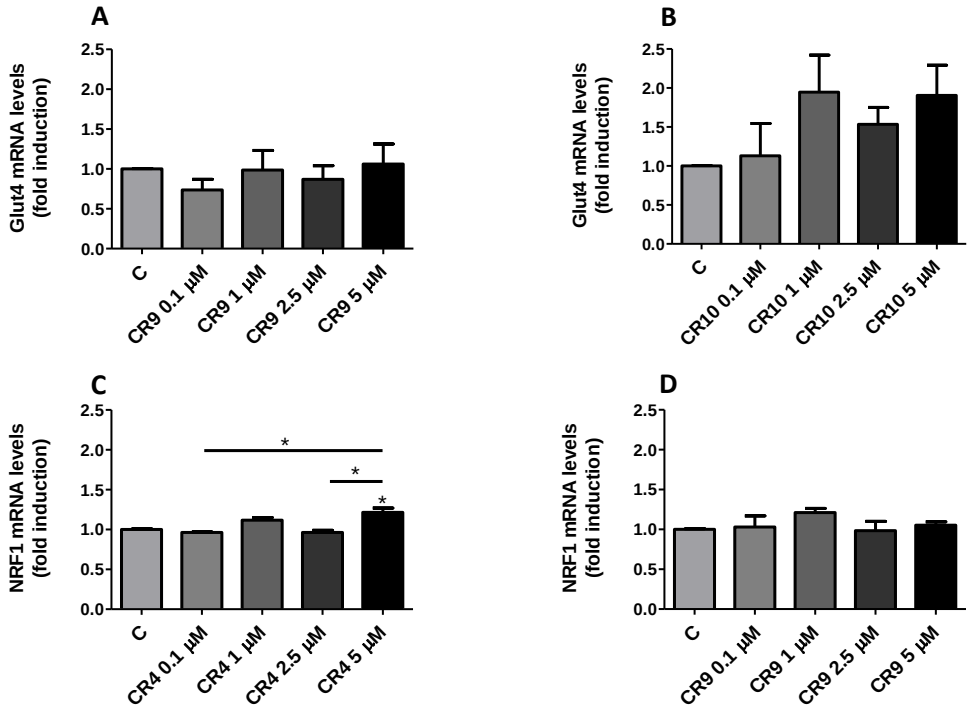

Figure III.5. Relative Glut-4 and NRF-1 mRNA levels, in N2a cells after treatment with the selected compounds (CR4, CR5, CR9, CR10 and CR11) at different concentrations. Cells were treated with each of the five selected compounds, at four different concentrations: 0.1 µM, 1 µM, 2.5 µM and 5 µM; and then incubated for 7 h, as described in 'Materials and Methods'. Total RNA was extracted from each sample and Glut-4 mRNA levels (upper panel – A, B) and NRF-1 mRNA levels (lower panel – C, D) were determined by reverse transcription quantitative PCR. Glut-4 mRNA levels in N2a treated with: **A.** CR9 and **B.** CR10 and NRF-1 mRNA levels in N2a treated with: **C.** CR4 and **D.** CR9 are depicted. mRNA relative levels of EEF were determined in parallel as a housekeeping gene and used as a normalization tool, resorting to the $\Delta\Delta C_T$ method. Results are representative of 3 independent experiments, for Glut-4 mRNA levels and of 2 independent experiments, for NRF-1 mRNA levels (* $p < 0.05$, ** $p < 0.01$, *** $p < 0.001$); the symbol '*' refers to the change vs control, except if otherwise indicated.

3. Evaluation of the effects of each selected compound in a cellular model of Parkinson's disease

In this study, MPP^+ was the chosen stimulus to recapitulate some biochemical features of Parkinson's disease, in the selected cellular model. Although this is a widely used model, a series of experiments were conducted to determine the effects of this neurotoxin on N2a cell viability and ATP levels.

Cells were treated with different concentrations of MPP^+, 100 µM, 250 µM, 500 µM and 1 mM and incubated for 16 h. An MTT assay was carried out, to assess the effects of MPP^+ on cell viability. All the tested MPP^+ concentrations affected cell viability, in a concentration-dependent manner. However, only the 500 µM and 1 mM concentrations showed statistical significance, when compared to the control (Figure III.6.). For this reason, the chosen concentration of MPP^+ to proceed with the following experiments was 1 mM.

Since MPP^+ is known to inhibit complex I, of the mitochondrial ETC, we next assessed the effects of different MPP^+ concentrations, on ATP levels. The concentrations used were the same described above for the MTT assay, although in these experiments we tested three different time-points (1 h, 3 h and 16 h), to follow the cellular response on ATP depletion and recovery (Figure III.7.). After 1 h incubation, cells suffered an ATP depletion, approximately by half, when compared to the control (untreated cells). Although, all tested concentrations were statistically different from the control condition, no statistical significance was found between the tested concentrations (Figure III.7. A). After 3 h incubation, again an ATP depletion was visible in all tested concentrations. At this time-point, all concentrations showed statistical significance, when compared to control cells. Additionally, the 1 mM concentration showed the highest depletion of ATP, being statistically different from all other tested concentrations (Figure III.7. B). However, at the 16 h incubation time-point no significant ATP depletion was found in any of the concentrations, suggesting a possible recovery of the cells (Figure III.7. C). Therefore, a concentration of 1 mM MPP^+ at the 3 h time-point, were the conditions chosen to proceed with the following experiments.

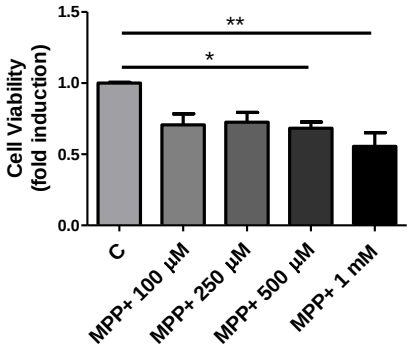

Figure III.6. N2a cell viability in response to MPP^+. N2a cells were treated with four different concentrations of MPP^+, 100 µM, 250 µM, 500 µM and 1 mM and incubated for 16 h, in order to assess the dose-response to MPP^+. Cell viability assessed by MTT was determined as fold induction of control (untreated cells). Results are representative of 3 independent experiments (* $p < 0.05$, ** $p < 0.01$, *** $p < 0.001$); the symbol '*' refers to the change vs control, except if otherwise indicated.

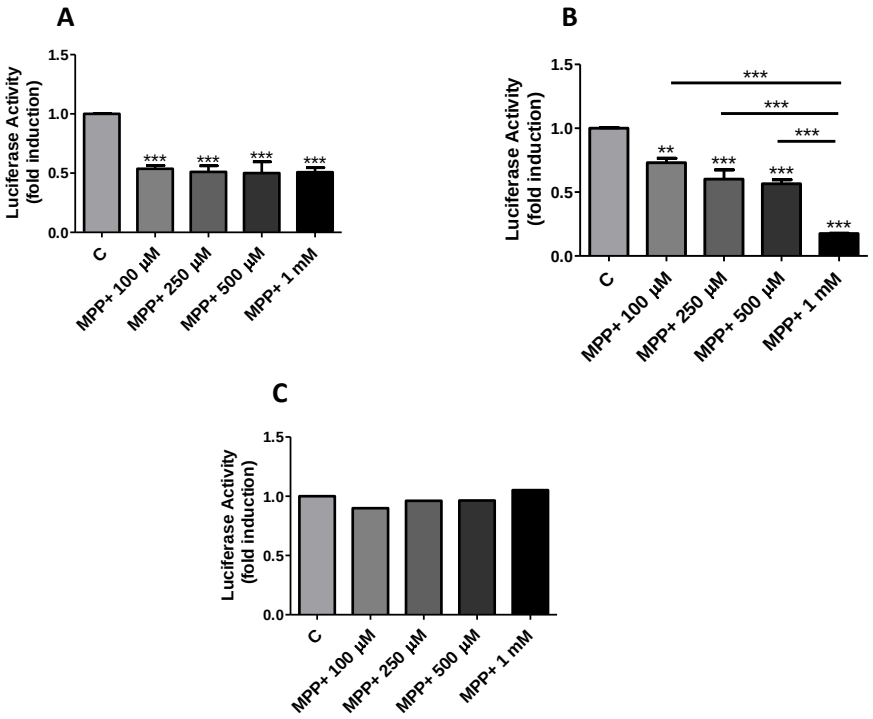

Figure III.7. ATP levels upon treatment with MPP^+ (time- and dose-response), in N2a cells. N2a cells were treated with four different concentrations of MPP^+, 100 µM, 250 µM, 500 µM and 1 mM, and incubated for **A.** 1 h, **B.** 3 h and **C.** 16 h. ATP levels assessed by Luciferase activity were determined as fold induction of control (untreated cells) and normalized to protein content, using Bradford assay. Results are representative of 4 independent experiments and 1 experiment for the 16 h incubation period (* $p < 0.05$, ** $p < 0.01$, *** $p < 0.001$); the symbol '*' refers to the change vs control, except if otherwise indicated.

3.1. Effect of compounds on cell viability, ATP levels and ROS production upon MPP^+ treatment

To understand if the selected compounds had any preventive/protective effect on cell viability after treatment with MPP^+, cells were pre-treated with each of the compounds, and then treated with the neurotoxin, as described in "Materials and Methods".

Figure III.8. shows that all the tested compounds were able to reverse the MPP^+ effects on cell viability, to some extent, with the exception of CR9 and CR10.

Although CR9 (Figure III.8. C) didn't present a significant toxicity to cells, when treated simultaneously with the neurotoxin, it was also not able to recover cell viability to the levels of cells treated only with the compound.

In the case of CR10 (Figure III.8. D), the compound itself demonstrated toxicity to cells, showing to be statistical different from the control condition, in accordance with what we have already seen in the first cell viability assays (Figure III.2.). MPP^+ showed more toxicity than the compound and when cells were treated with both, CR10 and MPP^+ present similar viability levels as displayed by cells treated only with the compound.

While all other compounds showed a tendency to revert MPP^+ toxicity, none could recover cell viability to similar levels of cells treated only with the compound.

Together, these results suggest a protective effect to cells by CR4, CR5 and CR11 compounds, although no full recovery of cell viability was observed.

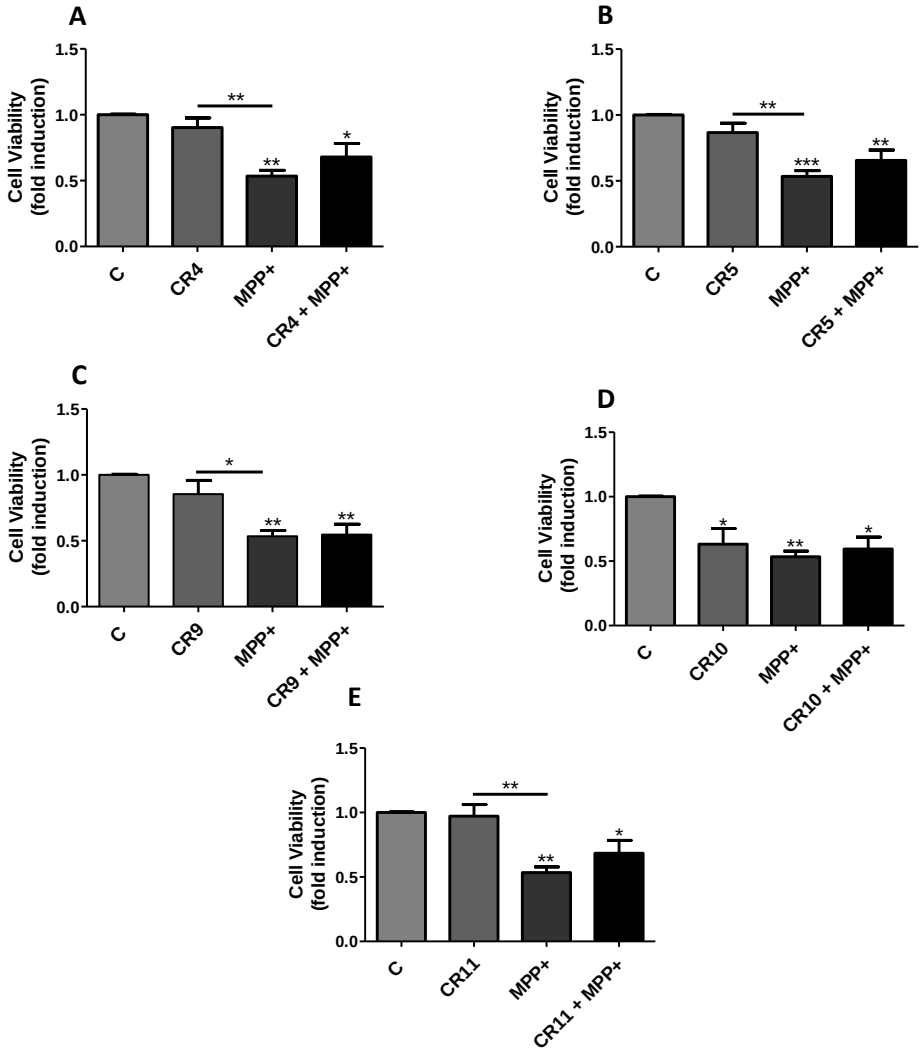

Figure III.8. Effect of CR compounds on cell viability upon MPP^+ treatment. N2a cells were treated with five compounds, **A.** CR4, **B.** CR5, **C.** CR9, **D.** CR10 and **E.** CR11, at a concentration of 1 µM, for 7 h and treated with MPP^+ 1 mM, for 16 h, as described in 'Materials and Methods'. Cell viability assessed by MTT was determined as fold induction of control (untreated cells). Results are representative of 4 independent experiments (* $p < 0.05$, ** $p < 0.01$, *** $p < 0.001$); the symbol '*' refers to the change vs control, except if otherwise indicated.

As depicted in Figure III.9., MPP^+ seemed to induce a decrease in the ATP levels when compared to the control condition, although statistical significance was not achieved. Additionally, most of the tested compounds showed a tendency to increase the ATP levels in N2a cells before and/or after MPP^+ treatment, with CR4 (Figure III.9. A) demonstrating a significant increase, when compared with the MPP^+ treatment and with the combined (compound and neurotoxin) treatment. Following CR4, the compounds that showed the highest trend to recover ATP levels were, respectively, CR10, CR11, CR9 and finally, CR5 (Figure III.9.).

Again, all tested compounds showed a tendency to recover the ATP levels, when compared to the MPP^+ treated condition. CR10 was the most efficient in recovering ATP levels upon treatment with the neurotoxin, leading to a full restoration of ATP levels, even, when compared with both the control and the cells treated only with the compound. Furthermore, although combined treatment with CR4 and MPP^+ leads to lower ATP levels, as compared to CR4 alone, the statistical significance is smaller than if we compare CR4 to MPP^+ alone, suggesting that the presence of CR4 might somehow avoid a more pronounced ATP decrease induced by MPP^+. Following these two compounds, CR5 and CR11 were the ones that showed the highest tendency to reverse MPP^+ decrease in ATP levels, when comparing to control and to the compound treatment. However, no statistical significance was found.

Taken together, the results regarding cell viability and ATP levels, show that CR4, CR5 and CR11 showed a tendency to recover both parameters. Although CR10 was the compound that demonstrated the highest recovery in the ATP levels of N2a cells, it was also the compound that presented more toxicity and therefore, could only partially revert the loss of cell viability induced by MPP^+ (Figure III.8. D).

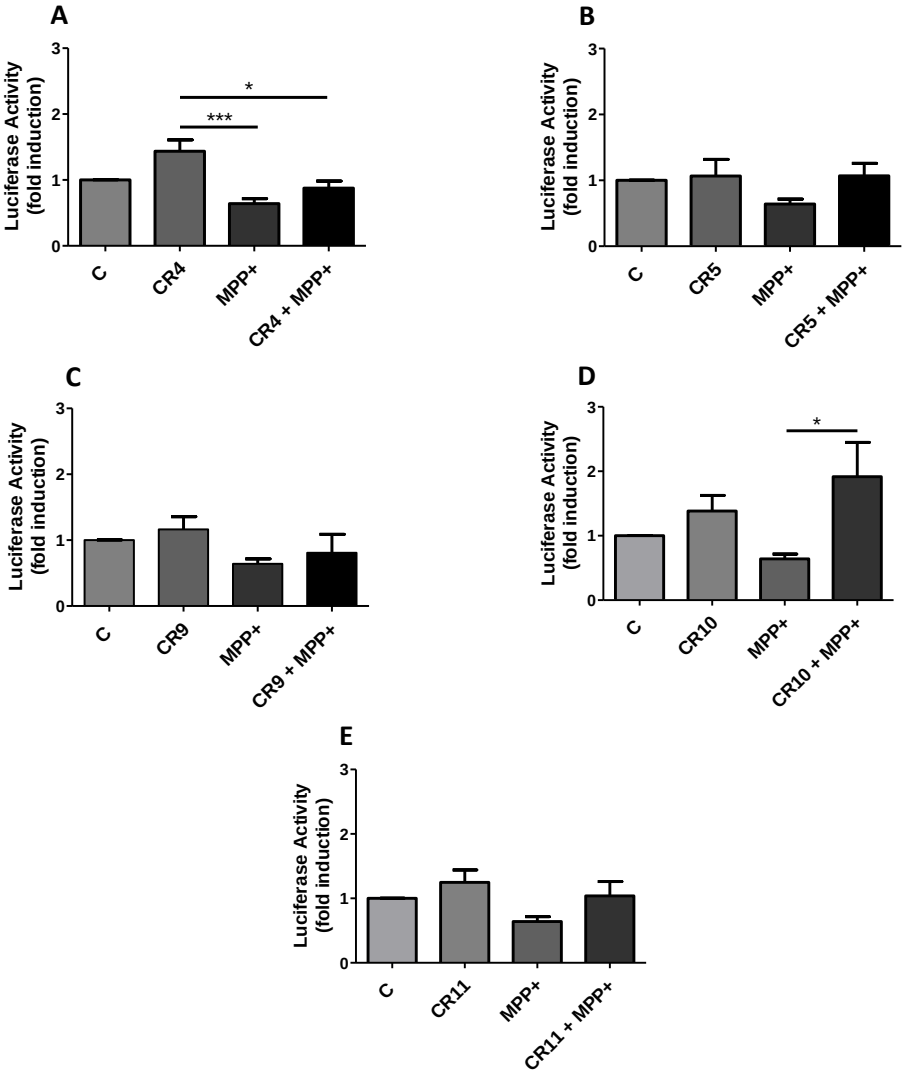

Figure III.9. ATP levels on N2a cells assessed by a Luciferase activity assay, after treatment with either each one of the compounds, MPP^+ or the combined treatment. N2a cells were treated with five compounds, **A.** CR4, **B.** CR5, **C.** CR9, **D.** CR10 and **E.** CR11, at a concentration of 1 µM, for 7 h and treated with MPP^+ 1 mM, for 3 h, as described in 'Materials and Methods'. ATP levels assessed by Luciferase activity were determined as fold induction of control (untreated cells) and normalized to protein content, using Bradford assay. Results are representative of 4 independent experiments (* $p < 0.05$, ** $p < 0.01$, *** $p < 0.001$); the symbol '*' refers to the change vs control, except if otherwise indicated.

Since ROS accumulation is a common feature in PD and cellular models of PD treated with MPP^+, a ROS production assay using a 2',7'-dichlorofluorescein diacetate probe was performed[75,164]. The aim of this assay was to evaluate the levels of ROS production, upon treatment with either the selected compounds, MPP^+ or the combined treatment and to assess any protective effects of the compounds over this feature.

Figure III.10. shows that MPP^+ seemed to increase ROS production levels, when compared to the control, although no statistical significance was found. In general, all the tested compounds showed a tendency to slightly increase ROS production, although CR4 to a lower extent (Figure III.10. A). Additionally, CR10 (Figure III.10. D) and CR11 (Figure III.10. E) were the compounds that seemed to show the highest levels of ROS production, almost achieving the levels of the MPP^+-treated cells.

Interestingly, all the compounds exhibited a decrease in ROS production in the combined treatment (compound and MPP^+), when compared to the MPP^+ treated cells, suggesting a possible protective effect. Moreover, CR9 (Figure III.10. C) followed by CR4 demonstrated the higher capacity to restore the levels of ROS production, in comparison to the control condition.

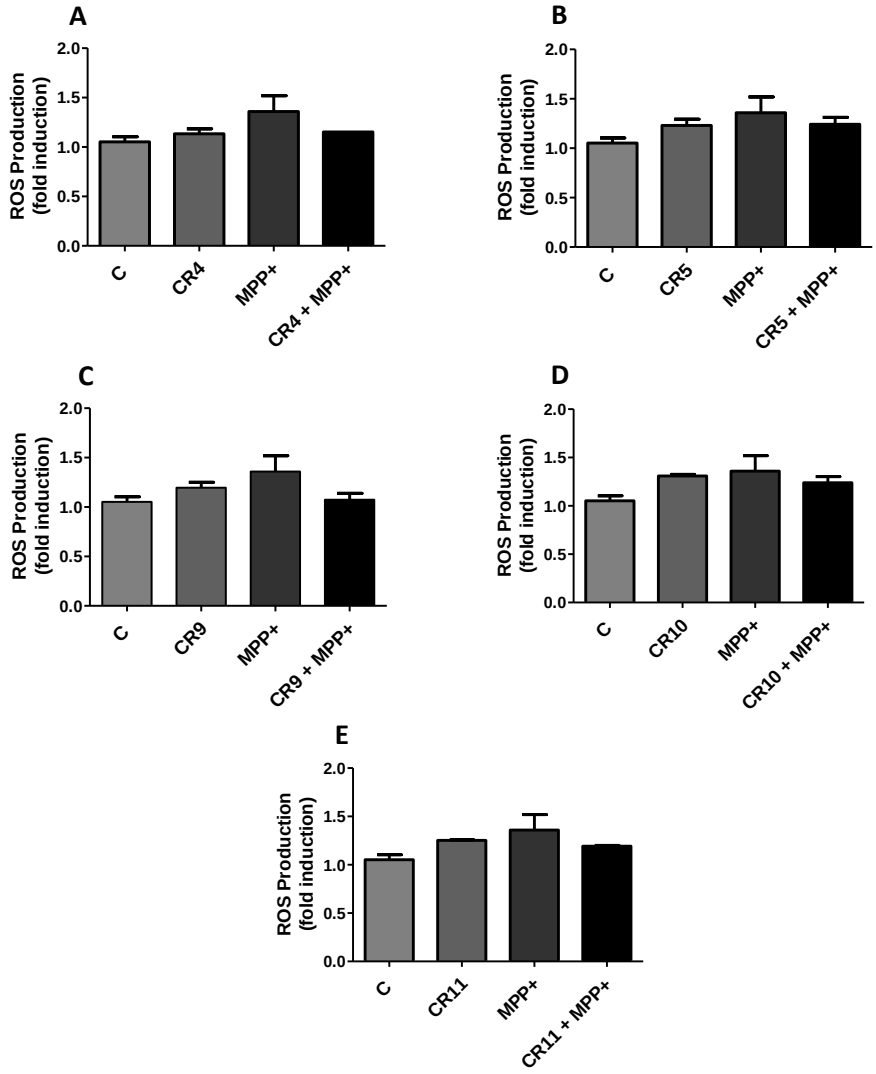

Figure III.10. ROS production in N2a cells after treatment with either each one of the compounds, MPP^+ or the combined treatment. N2a cells were treated with five compounds, **A.** CR4, **B.** CR5, **C.** CR9, **D.** CR10 and **E.** CR11 at a concentration of 1 µM, for 7 h and treated with MPP^+ 1 mM, for 3 h, as described in 'Materials and Methods'. ROS production levels were assessed using a H_2DCF-DA fluorescent probe. Levels of ROS production were determined as fold induction of control (untreated cells) and normalized to protein content, using Bradford assay. Results are representative of 2 independent experiments.

3.2. Effect of compounds on PGC-1α1 downstream targets upon MPP^+ treatment

In order to understand how each selected compound would modulate PGC-1α1, consequently leading to changes in its downstream targets, in the presence or absence of MPP^+, seven downstream targets were evaluated by qPCR, namely ERRα, NRF-1, CPT1α, Glut-4, UCP1, SREBP1c and XBP1s.

At the 1 μM concentration, CR4 was only able to increase NRF-1 mRNA relative expression levels, showing statistical significance (Figure III.11. A). However, no differences were found between MPP^+ treatment and the combined treatment (compound and MPP^+).

Regarding CR9, it tended to increase the mRNA levels of CPT1α (Figure III.12. A) and, although it was not able to increase SREBP1c mRNA levels, it seemed to restore these levels to control levels, upon treatment with MPP^+ (Figure III.14. A).

CR10 seemed to exhibit an increase in both mRNA levels of Glut-4 (data not shown) and of UCP1 (Figure III.13. B), although no statistical significance was found. Curiously, this compound seemed to downregulate CPT1α mRNA levels (Figure III.12. B) and, although it showed a tendency to reverse the effects of MPP^+ stimulus, it was not able to modulate the mRNA levels of both SREBP1c (Figure III.14. B) and XBP-1s (Figure III.15. A), when cells were treated with the compound, alone.

Finally, CR11 was the compound that showed a tendency to increase most of the tested genes, namely ERRα (data not shown), NRF-1 (Figure III.11. B), Glut-4 (data not shown), UCP1 (Figure III.13. C), SREBP1c (Figure III.14. C) and XBP-1s (Figure III.15. B). However, no statistical significance was found in these experiments.

Although we were evaluating PGC-1α1 downstream targets, to assess its stabilization, the fact that some compounds didn't increase some of the targets' mRNA levels, doesn't mean that a positive modulation on PGC-1α1 hasn't occur. Accordingly, each of the tested downstream targets are involved in different functions and play different roles in the pathways regulated by PGC-1α1, suggesting that in a given scenario some pathways might be active to the detriment of others.

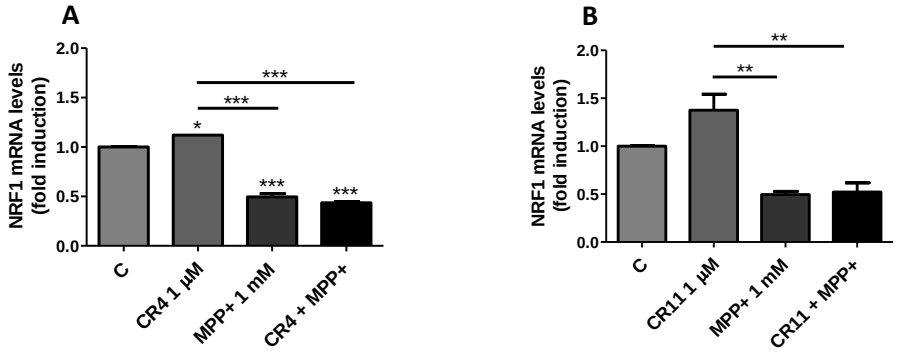

Figure III.11. NRF-1 relative mRNA levels, in N2a cells after treatment with either each one of the compounds, MPP^+ or the combined treatment. Cells were pre-treated with each of the five selected compounds, at the concentration of 1 µM and incubated for 7 h. After this treatment, cells were subjected to a new treatment with MPP^+ 1 mM, for 16 h, as described in 'Materials and Methods'. Total RNA was extracted from each sample and NRF-1 mRNA levels were determined by reverse transcription quantitative PCR. NRF-1 mRNA levels in N2a treated with: **A.** CR4 and **B.** CR11 are depicted. mRNA relative levels of EEF were determined in parallel as a housekeeping gene and used as a normalization factor, resorting to the $\Delta\Delta C_T$ method. Results are representative of 3 independent experiments (* $p < 0.05$, ** $p < 0.01$, *** $p < 0.001$); the symbol '*' refers to the change vs control, except if otherwise indicated.

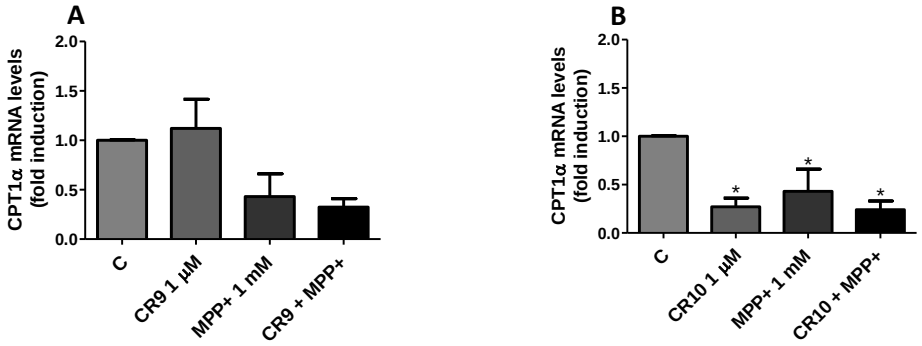

Figure III.12. CPT1α relative mRNA levels, in N2a cells after treatment with either each one of the compounds, MPP^+ or the combined treatment. Cells were pre-treated with each of the five selected compounds, at the concentration of 1 µM and incubated for 7 h. After this treatment, cells were subjected to a new treatment with MPP^+ 1 mM, for 16 h, as described in 'Materials and Methods'. Total RNA was extracted from each sample and CPT1α mRNA levels were determined by reverse transcription quantitative PCR. CPT1α mRNA levels in N2a treated with: **A.** CR9 and **B.** CR10 are depicted. mRNA relative levels of EEF were determined in parallel as a housekeeping gene and used as a normalization factor, resorting to the $\Delta\Delta C_T$ method. Results are representative of 3 independent experiments (* $p < 0.05$, ** $p < 0.01$, *** $p < 0.001$); the symbol '*' refers to the change vs control, except if otherwise indicated.

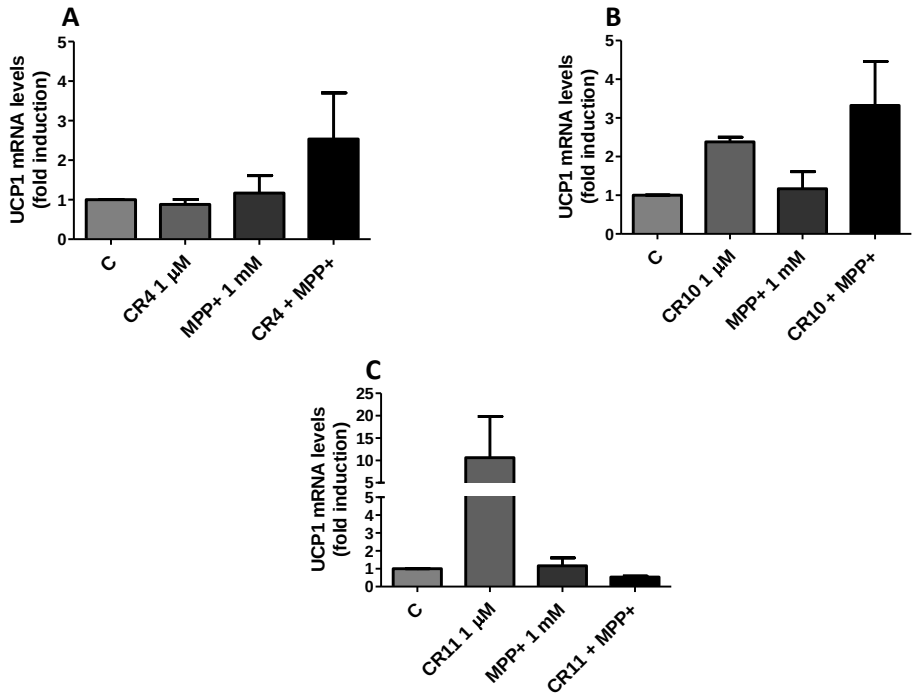

Figure III.13. UCP1 relative mRNA levels, in N2a cells after treatment with either each one of the compounds, MPP^+ or the combined treatment. Cells were pre-treated with each of the five selected compounds, at the concentration of 1 µM and incubated for 7 h. After this treatment, cells were subjected to a new treatment with MPP^+ 1 mM, for 16 h, as described in 'Materials and Methods'. Total RNA was extracted from each sample and UCP1 mRNA levels were determined by reverse transcription quantitative PCR. UCP1 mRNA levels in N2a treated with: **A.** CR4; **B.** CR10 and **C.** CR11 are depicted. mRNA relative levels of EEF were determined in parallel as a housekeeping gene and used as a normalization factor, resorting to the $\Delta\Delta C_T$ method. Results are representative of 3 independent experiments.

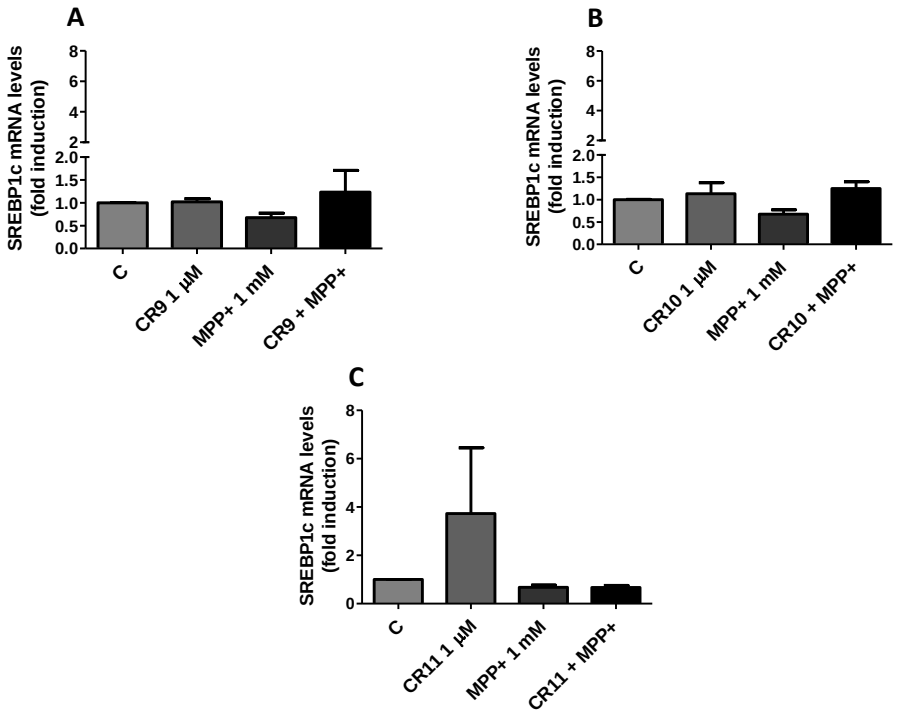

Figure III.14. SREBP1c relative mRNA levels, in N2a cells after treatment with either each one of the compounds, MPP^+ or the combined treatment. Cells were pre-treated with each of the five selected compounds, at the concentration of 1 µM and incubated for 7 h. After this treatment, cells were subjected to a new treatment with MPP^+ 1 mM, for 16 h, as described in 'Materials and Methods'. Total RNA was extracted from each sample and SREBP1c mRNA levels were determined by reverse transcription quantitative PCR. SREBP1c mRNA levels in N2a treated with: **A.** CR9; **B.** CR10 and **C.** CR11 are depicted. mRNA relative levels of EEF were determined in parallel as a housekeeping gene and used as a normalization factor, resorting to the $\Delta\Delta C_T$ method. Results are representative of 3 independent experiments.

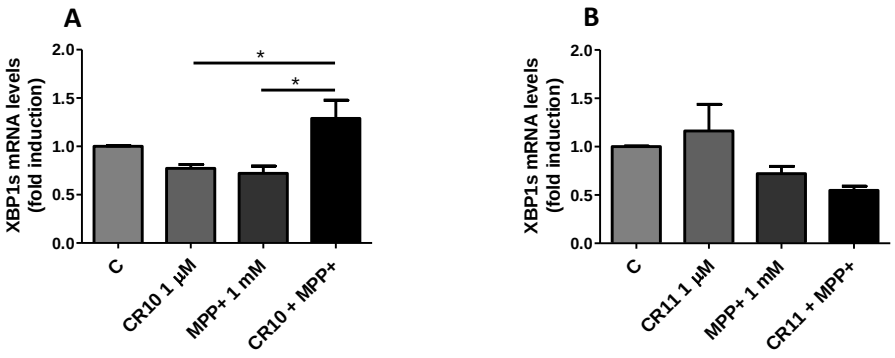

Figure III.15. Relative XBP1s mRNA levels, in N2a cells after treatment with either each one of the compounds, MPP^+ or the combined treatment. Cells were pre-treated with each of the five selected compounds, at the concentration of 1 µM and incubated for 7 h. After this treatment, cells were subjected to a new treatment with MPP^+ 1 mM, for 16 h, as described in 'Materials and Methods'. Total RNA was extracted from each sample and XBP1s mRNA levels were determined by reverse transcription quantitative PCR. XBP1s mRNA levels in N2a treated with: **A.** CR10 and **B.** CR11 are determined. mRNA relative levels of EEF were determined in parallel as a housekeeping gene and used as a normalization tool, resorting to the $\Delta\Delta C_T$ method. Results are representative of 3 independent experiments (* $p < 0.05$, ** $p < 0.01$, *** $p < 0.001$); the symbol '*' refers to the change vs control, except if otherwise indicated.

4. The p-CREB pathway appears to be involved in PGC-1α1 regulation by CR10

CREB is one of the main pathways involved in the activation of PGC-1α1. Its phosphorylation can be promoted by several different stimuli that will lead to its binding to a CRE at the PGC-1α promoter. Increasing PGC-1α1 gene transcription will consequently induce the expression of PGC-1α1 downstream targets, such as NRF-1, Tfam and Cyt C[165,166]. Therefore, we determined CREB protein and phosphorylation levels in N2a cells treated with either the selected compounds, MPP^+ or the combination of both.

Figure III.16. shows that, from all the selected compounds, only CR10 tended to increase the levels of CREB phosphorylation, although no statistical significance was found (Figure III.16. D). Interestingly, for all tested compounds both conditions treated with MPP^+ demonstrated a tendency to increase the phosphorylated form of CREB. Furthermore, the increase observed in N2a cells treated with both CR10 and MPP^+, suggest an accumulation of the effect observed in the CR10 and the MPP^+ treatments, alone, although not statistically significant.

Evaluating the modulation of the p-CREB expression levels could be an indirect way to assess the activation of PGC-1α1, by the selected compounds. Furthermore, understanding if any of the compounds possesses the capacity to positively influence CREB phosphorylation give us the notion of the pathway by which PGC-1α1 is being activated. Nonetheless, the fact that most of the selected compounds didn't positively regulate CREB doesn't mean that they are not having a positive effect over PGC-1α1, since they could be activating it through other pathways that don't involve CREB.

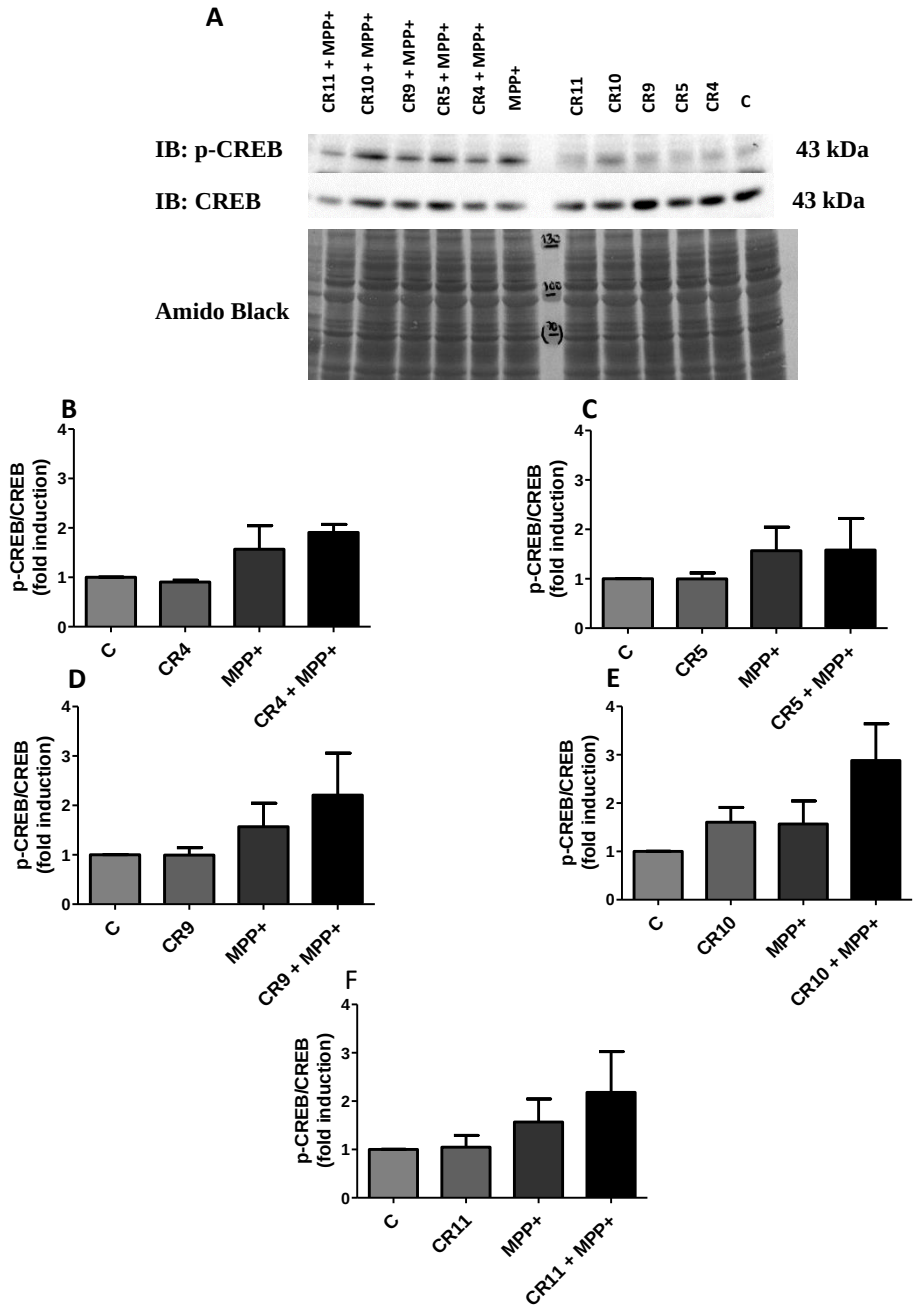

Figure III.16. p-CREB protein expression levels, in N2a cells after treatment with either each one of the compounds, MPP^+ or the combined treatment. Cells were pre-treated with each of the five selected compounds, at the concentration of 1 µM and incubated for 7 h. After this treatment, cells were subjected to a new treatment with MPP^+ 1 mM, for 16 h, as described in 'Materials and Methods'. **A.** Protein extracts were separated by SDS/PAGE and the corresponding immunoblots were probed with a p-CREB and Total-CREB antibodies. Expression values of the protein were obtained by determination of the ratio with the total protein levels and analysis of Amido black was performed in parallel as a loading control. Data were separated into different graphs, each representing p-CREB protein expression levels referring to the respective compound treatment: **B.** CR4; **C.** CR5; **D.** CR9; **E.**CR10 and **F.** CR11. Data are expressed as the mean values ± SEM and p-CREB/Total-CREB ratios are shown as fold induction over untreated control. Results are representative of 3 independent experiments.

Another interesting pathway that should be considered is the regulation of PGC-1α1 through Parkin-PARIS, as already described[103]. Indeed, a group of experiments were conducted by Western Blot to assess the protein expression levels of both Parkin and its substrate PARIS, to evaluate the possibility of some of the compounds to be stabilizing PGC-1α1, through this pathway (data not shown). However, it was not possible to take any conclusions from the preliminary results obtained. Furthermore, more independent experiments need to be conducted, in order to conclude any possible intervention of this pathway, on the presence of the selected compounds.

IV. DISCUSSION

Severe mitochondrial alterations, leading to decreased mitochondrial function and energy production, have been associated to axonal and neuronal loss in neurodegenerative diseases[49,50]. PGC-1α1 is a key regulator of mitochondrial biogenesis and metabolism and coordinates crucial mitochondrial processes, such as antioxidant defence mechanisms, energy metabolism and mitochondrial DNA transcription[30,131,132] .

In the present study we explored the biological capacity of a group of eleven small molecules, previously selected from a cell-based HTS, to stabilize PGC-1α1, in a mouse neuroblastoma cell-line, under physiological conditions and upon a neurotoxic insult.

The selection of compounds was extracted from the study where they were identified and validated using brown adipocyte cultures, where PGC-1α was first identified[114]. Furthermore, brown adipose tissue, skeletal muscle and fasted liver correspond to the tissues with the highest levels of expression of this coactivator, whereas the brain was shown to express only moderate levels, despite being a highly energy demanding tissue[164]. From the first steps of this validation process we selected the 1 μM concentration to all compounds, since it didn't display toxicity to N2a cells. This concentration corresponds to one tenth of the concentration used by Ruas and col. in brown adipocytes[163]. This suggests a higher sensitization of neuronal cells, to the compounds when compared to brown adipocytes. It can also suggest that N2a cells are more efficient at internalizing the compound than adipocytes, so that the intracellular concentration would be higher in N2a, despite being treated with lower doses.

Several studies have demonstrated that NRF-1, ERRα and PPARs are some of the downstream targets of PGC-1α1, showing increased expression levels in response to upregulation of this coactivator. Moreover, this leads to upregulation of components of the mitochondrial complexes I-V, as well as an increase in Tfam and Cyt C expression levels[167,142,168]. In addition, PGC-1α1 is also known to increase the expression of genes involved in ROS removal, such as SOD2 and GPx1[168] and UCPs, namely 1, 2 and 3[114,142]. Some of these genes and a group of others, also known to increase along with increased stability in PGC-1α1, such as Glut-4 and CPT1α were evaluated, at the level of their mRNA expression. In accordance, some compounds seemed to positively modulate the levels of expression of some of these genes, at the chosen concentration, although not at the same extent. Additionally, not all compounds were able to modulate the same tested genes, reinforcing the notion that these compounds might act through different mechanisms. For example, CR4 was only able to increase NRF-1 mRNA levels of expression, not affecting the levels of Tfam or ERRα, at the selected concentration. Conversely,

CR10 only tended to increase the expression levels of Glut-4. These results strongly suggest that, if the compounds are stabilizing PGC-1α1 they are probably modulating its levels through different pathways. Indeed, NRF-1 does not only promote the direct increase of Tfam, but also of Cyt C, although through cAMP activation and, consequently through CREB phosphorylation[168,165,166]. These changes in NRF-1 mRNA levels could then be responsible for a cellular adaptation to the stimulus by inducing respiratory mechanisms instead of mitochondrial biogenesis[168].

Upon the understanding that some of the compounds could indeed be stabilizing PGC-1α1, we next evaluated the possible protective effects of pre-conditioning, by treating N2a cells with the selected compounds and subsequently with MPP^+.

Since MPP^+ is a widely used model to recapitulate some cellular features of PD[2], we were able to observe a significant decrease in cell viability, assessed by MTT, in N2a cells treated with MPP^+ 1 mM. Additionally, we also observed a trend for increased levels of ROS, as observed by Requejo-Aguilar and Bolaños[52] and decreased levels of ATP, as previously described by Maruoka *et. al* and Burté *et. al*[83,78].

The dual behaviour of cells, upon treatment with different concentrations of MPP^+, observed in the different incubation periods of the ATP levels and the MTT assays, suggests an interesting response of cells to the stimulus. On one hand, after a short period of incubation with the neurotoxin, cells first respond to the decreased levels of ATP, since by inhibiting the mitochondria complex I, MPP^+ leads to a rapid perturbation of the whole ETC and, consequently of ATP production. On the other hand, after a longer period of incubation, although cells were able to restore their ATP content, the prolonged exposure to the neurotoxin will lead to dampening of other cellular processes and consequently to loss of viability and ultimately to cell death.

Remarkably, cancer cells are known to shift from oxidative phosphorylation to glycolysis to produce energy, which is known as the Warburg effect[52]. N2a cells are tumour-derived and may exhibit this intrinsic property. Since MPP^+ hampers oxidative phosphorylation, they could become dependent on glycolysis for ATP production, explaining the restoration of ATP content, after 16 h under MPP^+ stimulus.

CR10 and CR11 were the compounds that showed a tendency to increase ATP levels the most, both in the treatment with the compound and in the combined treatment. Additionally, CR10 was the compound that most significantly restored and even increased ATP levels, upon MPP^+ treatment. Interestingly, these two compounds were also the ones that exhibited the highest trend to induce Glut-4 and UCP1 mRNA levels. Activation of PGC-1α1 can be followed by

increased levels of Glut-4[169,170] and of UCP1[163]. According to Ruas and col., when measuring oxygen consumption rates in brown adipocytes, both CR10 (AM31) and CR11 (AM80), significantly increased basal respiration and uncoupled respiration by 38% and 16%, respectively[163]. However, no change in ATP coupled respiration was demonstrated and only CR11 showed a tendency to increase the maximal respiratory capacity. Assuming that this behaviour is maintained in neuronal cells, which appears to be, considering the UCP1 mRNA levels, the increase in ATP levels that tended to be promoted by these two compounds can be explained by increased glycolysis. The increased levels of Glut-4 suggest an increased glucose uptake by cells, which could be due to higher glucose utilization for energy production, through glycolysis.

Studies have showed that the production of energy by astrocytes is mainly glycolytic[171,172], while neurons rely on oxidative phosphorylation[173], being the first cells responsible for responding to the energy needs of the latter[174]. Although, another study has revealed that neurons might rely on glycolysis, under specific high energy demanding cellular events, such as synaptic transmission[175]. Indeed, it was demonstrated that Glut-4 is recruited during neuronal activity to increase glucose uptake and upregulate glycolysis. This process is thought to occur with the help of cytosolic malate dehydrogenase, that by converting aspartate into malate, leads to re-oxidation of NADH. Meanwhile, mitochondrial NADH is thought to create a proton gradient in the ETC, used by complex V to produce ATP[176].

CR4 was the third compound to induce the highest levels of ATP, even demonstrating a restoration of these levels after treatment with MPP^+. Indeed, CR4 was also the compound that showed the most significant increase in NRF-1 mRNA levels, which according with what was described above, could be promoting cell respiratory capacity through cAMP/CREB/Cyt C. However, when N2a cells were treated with both CR4 and MPP^+, NRF-1 mRNA levels were decreased at the same extent that when cells were only treated with MPP^+. Thus, CR4 seemed to be able to almost completely restore ATP levels, upon MPP^+ stimulus, suggesting the existence of a parallel pathway, involved in the protective effects of this compounds, over MPP^+.

Although, several of the results presented in this thesis didn't show statistical significance and can only be represented as tendencies, that does not necessary mean that biological differences aren't meaningful within cells and that PGC-1α1 is not being stabilized. Indeed, PGC-1α1 is known to possess a short half-life, under unstimulated and ectopic expression conditions[3,163,166]. In addition, PGC-1α overexpression might also, in some conditions, aggravate neuron degeneration[164], suggesting that the beneficial effects of this coactivator overexpression are

within moderate levels at the physiological range. A great caution is needed when modulating PGC-1α1 to not exceed these levels. Therefore, our compounds could be modulating the expression of PGC-1α1, near physiological levels, partially explaining the reason why no statistical significance was achieved.

Another interesting feature that we observed in our results, was the possibility of MPP^+ also be inducing PGC-1α1 expression. From our results we could observe that both UCP1 and Glut-4 mRNA levels were increased upon treatment with MPP^+. In addition, p-CREB protein expression levels also showed a tendency to increase under MPP^+ stimulus. Accordingly, Ye *et al.* observed that under MPP^+ treatment PGC-1α mRNA levels were increased, although a decrease in its protein expression levels, along with ERRα and NRF-1 expression levels were also observed[167]. Furthermore, another study has revealed that mitochondrial biogenesis can be triggered by environmental stresses that ultimately lead to oxidative stress[177]. A different study conducted in animal models of PD revealed that ninety minutes after MPTP acute administration, three different isoforms of PGC-1α, full-length, NT- and CNS-, were all increased in three different regions of the mice's brains, namely *striatum*, cortex and *cerebellum*[178]. Additionally, seven days after the last MPTP administration the levels of these three isoforms were all decreased, especially the CNS-isoform. Comparing this acute treatment with a low-dose chronic administration of MPTP, Torok and colleagues were not able to observe the same increase in the PGC-1α isoforms[178].

Interestingly, a study using lead as an oxidative stress inducer, showed that when cells were exposed to this toxin for a short period of 3 h, the tested concentrations of 100 μM and 500 μM were both able to significantly increase PGC-1α transcriptional levels. Additionally, after an incubation period of 48 h, only the lowest tested concentration was able to sustain this increase, along with increased levels of PGC-1α downstream targets, such as NRF-1 and Tfam[179].

Taken together, these results might be suggesting a short-term compensatory and protective response against the neurotoxin, that is evident under short incubation periods. These findings could be also revealing that the incubation periods are very important to assess PGC-1α1 stabilization and that, probably longer periods of incubation should also be tested, in the form of a chronic treatment, with MPP^+ and/or the selected compounds, to better understand its protective effects in cell death and its effects in PGC-1α1 stabilization.

Another interesting fact that we observed and corroborates the importance of choosing the right incubation periods, is the significant increase of NRF-1 mRNA levels by CR4 and a significant decrease of this same target gene and others, such as ERRα by CR10. However, when assessing p-CREB protein expression levels, which could be an indicative of PGC-1α1 activation and of

its downstream targets, only CR10 showed a tendency to increase these levels, with CR4 even exhibiting a slightly trend to decrease these same levels. Since, both mRNA levels and protein expression levels were assessed after a 16 h incubation period and differences in these two cellular events may not be observed within the same time-points, this could suggest that what we observe in both cases could be either a reminiscence of the response to the compounds or a begin of the same response.

Understanding through which pathways PGC-1α1 is being activated is very important to assess the mechanism by which each compound could be affecting its stabilization. For instance, phosphorylation of PGC-1α1 through p38 MAPK is known to increase its half-life, stabilizing this coactivator and enhancing its co-transcriptional activity[166]. Indeed, PGC-1α1 can suffer different PTM that depending on the external signal, can either downregulate or upregulate its expression. Moreover, PTMs are also very important in the targeting of specific genes[111], as well as regulation of protein stability, function and localization[126]. Therefore, the selected compounds could be regulating these modifications towards PGC-1α1 stabilization, targeting its function to the regulation of specific genes, such as increasing cellular glucose uptake or respiration.

Although the biological activity of the tested compounds is not known, we observed that some of these compounds demonstrated protective effects in MPP^+-treated cells, with the most interesting results regarding ATP levels and cell viability. Indeed, we were able to observe a restoration, or at least a tendency, to increase both the ATP levels and cell viability of N2a cells, upon pre-conditioning with the selected compounds and treatment with MPP^+. While PGC-1α1 downstream targets mRNA levels and protein expression levels of other proteins involved in its activation pathways were not very elucidative, efforts should be made to try to understand if the compounds could be having positive effects on its regulation. In the future, it would also be interesting to address the oxygen consumption rate capacity of some of the selected compounds, especially the ones demonstrating the highest capacity to increase ATP levels, in N2a cells. Moreover, other pathways involved in PGC-1α1 activation should be tested, in N2a cells, such as the insulin receptor substrate 1 and other downstream targets and its respective proteins expression levels, namely Cyt C, UCP 2 and 3. Measuring the levels of certain glycolytic enzymes, such as phosphofructokinase or pyruvate kinase, could also be interesting. Furthermore, a more extensive study on the different concentrations of the tested compounds should be taken into consideration, since some of the selected compounds didn't present toxicity to cells at the higher tested concentrations. Although, due to time management we selected a single concentration to all compounds, a more extensive approach using higher concentrations

could be beneficial to this project and positive results could be obtained, regarding the effects of these compounds on cells. Understanding the interplay between primary cultured neurons and astrocytes and the possible effects of each selected compounds in both cell types would also be interesting, since effects could be more prominent in astrocytes than neurons and in the spectrum of the whole brain, all types of cells interact between themselves.

PGC-1α has been shown to be a major coactivator in several tissues, with more relevance to oxidative tissues. Finding compounds that modulate and stabilize this coactivator, within physiological levels, in these tissues, is of great importance in order to allow the development of common or similar therapeutic strategies, for different origin diseases, that might involve this coactivator.

V. REFERENCES

1. Dexter, D. T. & Jenner, P. Parkinson disease: from pathology to molecular disease mechanisms. *Free Radic. Biol. Med.* **62**, 132–144 (2013).

2. Dauer, W. & Przedborski, S. Parkinson's Disease: Mechanisms and Models. **39**, 889–909 (2003).

3. Hauser, David N; Hastings, T. G. Mitochondrial dysfunction and oxidative stress in Parkinson's disease and monogenic parkinsonism. *Neurobiol. Dis.* 35–42

4. Winklhofer, Konstanze F.; Haass, C. Mitochondrial dysfunction in Parkinson's disease. *Biochim. Biophys. Acta* **1802**, 29–44 (2010).

5. Berardelli, A., Rothwell, J. C., Thompson, P. D. & Hallett, M. Pathophysiology of bradykinesia in Parkinson's disease. 2131–2146 (2001).

6. Yuan, H. *et al.* Treatment strategies for Parkinson's disease. **26**, 66–76 (2010).

7. Ikeda, H., Markey, C. J. & Markey, S. P. Search for neurotoxins structurally related to 1-methyl-4-phenylpyridine (MPP^+) in the pathogenesis of Parkinson's disease. *Brain Res.* **575**, 285–298 (1992).

8. Houlden, Henry; Singleton, A. B. The genetics and neuropathology of Parkinson's disease. **124**, 325–338 (2013).

9. Klein, C. & Westenberger, A. Genetics of Parkinson's disease. *Cold Spring Harb. Perspect. Med.* **2**, (2012).

10. Galvin, J. E. *et al.* Monoclonal antibodies to purified cortical lewy bodies recognize the mid-size neurofilament subunit. *Ann. Neurol.* **42**, 595–603 (2004).

11. Auluck, P. K., Chan, H. Y. E., Trojanowski, J. Q., Lee, V. M.-Y. & Bonini, N. M. Chaperone Suppression of α-Synuclein Toxicity in a Model for Parkinson's Disease. *Science.* **295**, (2002).

12. Tappel, A. & Tappel, A. Oxidant free radical initiated chain polymerization of protein and other biomolecules and its relationship to diseases. *Med. Hypotheses* **63**, 98–99 (2018).

13. Chaari, A., Hoarau-Véchot, J. & Ladjimi, M. Applying chaperones to protein-misfolding disorders: Molecular chaperones against α-synuclein in Parkinson's disease. *Int. J. Biol. Macromol.* **60**, 196–205 (2013).

14. Makwana, P. K. & Sundd, M. Review Article Alpha-synuclein structure, aggregation and modulators. **7**, 1–29 (2016).

15. Corona, J. C. & Duchen, M. R. PPARγ and PGC-1α as Therapeutic Targets in Parkinson's. *Neurochem. Res.* **40**, 308–316 (2014).

16. Braak, H. *et al.* Staging of brain pathology related to sporadic Parkinson's disease. **24**, 197–

211 (2003).
17. Kolb, B. & Whishaw, I. Q. Fundamentals of human neuropsychology, 5th ed. Fundamentals of human neuropsychology, *5th ed.* (Worth Publishers, 2003).
18. Youdim, M. B. H. & Bakhle, Y. S. Monoamine oxidase: isoforms and inhibitors in Parkinson's disease and depressive illness. (2006).
19. Nashatizadeh, M. M., Lyons, K. E. & Pahwa, R. A review of ropinirole prolonged release in Parkinson's disease. *Clin. Interv. Aging.* 179–186 (2012).
20. Binder, S., Deuschl, G. & Volkmann, J. Effect of Cabergoline on Parkinsonian Tremor Assessed by Long-Term Actigraphy. *Eur. Neurol.* **61**, 149–153 (2009).
21. Uzun, M. *et al.* The investigation of selegiline and rasagiline administration on QT interval in conscious rabbits. *Eur. Rev. Med. Pharmacol. Sci.* **13**, 95–98 (2008).
22. Müller, T. Drug therapy in patients with Parkinson' s disease. *Transl. Neurodegener.* **1**, 1–13 (2012).
23. Groiss, S. J., Wojtecki, L., Su, M. & Schnitzler, A. Deep brain stimulation in Parkinson' s disease. *Ther. Adv. Neurol. Disord.* 379–391 (2009).
24. Article, R., Moon, H. E. & Paek, S. H. Mitochondrial Dysfunction in Parkinson' s Disease. *Exp. Neurobiol.* **24**, 103–116 (2015).
25. Scarpulla, R. C. Transcriptional activators and coactivators in the nuclear control of mitochondrial function in mammalian cells. *Gene*, **286**, 81–89 (2002).
26. Giuseppe, A. & Schatz, G. Biogenesis of Mitochondria. *Annu Rev Cell Biol.* **4**, 289–333 (1988).
27. Spinazzi, M., Casarin, A., Pertegato, V., Salviati, L. & Angelini, C. Assessment of mitochondrial respiratory chain enzymatic activities on tissues and cultured cells. *Nat. Protoc.* **7**, 1235–1246 (2012).
28. Lambert, A. J. & Brand, M. D. Reactive Oxygen Species Production by Mitochondria BT - Mitochondrial DNA: Methods and Protocols. 165–181 (Humana Press, 2009).
29. Dorn II, G. W. Mitochondrial dynamism and heart disease: changing shape and shaping change. *EMBO Mol. Med.* **7**, 865–877 (2015).
30. St-Pierre, J. *et al.* Bioenergetic analysis of peroxisome proliferator-activated receptor γ coactivators 1α and 1β (PGC-1α and PGC-1β) in muscle cells. *J. Biol. Chem.* **278**, 26597–26603 (2003).
31. Brown, G. U. Y. C. Cellular Energy Utilization of Standard Metabolic and Molecular Origin Rate in Mammals. *Physiol Rev.* **77**, (2018).
32. Arsenijevic, D. *et al.* Disruption of the uncoupling protein-2 gene in mice reveals a role in

immunity and reactive oxygen species production. *Nat. Genet.* **26**, 435–439 (2000).

33. Echtay, K. S. *et al.* Superoxide activates mitochondrial uncoupling proteins. *Nature* **415**, 96–99 (2002).

34. McInnes, J. Insights on altered mitochondrial function and dynamics in the pathogenesis of neurodegeneration. *Transl. Neurodegener.* **2** (2013).

35. Santos, D. & Cardoso, S. M. Mitochondrial dynamics and neuronal fate in Parkinson's disease. *Mitochondrion* **12**, 428–437 (2012).

36. Barsoum, M. J. *et al.* Nitric oxide-induced mitochondrial fission is regulated by dynamin-related GTPases in neurons. *EMBO J.* **25**, 3900–3911 (2006).

37. Ali, S. & Mcstay, G. P. Regulation of Mitochondrial Dynamics by Proteolytic Processing and Protein Turnover. **1**, 1–15 (2018).

38. Benard, G. & Karbowski, M. Mitochondrial fusion and division: Regulation and role in cell viability. *Semin. Cell Dev. Biol.* **20**, 365–374 (2009).

39. Smirnova, E., Griparic, L., Shurland, D. L. & van der Bliek, A. M. Dynamin-related protein Drp1 is required for mitochondrial division in mammalian cells. *Mol. Biol. Cell* **12**, 2245–2256 (2001).

40. Otera, H. *et al.* Mff is an essential factor for mitochondrial recruitment of Drp1 during mitochondrial fission in mammalian cells. *J. Cell Biol.* **191**, 1141–1158 (2010).

41. Palmer, C. S. *et al.* MiD49 and MiD51, new components of the mitochondrial fission machinery. *EMBO Rep.* **12**, 565–573 (2011).

42. Korovila, I. *et al.* Proteostasis, oxidative stress and aging. *Redox Biol.* **13**, 550–567 (2017).

43. Trifunovic, A. & Larsson, N. Mitochondrial dysfunction as a cause of ageing. 167–178 (2008).

44. Reeve, A. K., Krishnan, K. J. & Turnbull, D. Mitochondrial DNA Mutations in Disease, Aging, and Neurodegeneration. *Ann. N. Y. Acad. Sci.* **1147**, 21–29 (2008).

45. DiMauro, S. & Davidzon, G. Mitochondrial DNA and disease. *Ann. Med.* **37**, 222–232 (2005).

46. Khrapko, K. & Vijg, J. Mitochondrial DNA mutations and aging: devils in the details? *Trends Genet.* **25**, 91–98 (2009).

47. Rossignol, R. *et al.* Mitochondrial threshold effects. *Biochem. J.* **370**, 751–762 (2003).

48. Engelhardt, J. F. Redox-Mediated Gene Therapies for Environmental Injury: Approaches and Concepts. *Antioxid. Redox Signal.* **1**, 5–27 (1999).

49. Hoepken, H. *et al.* Mitochondrial dysfunction, peroxidation damage and changes in glutathione metabolism in PARK6. **25**, 401–411 (2007).

50. Pacelli, C. *et al.* Elevated Mitochondrial Bioenergetics and Axonal Arborization Size Are Key Contributors to the Vulnerability of Dopamine Neurons. *Curr. Biol.* **25**, 2349–2360 (2015).
51. Benskey, M. *et al.* Recovery of hypothalamic tuberoinfundibular dopamine neurons from acute toxicant exposure is dependent upon protein synthesis and associated with an increase in parkin and ubiquitin carboxy-terminal hydrolase-L1 expression. *Neurotoxicology* **33**, 321–331 (2012).
52. Requejo-Aguilar, Raquel; Bolaños, J. P. Mitochondrial control of cell bioenergetics in Parkinson's disease. *Free Radic. Biol. Med.* 123–137 (2017).
53. Chinta, S. J. & Andersen, J. K. Redox imbalance in Parkinson's disease. *Biochim. Biophys. Acta* **1780**, 1362–1367 (2008).
54. Alam, Z. I. *et al.* Oxidative DNA Damage in the Parkinsonian Brain: An Apparent Selective Increase in 8-Hydroxyguanine Levels in Substantia Nigra. *J. Neurochem.* **69**, 1196–1203 (1997).
55. Dexter, D. T. *et al.* Basal Lipid Peroxidation in Substantia Nigra Is Increased in Parkinson's Disease. *J. Neurochem.* **52**, 381–389 (1989).
56. Floor, E. & Wetzel, M. G. Increased Protein Oxidation in Human Substantia Nigra Pars Compacta in Comparison with Basal Ganglia and Prefrontal Cortex Measured with an Improved Dinitrophenylhydrazine Assay. *J. Neurochem.* **70**, 268–275 (1998).
57. Winkler-Stuck, K., Wiedemann, F. R., Wallesch, C.-W. & Kunz, W. S. Effect of coenzyme Q_{10} on the mitochondrial function of skin fibroblasts from Parkinson patients. *J. Neurol. Sci.* **220**, 41–48 (2004).
58. Bindoff, L. A., Birch-Machin, M. A., Cartlidge, N. E. F., Parker Jr., W. D. & Turnbull, D. M. Respiratory chain abnormalities in skeletal muscle from patients with Parkinson's disease. *J. Neurol. Sci.* **104**, 203–208 (1991).
59. Yoshino, H., Kondo, T. & Mizuno, Y. Mitochondrial complex I and II activities of lymphocytes and platelets in Parkinson's disease. *J. Neural Transm.* 27–34 (1992).
60. Parker Jr., W. D. & Swerdlow, R. H. Mitochondrial Dysfunction in Idiopathic Parkinson Disease. *Am. J. Hum. Genet.* **62**, 758–762 (1998).
61. Shults, C. W. Mitochondrial dysfunction and possible treatments in Parkinson's disease - a review. *Mitochondrion* **4**, 641–648 (2004).
62. Thyagarajan, D. *et al.* A novel mitochondrial 12SrRNA point mutation in parkinsonism, deafness, and neuropathy. *Ann. Neurol.* **48**, 730–736 (2000).
63. Hindle, J. V. Ageing, neurodegeneration and Parkinson's disease. *Age Ageing* **39**, 156–161 (2010).

64. Levy, G. The Relationship of Parkinson Disease With Aging. *JAMA Neurol.* **64**, 1242–1246 (2007).

65. Meredith, G. E. & Rademacher, D. J. MPTP mouse models of Parkinson's disease: an update. *J. Parkinsons. Dis.* **1**, 19–33 (2011).

66. Marini, A. M., Lipsky, R. H., Schwartz, J. P. & Kopin, I. J. Accumulation of 1-Methyl-4-Phenyl-1,2,3,6-Tetrahydropyridine in Cultured Cerebellar Astrocytes. *J Neurochem.* **4**, 1250–1258 (1992).

67. Javitch, J. A., D'Amato, R. J., Strittmatter, S. M. & Snyder, S. H. Parkinsonism-inducing neurotoxin, N-methyl-4-phenyl-1,2,3,6-tetrahydropyridine: uptake of the metabolite N-methyl-4-phenylpyridine by dopamine neurons explains selective toxicity. *Proc. Natl. Acad. Sci. U. S. A.* **82**, 2173–2177 (1985).

68. William Langston, J., Forno, L. S., Rebert, C. S. & Irwin, I. Selective nigral toxicity after systemic administration of 1-methyl-4-phenyl-1,2,5,6-tetrahydropyrine (MPTP) in the squirrel monkey. *Brain Res.* **292**, 390–394 (1984).

69. Chiueh, C. C. *et al.* Neurochemical and behavioral effects of systematic and intranigral administration of N-methyl-4-phenyl-1,2,3,6-tetrahydropyridine in the rat. *Eur. J. Pharmacol.* **100**, 189–194 (1984).

70. Liu, Y., Roghani, A. & Edwards, R. H. Gene transfer of a reserpine-sensitive mechanism of resistance to N-methyl-4-phenylpyridinium. *Proc. Natl. Acad. Sci. U. S. A.* **89**, 9074–9078 (1992).

71. Klaidman, L. K., Adams, J. D., Leung, A. C., Sam Kim, S. & Cadenas, E. Redox cycling of MPP^+: Evidence for a new mechanism involving hydride transfer with xanthine oxidase, aldehyde dehydrogenase, and lipoamide dehydrogenase. *Free Radic. Biol. Med.* **15**, 169–179 (1993).

72. Rarnsaysb, Rona R; Singer, T. P. Energy-dependent Uptake of Energy-dependent Uptake of N-Methyl-4-phenylpyridinium, the NeurotoxicMetabolite of l-Methyl-4-Phenyl-1,2,3,6-tetrahydropyridine, by Mitochondria. **261**, 7585–7587 (1986).

73. Przedborski, S. & Jackson-Lewis, V. Mechanisms of MPTP toxicity. *Mov. Disord.* **13 Suppl 1**, 35–38 (1998).

74. Tipton, K. F. & Singer, T. P. Advances in Our Understanding of the Mechanisms of the Neurotoxicity of MPTP and Related Compounds. *J. Neurochem.* **61**, 1191–1206 (1993).

75. Fabre, E., Monserrat, J., Herrero, A., Barja, G. & Leret, M. L. Effect of MPTP on brain mitochondrial H2O2 and ATP production and on dopamine and DOPAC in the striatum. *J. Physiol. Biochem.* **55**, 325–331 (1999).

76. Desai, V. G., Feuers, R. J., Hart, R. W. & Ali, S. F. MPP^+-induced neurotoxicity in mouse is age-dependent: evidenced by the selective inhibition of complexes of electron transport. *Brain Res.* **715**, 1–8 (1996).

77. Piao, Y., Kim, H. G., Oh, M. S. & Pak, Y. K. Overexpression of TFAM, NRF-1 and myr AKT protects the MPP+-induced mitochondrial dysfunctions in neuronal cells. *Biochim. Biophys. Acta - Gen. Subj.* **1820**, 577–585 (2012).

78. Burté, F., De Girolamo, L. A., Hargreaves, A. J. & Billett, E. E. Alterations in the Mitochondrial Proteome of Neuroblastoma Cells in Response to Complex 1 Inhibition. *J. Proteome Res.* **100**, 1974–1986 (2011).

79. Zhang, X. *et al.* Region-specific protein abundance changes in the brain of MPTP-induced Parkinson's disease mouse model. *J. Proteome Res.* **9**, 1496–1509 (2010).

80. Chalmers-Redman, R. M. E., MacLean Fraser, A. D., Carlile, G. W., Pong, A. & Tatton, W. G. Glucose Protection from MPP^+-Induced Apoptosis Depends on Mitochondrial Membrane Potential and ATP Synthase. *Biochem. Biophys. Res. Commun.* **257**, 440–447 (1999).

81. Wu, E. Y., Langston, J. W. & Di Monte, D. A. Toxicity of the 1-methyl-4-phenyl-2,3-dihydropyridinium and 1-methyl-4-phenylpyridinium species in primary cultures of mouse astrocytes. *J. Pharmacol. Exp. Ther.* **262** (1992).

82. Mazzio, E. & Soliman, K. F. A. D-(+)-Glucose rescue against 1-methyl-4-phenylpyridinium toxicity through anaerobic glycolysis in neuroblastoma cells. **962**, 48–60 (2003).

83. Maruoka, N., Murata, T. & Omata, N. Biphasic mechanism of the toxicity induced by 1-methyl-4-phenylpyridinium ion (MPP^+) as revealed by dynamic changes in glucose metabolism in rat brain slices. **28**, 672–678 (2007).

84. Bolaños, Juan P.; Cadenas, E.; Duchen, MR; Hampton, MB; Mann, GE; Murphy, M. Introduction to Special Issue on Mitochondrial Redox Signaling in Health and Disease. *Free Radic. Biol. Med.* **100**, 1–4 (2016).

85. Bonifati, V. *et al.* Mutations in the DJ-1 Gene Associated with Autosomal Recessive Early-Onset Parkinsonism. *Science.* **299** (2003).

86. Kitada, T. *et al.* Mutations in the parkin gene cause autosomal recessive juvenile parkinsonism. *Nature* **392**, 605–608 (1998).

87. Valente, E. M. *et al.* Hereditary Early-Onset Parkinson's Disease Caused by Mutations in PINK1. *Science.* **304** (2004).

88. Pridgeon, J. W., Olzmann, J. A., Chin, L.-S. & Li, L. PINK1 protects against oxidative stress by phosphorylating mitochondrial chaperone TRAP1. *PLoS Biol.* **5** (2007).

89. Paterna, J.-C., Leng, A., Weber, E., Feldon, J. & Büeler, H. DJ-1 and Parkin Modulate Dopamine-dependent Behavior and Inhibit MPTP-induced Nigral Dopamine Neuron Loss in Mice. *Mol. Ther.* **15**, 698–704 (2007).

90. Park, J. *et al.* Drosophila DJ-1 mutants show oxidative stress-sensitive locomotive dysfunction. *Gene* **361**, 133–139 (2005).

91. Dagda, R. K. *et al.* Loss of PINK1 function promotes mitophagy through effects on oxidative stress and mitochondrial fission. *J. Biol. Chem.* **284**, 13843–13855 (2009).

92. Martin, Ian; Dawson, Valina L.; dawson, T. M. Recent Advances in the genetics of Parkinson's Disease. *Annu. Rev. Genomics Hum. Genet.* **60**, 301–325 (2014).

93. Bouman, L. *et al.* Parkin is transcriptionally regulated by ATF4: evidence for an interconnection between mitochondrial stress and ER stress. *Cell Death Differ.* **18**, 769–782 (2011).

94. Wang, B., Abraham, N., Gao, G. & Yang, Q. Dysregulation of autophagy and mitochondrial function in Parkinson's disease. *Transl. Neurodegener.* 1–9 (2016).

95. Han, J.-Y., Kim, J.-S. & Son, J. H. Mitochondrial homeostasis molecules: regulation by a trio of recessive Parkinson's disease genes. *Exp. Neurobiol.* **23**, 345–351 (2014).

96. Cui, M., Tang, X., Christian, W. V, Yoon, Y. & Tieu, K. Perturbations in mitochondrial dynamics induced by human mutant PINK1 can be rescued by the mitochondrial division inhibitor mdivi-1. *J. Biol. Chem.* **285**, 11740–11752 (2010).

97. Wang, H. *et al.* Parkin ubiquitinates Drp1 for proteasome-dependent degradation: implication of dysregulated mitochondrial dynamics in Parkinson disease. *J. Biol. Chem.* **286**, 11649–11658 (2011).

98. Irrcher, I. *et al.* Loss of the Parkinson's disease-linked gene DJ-1 perturbs mitochondrial dynamics. *Hum. Mol. Genet.* **19**, 3734–3746 (2010).

99. Xiong, H. *et al.* Parkin, PINK1, and DJ-1 form a ubiquitin E3 ligase complex promoting unfolded protein degradation. *J. Clin. Invest.* **119**, 650–660 (2009).

100. Henchcliffe, C. & Beal, M. F. Mitochondrial biology and oxidative stress in Parkinson disease pathogenesis. *Nat. Clin. Pract. Neurol.* **4**, 600–609 (2008).

101. Abou-Sleiman, P. M., Muqit, M. M. K. & Wood, N. W. Expanding insights of mitochondrial dysfunction in Parkinson's disease. *Nat. Rev. Neurosci.* **7**, 207–219 (2006).

102. Shin, J. H. *et al.* PARIS (ZNF746) repression of PGC-1α contributes to neurodegeneration in parkinson's disease. *Cell* **144**, 689–702 (2011).

103. Castillo-Quan, J. I. Parkin' control: regulation of PGC-1α through PARIS in Parkinson's disease. *Dis. Model. Mech.* **4** (2011).

104. Hershko, A. & Ciechanover, A. The Ubiquitin System. *Annu. Rev. Biochem.* **67**, 425–479 (1998).
105. Glickman, M. H. & Ciechanover, A. The Ubiquitin-Proteasome Proteolytic Pathway: Destruction for the Sake of Construction. *Physiol. Rev.* **82**, 373–428 (2002).
106. Chhangani, D. & Mishra, A. Protein quality control system in neurodegeneration: A healing company hard to beat but failure is fatal. *Mol. Neurobiol.* **48**, 141–156 (2013).
107. Schwartz, A. L. & Ciechanover, A. Targeting Proteins for Destruction by the Ubiquitin System: Implications for Human Pathobiology. *Annu. Rev. Pharmacol. Toxicol.* **49**, 73–96 (2009).
108. Voges, D., Zwickl, P. & Baumeister, W. The 26S proteasome: a molecular machine designed for controlled proteolysis. *Annu. Rev. Biochem.* **68**, 1015–1068 (1999).
109. Ross, J. M., Olson, L. & Coppotelli, G. Mitochondrial and Ubiquitin Proteasome System Dysfunction in Ageing and Disease: Two Sides of the Same Coin? *Int. J. Mol. Sci.* **16**, 19458–19476 (2015).
110. Rango, M. & Bresolin, M. Brain Mitochondria, Aging, and Parkinson's Disease. *Genes*. **5**, (2018).
111. Austin, S. & St-Pierre, J. PGC1α and mitochondrial metabolism - emerging concepts and relevance in ageing and neurodegenerative disorders. *J. Cell Sci.* **125**, 4963–4971 (2012).
112. Handschin, C. The biology of PGC-1α and its therapeutic potential. *Trends Pharmacol. Sci.* **30**, 322–329 (2009).
113. Uldry, M. *et al.* Complementary action of the PGC-1 coactivators in mitochondrial biogenesis and brown fat differentiation. *Cell Metab.* **3**, 333–341 (2006).
114. Puigserver, P. *et al.* A Cold-Inducible Coactivator of Nuclear Receptors Linked to Adaptive Thermogenesis. **92**, 829–839 (1998).
115. Tsunemi, T. & La, A. R. PGC-1a at the intersection of bioenergetics regulation and neuron function: From Huntington's disease to Parkinson's disease and beyond. *Prog. Neurobiol.* **97**, 142–151 (2012).
116. Correia, J. C., Ferreira, D. M. S. & Ruas, J. L. Intercellular: Local and systemic actions of skeletal muscle PGC-1s. *Trends Endocrinol. Metab.* **26**, 305–314 (2015).
117. Miura, S., Kai, Y., Kamei, Y. & Ezaki, O. Isoform-Specific Increases in Murine Skeletal Muscle Peroxisome Proliferator-Activated Receptor-γ Coactivator-1α (PGC-1α) mRNA in Response to β2-Adrenergic Receptor Activation and Exercise. *Endocrinology* **149**, 4527–4533 (2008).
118. Zhang, Y. *et al.* Alternative mRNA Splicing Produces a Novel Biologically Active Short

Isoform of PGC-1α. *J. Biol. Chem.* **284**, 32813–32826 (2009).

119. Chang, J. S. *et al.* NT-PGC-1α Protein Is Sufficient to Link β(3)-Adrenergic Receptor Activation to Transcriptional and Physiological Components of Adaptive Thermogenesis. *J. Biol. Chem.* **287**, 9100–9111 (2012).

120. Wen, X. *et al.* Effect of Exercise Intensity on Isoform-Specific Expressions of NT-PGC-1 α mRNA in Mouse Skeletal Muscle. *Biomed Res. Int.* **2014** (2014).

121. Ruas, J. L. *et al.* A PGC-1α isoform induced by resistance training regulates skeletal muscle hypertrophy. *Cell* **151**, 1319–1331 (2012).

122. Barger, P. M., Browning, A. C., Garner, A. N. & Kelly, D. P. p38 Mitogen-activated Protein Kinase Activates Peroxisome Proliferator-activated Receptor alpha: A potential role in the cardiac metabolic stress response. *J. Biol. Chem.* **276**, 44495–44501 (2001).

123. Rodgers, J. T. *et al.* Nutrient control of glucose homeostasis through a complex of PGC-1α and SIRT1. *Nature* **434**, 113 (2005).

124. Rytinki, M. M. & Palvimo, J. J. SUMOylation Attenuates the Function of PGC-1α. *J. Biol. Chem.* **284**, 26184–26193 (2009).

125. Qian, X. *et al.* KDM3A Senses Oxygen Availability to Regulate PGC- Article KDM3A Senses Oxygen Availability to Regulate PGC-1 a -Mediated Mitochondrial Biogenesis. *Mol. Cell* 1–11 (2019). doi:10.1016/j.molcel.2019.09.019

126. Li, S. & Shang, Y. Regulation of SRC family coactivators by post-translational modifications. *Cell. Signal.* **19**, 1101—1112 (2007).

127. Lonard, D. M. & O'Malley, B. W. Nuclear Receptor Coregulators: Judges, Juries, and Executioners of Cellular Regulation. *Mol. Cell* **27**, 691–700 (2007).

128. Rosenfeld, M. G., Lunyak, V. V & Glass, C. K. Integrating signal-dependent programs of transcriptional response Sensors and signals: a coactivator/corepressor/epigenetic code for integrating signal-dependent programs of transcriptional response. *Genes Dev.* **20**, 1405–1428 (2006).

129. Han, S. J., Lonard, D. M. & O'Malley, B. W. Multi-modulation of nuclear receptor coactivators through posttranslational modifications. *Trends Endocrinol. Metab.* **20**, 8–15 (2009).

130. Handschin, C. & Spiegelman, B. M. Peroxisome Proliferator-Activated Receptor γ Coactivator 1 Coactivators, Energy Homeostasis, and Metabolism. *Endocr. Rev.* **27**, 728–735 (2006).

131. St-Pierre, J. *et al.* Suppression of Reactive Oxygen Species and Neurodegeneration by the PGC-1 Transcriptional Coactivators. *Cell* **127**, 397–408 (2006).

132. Valle, I., Álvarez-Barrientos, A., Arza, E., Lamas, S. & Monsalve, M. PGC-1α regulates the mitochondrial antioxidant defense system in vascular endothelial cells. *Cardiovasc. Res.* **66**, 562–573 (2005).

133. Fernandez-marcos, P. J. & Auwerx, J. Regulation of PGC-1 a , a nodal regulator of mitochondrial biogenesis. **93**, 884–890 (2011).

134. Mudò, G. *et al.* Transgenic expression and activation of PGC-1α protect dopaminergic neurons in the MPTP mouse model of Parkinsons disease. *Cell. Mol. Life Sci.* **69**, 1153–1165 (2012).

135. Rodgers, J. T., Lerin, C., Gerhart-Hines, Z. & Puigserver, P. Metabolic Adaptations through the PGC-1α and SIRT1 Pathways. *FEBS Lett.* **582**, 46–53 (2008).

136. Handschin, C., Rhee, J., Lin, J., Tarr, P. T. & Spiegelman, B. M. An autoregulatory loop controls peroxisome expression in muscle. *Proc Natl Acad Sci U S A.* **100**, (2003).

137. Lagouge, M. *et al.* Resveratrol Improves Mitochondrial Function and Protects against Metabolic Disease by Activating SIRT1 and PGC-1α. *Cell* **127**, 1109–1122 (2006).

138. Sahin, E. *et al.* Telomere dysfunction induces metabolic and mitochondrial compromise. *Nature* **470**, 359 (2011).

139. Zheng, B. *et al.* PGC-1α, A Potential Therapeutic Target for Early Intervention in Parkinson's Disease. *Sci. Transl. Med.* **2** (2010).

140. Breidert, T. *et al.* Protective action of the peroxisome proliferator-activated receptor-γ agonist pioglitazone in a mouse model of Parkinson's disease. *J. Neurochem.* **82**, 615–624 (2002).

141. Lin, J. *et al.* Defects in adaptive energy metabolism with CNS linked hyperactivity in PGC 1 alpha null mice. *Cell* **119**, 121–135 (2004).

142. Lv, J. *et al.* PGC-1α sparks the fire of neuroprotection against neurodegenerative disorders. *Ageing Res. Rev.* **44**, 8–21 (2018).

143. Falkenburger, Bjorn H.; Saridaki, Theodora; Dinter, E. Cellular Models for Parkinson's Disease. *J. Neurochem.* **139**, 121–130 (2016).

144. Gordon, J., Amini, S. & White, M. K. General overview of neuronal cell culture. *Methods Mol. Biol.* **1078**, 1–8 (2013).

145. Hasegawa, T. *et al.* Accelerated alpha-synuclein aggregation after differentiation of SH-SY5Y neuroblastoma cells. *Brain Res.* **1013**, 51–59 (2004).

146. Roberti, M. J., Bertoncini, C. W., Klement, R., Jares-Erijman, E. A. & Jovin, T. M. Fluorescence imaging of amyloid formation in living cells by a functional, tetracysteine-tagged α-synuclein. *Nat. Methods* **4**, 345–351 (2007).

147. Jang, W., Kim, H. J., Li, H., Jo, K. D. & Lee, M. K. The Neuroprotective Effect of Erythropoietin on Rotenone-Induced Neurotoxicity in SH-SY5Y Cells Through the Induction of Autophagy. *Mol Neurobiol.* **6** (2015).

148. Narotzky, R. & Bondareff, W. Biogenic amines in cultured neuroblastoma and astrocytoma cells. *J. Cell Biol.* **63**, 64–70 (1974).

149. Zhou, X.-W., Winblad, B., Guan, Z. & Pei, J.-J. Interactions between glycogen synthase kinase 3beta, protein kinase B, and protein phosphatase 2A in tau phosphorylation in mouse N2a neuroblastoma cells. *J. Alzheimers. Dis.* **17**, 929–937 (2009).

150. Amazzal, L., Lapôtre, A., Quignon, F. & Bagrel, D. Mangiferin protects against 1-methyl-4-phenylpyridinium toxicity mediated by oxidative stress in N2A cells. *Neurosci. Lett.* **418**, 159–164 (2007).

151. An, W. F. & Tolliday, N. Cell-Based Assays for High-Throughput Screening. *Mol. Biotechnol.* **6**, 180–186 (2010).

152. Markowicz, M. & Mikiciuk-olasik, E. Adaptation of High-Throughput Screening in Drug Discovery - Toxicological Screening Tests. *Int J Mol Sci.* **1**, 427–452 (2012).

153. Hopkins, A. L. & Groom, C. R. The druggable genome. *Nat. Rev. Drug Discov.* **1**, 727–730 (2002).

154. Martis, E. A. & Radhakrishnan, R. High-Throughput Screening: The Hits and Leads of Drug Discovery - An Overview. **1**, 2–10 (2011).

155. Armstrong, B. Y. J. W. A review of high-throughput screening approaches for drug discovery. (1999).

156. Enslein, K. Computation of developmental toxicity potential by QSTR models in the TOPKAT program. *Adv. Anim. Altern. Saf. Effic. Test.* 159–167 (1998).

157. Mayr, L. M. & Bojanic, D. Novel trends in high-throughput screening. *Curr Opin Pharmacol.* **5**, 580–588 (2009).

158. Burns, S. *et al.* Identification of Small-Molecule Inhibitors of Protein Kinase B (PKB/AKT) in an AlphaScreen^{TM} High-Throughput Screen. *J. Biomol. Screen.* **7**, 822–827 (2006).

159. Swaney, S. *et al.* Characterization of a High-Throughput Screening Assay for Inhibitors of Elongation Factor P and Ribosomal Peptidyl Transferase Activity. *J. Biomol. Screen.* **11**, 736–742 (2006).

160. Spiegelman, B. M. & Heinrich, R. Biological Control through Regulated Transcriptional Coactivators. *Cell* **119**, 157–167 (2004).

161. Arany, Z. *et al.* Gene expression-based screening identifies microtubule inhibitors as

inducers of PGC-1alpha and oxidative phosphorylation. *Proc Natl Acad Sci U S A.* **105**, 4721–4726 (2008).

162. Lynch, C. *et al.* Identification of Compounds That Inhibit Estrogen-Related Receptor Alpha Signaling Using High-Throughput Screening Assays. *Molecules* **24**, (2019).

163. Izadi, M., Ferreira, D. M. S., Cervenka, I. & Correia, J. C. Small molecule PGC-1a1 protein stabilizers induce adipocyte Ucp1 expression and uncoupled mitochondrial respiration. *Mol Metab.* **9**, (2018).

164. Villena, J. A. New insights into PGC-1 coactivators: redefining their role in the regulation of mitochondrial function and beyond. *FEBS. J.* **282**, 647–672 (2014).

165. Scarpulla, R. C. Nuclear Control of Respiratory Chain Expression by Nuclear Respiratory Factors and PGC-1-Related Coactivator. *Ann. N. Y. Acad. Sci.* 321–334 (2010).

166. Wenz, T. Regulation of mitochondrial biogenesis and PGC-1α under cellular stress. *Mitochondrion* **13**, 134–142 (2013).

167.Ye, Q. *et al.* Mitochondrial Effects of PGC-1alpha Silencing in MPP^+ Treated Human SH-SY5Y Neuroblastoma Cells. *Front. Mol. Neurosci.* **10**, 1–13 (2017).

168. Kelly, D. P. & Scarpulla, R. C. Transcriptional regulatory circuits controlling mitochondrial biogenesis and function. *Genes Dev.* **18**, 357–368 (2004).

169. Fang, P., He, B., Yu, M., Shi, M. & Zhu, Y. Treatment with celastrol protects against obesity through suppression of galanin-induced fat intake and activation of PGC-1α/GLUT4 axis-mediated glucose consumption. *BBA - Mol. Basis Dis.* **1865**, 1341-1350 (2019).

170. Puigserver, P. & Spiegelman, B. M. Peroxisome Proliferator-Activated Receptor gama Coactivator 1 alpha (PGC-1 alpha): Transcriptional Coactivator and Metabolic Regulator. *Endocr. Rev.* **24**, 78–90 (2003).

171. Loaiza, A., Porras, O. H. & Barros, L. F. Glutamate triggers rapid glucose transport stimulation in astrocytes as evidenced by real-time confocal microscopy. *J. Neurosci.* **23**, 7337–7342 (2003).

172. Porras, O., Ruminot, I., Loaiza, A. & Barros, L. Na^+-Ca^{2+} cosignaling in the stimulation of the glucose transporter GLUT1 in cultured astrocytes. *Glia* **56**, 59–68 (2008).

173. Bouzier-Sore, A.-K. *et al.* Competition between glucose and lactate as oxidative energy substrates in both neurons and astrocytes: a comparative NMR study. *Eur. J. Neurosci.* **24**, 1687–1694 (2006).

174. Bolaños, J. P. Bioenergetics and redox adaptations of astrocytes to neuronal activity. *J. Neurochem.* **139**, 115–125 (2016).

175. Ashrafi, G. *et al.* GLUT4 Mobilization Supports Energetic Demands of Active Synapses.

Neuron **93** (2016).
176. Ashrafi, G. & Ryan, T. A. Glucose metabolism in nerve terminals. *Curr. Opin. Neurobiol.* 156–161 (2018).
177. Garnier, A. & Veksler, V. Transcriptional control of mitochondrial biogenesis: the central role of PGC-1a. *Cardiovasc. Res.* **79**, 208–217 (2008).
178. Torok, R. *et al.* Effect of MPTP on mRNA expression of PGC-1a in mouse brain. *Brain Res.* **1660**, 20–26 (2017).
179. Dabrowska, A. *et al.* PGC-1α controls mitochondrial biogenesis and dynamics in lead-induced neurotoxicity. *Aging* **7**, 629–643 (2015).